ORIENTATION AND DYNAMICS OF UNFILLED AND FILLED POLY(BUTADIENE) NETWORKS STUDIED BY DEUTERIUM NMR

Dissertation

zur Erlangung des akademischen Grades doktor rerum naturalium

(Dr. rer. nat.)

vorgelegt der

Mathematisch-Naturwissenschaftlich-Technischen Fakultät

der Martin-Luther-Universität Halle-Wittenberg

von Herrn Piyasiri Ekanayake

geb. am: 14. 09. 1965 in Senapura, Sri Lanka

Gutachter:

1. Prof. Dr. H. Schneider

2. Prof. Dr. E. Straube

3. Prof. Dr. W. Gronski

Halle (Saale), den 07.02.2000

CONTENTS

ABSTRACT

Deuterium NMR has been employed to determine the average orientation $\overline{P_2(\cos\theta)}$ of chain segments in poly(butadiene) networks. It is shown that the free induction decay separates the contribution to the orientation arising from the network constraint to that from chain interactions. The NMR spectrum lineshape reveals the orientational distribution of network vectors due to the crosslinks, whereas the observed splitting gives information about the orientation due to segmental interactions. Both the lineshape and splitting have been fitted simultaneously for a range of deformed poly(butadiene) networks. From the fitting parameters the separate contributions to the average orientation of the chain segments arising from the network constraint and from the interactions are calculated. These in turn are used to determine the molecular weight between crosslinks and the size of the segmental interactions, which we choose to express in terms of the Edward's screening length.

The NMR line splitting is investigated also in terms of network concentration and on the Flory interaction parameter χ. It is shown that one should take into account not only the χ parameter arising from different chemical structures but also that arising from the crosslinks of the network, in order to explain the experimental NMR line splitting. The latter is found to be proportional to $1/\sqrt{T}$. It is also shown that the Edward's screening length is independent of precursor chain length and crosslink density.

Deuterium NMR line shapes of carbon black (N220) filled cis-1,4 poly(butadiene) networks have been examined. The effect of the susceptibility of the filler on the NMR line shape has been considered. The theory constructed in this study for deuterium NMR line splitting from polymer networks was used to fit the experimental data. It was found that the polymer segments nearby the surface of a filler particle experience a different local magnetic field from the remaining segments, due to the susceptibility of the carbon black. This effect gives rise to an asymmetry in the NMR spectrum, which until now has not been explained. Additionally, this analysis determines the fraction of polymer units affected by the local field of the filler particles and provides information about the effect of the macroscopic deformation on these attached chains.

The sine correlation function (introduced by Callaghan et al.) and the NMR relaxation function (introduced by Simon et al.) were also employed to study the NMR response of the poly(butadiene) networks and linear chains. Finally, the residual quadrupolar interaction determined by all the above mentioned procedures was compared.

SUMMARY

Investigation of orientation and dynamics of polymeric chains is one of the main concerns in the field of polymers since it fully influences to properties of polymer products, such as plastics, rubber, adhesives, fibers and paints. In order to enhance mechanical properties of some polymer products, e.g. car tyres, different types of filler materials are mixed together with polymer. Although elastomers are vastly studied, there exist still open questions such as to understand and determine the orientation and dynamics of polymer network chains under deformation, in terms of basic polymer physics and also to understand the effect of filler on polymer network chains. In this work the main aim is to cope with the latter questions by means of nuclear magnetic resonance (NMR). Deuterium NMR is mainly used throughout this study since its capability of labeling polymer chains and hence giving opportunity to study the chains or segments discretely.

For an undeformed rubber a single resonance line in the deuterium NMR spectrum is observed[26]. Under uniaxial deformation the spectrum splits into a well-defined doublet structure corresponding to an oscillation in the free induction decay[27]. A non interacting phantom Gaussian network theoretically shows no splitting under deformation[28]. These results therefore indicate that to model the chain reorientation in a strained elastomer one must introduce segmental interactions[29]. In strained rubbers there is a higher degree of anisotropy than that merely induced by the crosslinks. Several explanations have been put forward to account for the oscillations seen in the free induction decay from strained deuterated networks, these include: nematic interactions[30], excluded volume interactions[31], and anisotropic junction fluctuations[32].

In this work it is shown, without the need to assume a particular model for the chain interactions, that the oscillations are indicative of an anisotropic mean field due to the many segmental interactions. Furthermore the decay envelope of the oscillations reveals the distribution of network vectors, each formed by connecting together consecutive crosslinks. A general analytic result that includes the effect of anisotropic mean field and network constraint will then be derived.

It is shown from analysing a range of deformed network sample signals, that for small deformations the assumption of initially Gaussian distributed network vectors, that then undergo affine deformation, adequately describes the NMR response. The NMR interaction term, the static quadrupolar constant, is effectively reduced in magnitude by rapid local level reorientations subject to both the constraint from the monomers being attached between crosslinks and the interactions of the segments with their environment. In a network a polymer segment interacts with many neighbouring ones. These many interactions can be described by an effective mean field[33,34]. NMR is able to monitor the average orientation due to the crosslinks and this mean field separately, allowing the two contributions to the total average orientation $\overline{P_2(\cos\theta)}$ to be evaluated. A theoretical interpretation by Brereton and Ries[31] attributes the higher degree of anisotropy implied by the splitting to excluded volume interactions within the rubber. Under deformation the distribution of monomeric units generate, through their excluded volume interactions, an

anisotropic mean field. All chains within the rubber matrix experience this mean field that causes an induced alignment along the strain direction. The resultant splitting due to this interaction is dependent on the size of the excluded volume interaction.

This work is based on an earlier NMR study that analysed a range of linear poly(butadiene) melts[39]. In that work the deuterium transverse relaxation was investigated to determine the size of a statistical segment and the magnitude of its corresponding rescaled quadrupolar coupling constant v_o. Rapid internal conformational changes within a single statistical segment reduce the magnitude of the static quadrupolar coupling constant, giving rise to a rescaled value. These two parameters found from well-characterised monodisperse linear chains are required in analysing the spectra from strained deuterated networks.

The NMR line splitting depends on the network concentration and also on the Flory interaction parameter χ. It is shown that one should take into account the χ parameter not only arising from different chemical structures but also that arising from the crosslinks of the network, in order to explain the experimental NMR line splitting. The temperature dependence of NMR line splitting is studied and it is shown that the dependency is in the order of $1/\sqrt{T}$. It is also shown that the Edward's screening length is independent of precursor chain length and crosslink density.

The next attempt is to explain the asymmetric NMR spectra observed from deformed carbon black filled poly(butadiene) networks. The effect of the susceptibility of the carbon black filler on the local field of polymer chains that are in the vicinity of these particles is considered. It is proposed for the interpretation that the magnetic field near carbon black particles is different to the rest of the sample. Therefore, the polymer chains near to the filler particles experience a different resonance frequency. This change in frequency causes a shift of their NMR spectrum in the Fourier transformed signal relatively to the unbound segments. In order to quantify this shift we employed our theoretical expression, which will be constructed at the beginning of the study, to model the NMR lineshape and splitting. Then the expected shift in frequency is calculated by using susceptibility data of carbon black and shows that this compares favorably with the results obtained from our fitting procedure. As well as the susceptibility of the carbon black filler we also consider that the applied macroscopic deformation does not affect the chains closely attached to filler particles to the same degree as it does the remaining chains. Also it is shown experimental evidence for the existence of the shifted spectrum of the carbon black closely associated segment.

The sine correlation function (introduced by Callaghan et al.)[73] and the NMR relaxation function (introduced by Simon et al.)[20] were also employed to study the NMR response of the poly(butadiene) networks and linear chains. The residual quadrupolar interaction determined by all the above mentioned procedures was compared. It is shown that the results from sine correlation function and conventional NMR relaxation show the same tendency though they differ in the numbers.

ZUSAMMENFASSUNG

Eine wichtige Fragestellung auf dem Gebiet der Polymere besteht in der Untersuchung von Orientierung und Dynamik polymerer Ketten, da diese wesentlich die anwendungstechnischen Eigenschaften vieler Polymerprodukte wie Plaste, Gummi, Beschichtungen, Fasern und Farbanstriche beeinflusst. Um die mechanischen Eigenschaften solcher Polymerprodukte, wie z.B. Autoreifen, zu verbessern, wurden verschiedenen Typen von Füllstoffmaterialien mit dem Polymer zusammengemischt. Obwohl Polymere bereits vielfach untersucht wurden, existieren noch immer offenen Fragen hinsichtlich der Bestimmung und dem Verständnis der Orientierung von Polymerketten sowie dem Einfluss von Füllstoffen auf die Polymerkette. Das Hauptziel dieser Arbeit besteht in der Bearbeitung dieser Fragestellungen nittels der Magnetischen Kernresonanz (NMR). Aufgrund ihres Potentiales an deuterierten Polymerketten wurde im Rahmen dieser Arbeit weitgehend die Deuteronen-NMR zur Untersuchung verwendet, da diese die Möglichkeit zur diskreten Untersuchung von einzelnen Ketten bzw. Segmenten eröffnet.

Für nichtdeformierte Elastomere wird im Deuteriumspektrum eine einzelne Linie beobachtet[26]. Bei uniaxialer Deformation ergibt sich im Spektrum eine wohldefinierte Dublettstruktur, die einer Oszillation im freien Induktionsabfall (FID) entspricht.[27]. Ein Gauß'sches Phantomnetzwerk ohne Wechselwirkung zeigt theoretisch keine Aufspaltung bei Deformation[28]. Dieses Ergebnis zeigt daher, daß zur Beschreibung der Kettenreorientierung in einem gedehnten Elastomer Segmentwechselwirkungen in Betracht gezogen werden müssen[29]. In gedehnten Elastomeren existiert ein höherer Anisotropiegrad als der, der nur durch die Vernetzungspunkte eingebracht wird.

Zur Beschreibung der im freiem Induktionsabfall gedehnter deuterierter Netzwerke beobachteten Oszillationen wurden verschiedene Erklärungen in Betracht gezogen, unter ihnen: nematische Wechselwirkungen[30], ausgeschlossenes Volumen[31] und anisotrope Knotenfluktuationen[32].

In dieser Arbeit wird, ohne ein bestimmtes Modell für die Kettenwechselwirkung anzunehmen, gezeigt, daß diese Oszillationen durch ein aufgrund der vielen Segmentwechselwirkungen anisotropes "mean field" hervorgerufen werden. Weiterhin spiegelt die Einhüllende der Oszillationen die Verteilung der Netzwerkvektoren wider, welche von den Verbindungsvektoren aufeinanderfolgender Netzknoten gebildet werden. Ein allgemeines analytisches Ergebnis, welches sowohl den Einfluß des anisotropen „mean" Feldes als auch der Netzwerkbehinderungen einschließt, wird abgeleitet.

An einer Reihe von deformierten Netzwerken wird gezeigt, daß für geringe Deformationen die Annahme einer Gaußverteilung der Netzwerkvektoren und deren affines Deformationsverhalten eine adäquate Beschreibung des NMR-Signals liefern. Der NMR-Wechselwirkungsterm, d.h. die statische Quadrupolkopplungskonstante, wird in seiner Stärke effektiv durch schnelle lokale Reorientierungen reduziert, welche sowohl von den Behinderungen der Monomere zwischen zwei Knoten als auch von den Wechselwirkungen der Segmente mit ihrer Umgebung beeinflußt werden. In einem

Netzwerk kann das Polymersegment mit vielen Nachbarn wechselwirken. Diese vielfachen Wechselwirkungen können durch ein effektives „mean"-Feld beschrieben werden[33,34] . Die NMR ist in der Lage, sowohl die mittlere Orientierung zwischen den Netzknoten als auch das „mean"-Feld separat zu beobachten, wobei die beiden Beiträge zur gesamten mittleren Orientierung $P_2(\cos\theta)$ getrennt werden können.

Ein theoretischer Zugang von Brereton und Ries beschreibt den als Aufspaltung beobachtbaren höheren Anisotropiegrad in Elastomeren als „excluded volume"-Wechselwirkung. Unter Deformation erzeugt die Verteilung der Monomereinheiten infolge der „excluded volume"-Wechselwirkung ein anisotropes „mean"-Feld. Alle Ketten innerhalb der Elastomermatrix erfahren dieses „mean"-Feld, welches zu einer induzierten Anordnung entlang der Zugrichtung führt. Die Aufgrund dieser Wechselwirkung resultierende Aufspaltung hängt von der Stärke der „excluded volume" Wechselwirkung.

Diese Arbeit baut auf einer früheren NMR-Arbeit zur Untersuchung von linearen Polybutadienschmelzen auf[39]. Darin wurde mittels transversaler Deuteriumrelaxation die Größe des statistischen Segmentes und die Stärke der entsprechenden reskalierten Quadrupolkopplungskonstante ν_0 bestimmt. Schnelle interne Konformationsänderungen innerhalb eines einzelnen statistischen Segmentes reduzieren die Stärke der statischen Quadrupolkopplungskonstante und liefern einen reskalierten Wert. Diese zwei Parameter wurden an gut charakterisierten monodispersen linearen Ketten bestimmt und hier zur Analyse der Spektren gedehnter deuterierter Netzwerke verwendet.

Die NMR-Linienaufspaltung hängt sowohl von der Netzwerkkonzentration als auch vom Flory-Wechselwirkungsparameter χ ab. Es wird gezeigt, daß zur Beschreibung der experimentell beobachteten NMR-Linienaufspaltung die Berücksichtigung eines χ-Parameters nötig ist, verursacht nicht nur durch chemisch unterschiedlichen Strukturen sondern auch durch Knoten im Netzwerk. Die Temperaturabhängigkeit der Linienaufspaltung wurde untersucht und es konnte gezeigt werden, daß diese eine $1/\sqrt{T}$ Abhängigkeit aufweist. Weiterhin wurde gezeigt, daß die Edwards „screening"-Länge unabhängig von der Ausgangskettenlänge und der Netzwerkdichte ist.

Der nächste Punkt besteht in der Erklärung der unsymmetrischen NMR-Spektren, wie sie an rußgefüllten Polybutadiennetzwerken beobachtet wurden. Der Einfluß der Suszeptibilität des Rußes auf das lokale Feld der Polymerketten, die sich in der Nähe der Füllstoffteilchen befinden, wird betrachtet. Es wird zur Interpretation vorgeschlagen, daß das Magnetfeld in der Nähe der Rußpartikel verschieden von dem in der restlichen Probe ist. Daher erfahren die Polymerketten in der Nähe der Rußpartikel eine andere Resonanzfrequenz. Dieser Frequenzunterschied führt zu einer Verschiebung des NMR-Teilspektrums im fouriertransformierten Signal relativ zu dem der ungebundenen Segmente. Zur Quantifizierung dieser Verschiebung wurde der eingangs vorgestellte theoretische Ausdruck zur Modellierung von Linienform und Aufspaltung verwendet. Danach wurde die zu erwartende Frequenzverschiebung bei Kenntnis der Suszeptibilität des verwendeten Rußes berechnet. Es konnte gezeigt werden, daß dieses Ergebnis hervorragend mit dem Resultat der Fitprozedur übereinstimmt. Neben der Suszeptibilität

der Rußfüllstoffes wurde ebenfalls beobachtet, daß die aufgebrachte makroskopische Deformation diejenigen Ketten, welche eng an die Füllstoffteilchen gebunden sind, nicht in demselben Maße beeinflußt wie die restliche Polymermatrix. Weiterhin wird ein experimenteller Beweis für die Existenz des verschobenen Spektrums gegeben, hervorgerufen durch Segmente, die eng an den Ruß gebunden sind.

Die „Sinus-Korrelationsfunktion" (eingeführt durch Callaghan et al.)[73] und die NMR Relaxationsfunktion (eingeführt von Simon et al.)[20] wurden ebenfalls zur Untersuchung des NMR-Signals von Polybutadiennetzwerken und linearen Polybutadienketten verwendet. Die nichtausgemittelte Restquadrupolwechselwirkung wurde mit allen oben erwähnten Methoden bestimmt und miteinander verglichen. Es konnte gezeigt werden, daß die Ergebnisse aus der"Sinus-Korrelationsfunktion" und den konventionalle Relaxationsuntersuchungen die gleiche Tendenz zeigen, allerdings in ihren Absolutwerten variieren.

CHAPTER 1

1.1 Introduction

1.1.1 Motivation

Investigation of orientation and dynamics of polymeric chains is one of the main concerns in the field of polymers since it fully influences to properties of polymer products, such as plastics, rubber, adhesives, fibers and paints. To enhance mechanical properties of some polymer products, e.g. car tyres, different types of filler materials are mixed together with polymer. Also crosslinking of technical elastomers such as poly(butadiene) is of crucial importance for the mechanical properties of rubber products. Therefore, these materials, either filled or unfilled, have been the subjects of a large numbers of investigations.

Although elastomers are vastly studied, there still exist open questions such as to understand and determine the orientation and dynamics of polymer network chains under deformation, in terms of basic polymer physics. Also, the effect of microscopic parameters, e.g. Edward's screening length, on the orientation of network chains and exact means of investigating these parameters are still not well revealed. In addition, despite of numerous investigations of filled elastomers by different physical and mechanical methods, the molecular origin of the reinforcement effect is still under discussion. The key problems which should be solved in order to reveal the molecular mechanism for improvement of the mechanical properties are the following: chain unit behaviour at the polymer-filler interface during deformation and chain orientation in deformed networks as a result of the complex network structure in the presence of filler.

Through measurements of spin relaxation times, Nuclear Magnetic Resonance (NMR) has been a profoundly useful technique for providing insights into segmental dynamics in polymers. The dipole-dipole interactions between a pair of protons and the quadrupolar interaction along the C-D bond are inherently the most sensitive ways to draw out dynamical information from NMR.

This work is to study the above mentioned questions by means of nuclear magnetic resonance. Deuterium NMR is mainly used throughout this study since its capability of labeling polymer chains and hence giving opportunity to study the chains or segments discretely. This chapter is devoted to describe the basic theory of Transverse NMR Relaxation. In Chapter 2, materials and methods are discussed. Chapter 3 is devoted to construct a frame work in order to understand the deuterium NMR line splitting observed from deformed elastomers, by means of basic polymer physics. An analytic result was derived that takes into account two contributions to the total orientation of the constituent polymer chains. It is shown that the free induction decay readily separates the effect of chain interactions with their environment from that of the network constraint, i.e. the presence of crosslinks within the rubber matrix, on the polymer segmental anisotropy. The analytic result for the NMR response of a strained network was compared to experimental data from a range of deformed poly(butadiene) rubbers.

The dependence of deuterium NMR line splitting of deformed poly(butadiene) on temperature, network chain concentration and Flory interaction parameter χ is discussed in Chapter 4. Carbon black filled poly(butadiene) networks were studied in order to reveal the effect of filler on the polymer network (Chapter 5). In Chapter 6 and Chapter 7, two different NMR methods, which are employed to study the molecular orientation and dynamics of polymer networks, are discussed and the results from these methods are compared with the results obtained in Chapter 3.

1.1.2 The Transverse NMR Relaxation

The relaxation of induced nuclear magnetic polarisation in a sample is described by two processes: longitudinal spin-lattice relaxation, and transverse spin-spin relaxation. This work is concerned with the latter and considers the information that it can reveal about polymeric structure and dynamics.

Basics of both the theoretical and experimental aspects of the transverse relaxation are presented in this chapter. This introduction is developed for proton NMR, but the analysis holds equally for deuterium work, as will be mentioned later in this chapter.

A proton possesses a nonzero spin and hence a magnetic moment. An applied magnetic field causes the spin to precess with an angular frequency ω_0 about the z-axis, defined as the field direction. This is termed the Larmor frequency, with its magnitude is given by[1]

$$\omega_0 = \gamma B_0 \quad , \tag{1.1}$$

where γ is the gyromagnetic ratio for a proton (2.6752×10^7 rad T^{-1} s^{-1}) and B_0 is the magnitude of the field. In a system of protons experiencing the same static field, all the spins would precess at this frequency. They are randomly distributed in phase about the field direction. Protons are spin ½ nuclei and either align themselves parallel or anti-parallel to the applied field. To align against the magnetic field direction requires a slightly higher energy level. Through the Boltzmann factor this produces a small excess of up spins, i.e. pointing in the same direction as the field. The magnetic moments of the protons can then be mathematically paired, up with down, leaving a slight resultant magnetisation in the positive z-direction, see Figure 1.1. This is known as the bulk or macroscopic magnetisation **M**, and defined as

$$M = \sum_{protons} \underline{\mu} \quad , \tag{1.2}$$

where $\underline{\mu}$ is the magnetic moment vector of a proton. It is through this slight asymmetry in the distribution of spins that NMR is possible. All NMR experiments are concerned with the behaviour of this macroscopic property **M**.
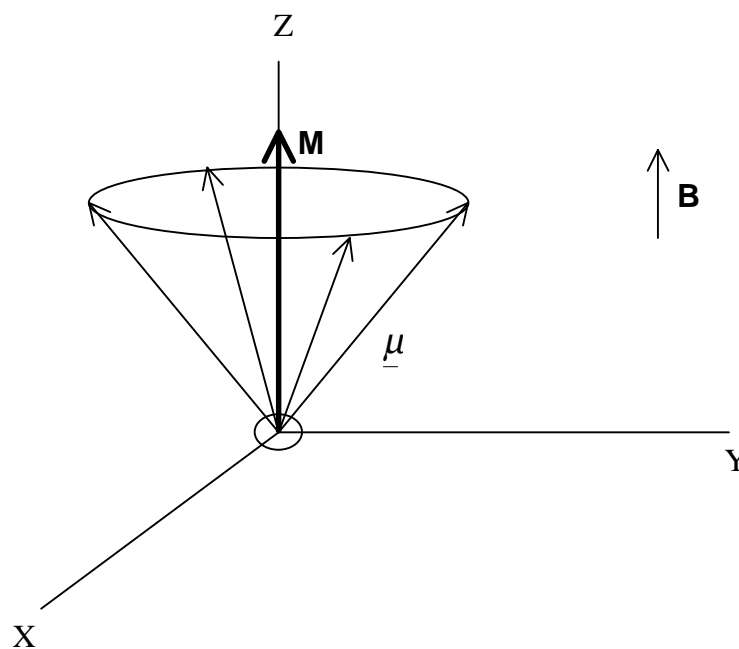
Figure 1.1 Macroscopic Magnetization for a system of protons

A pulse of high frequency radiation at the Lamore frequency causes an equalisation of the spin distribution in such a way that the falling population receive phase coherence in the x-y plane. Essentially this can be viewed as rotation of the vector **M** about the x-axis, see Figure 1.2.
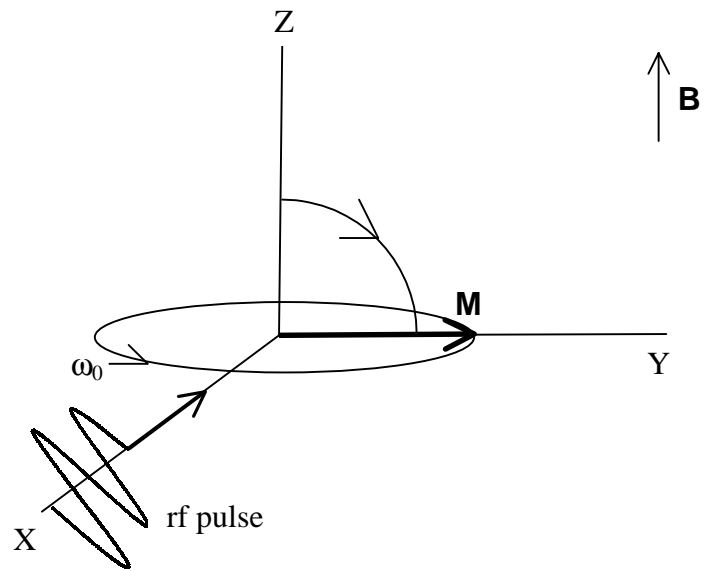
Figure 1.2 Rotation of **M** by a radio frequency (rf) pulse
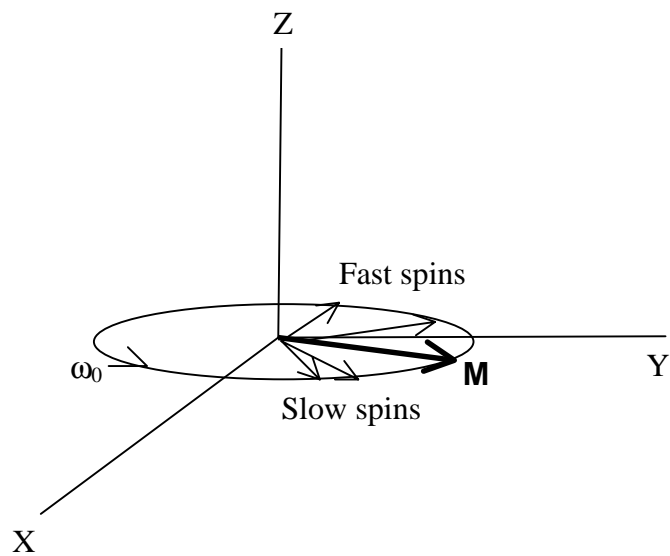
Figure 1.3 The dephasing of the bulk magnetisation **M**

The effect of dephasing is to reduce the magnitude of the bulk magnetisation. This is illustrated in Figure 1.4a.
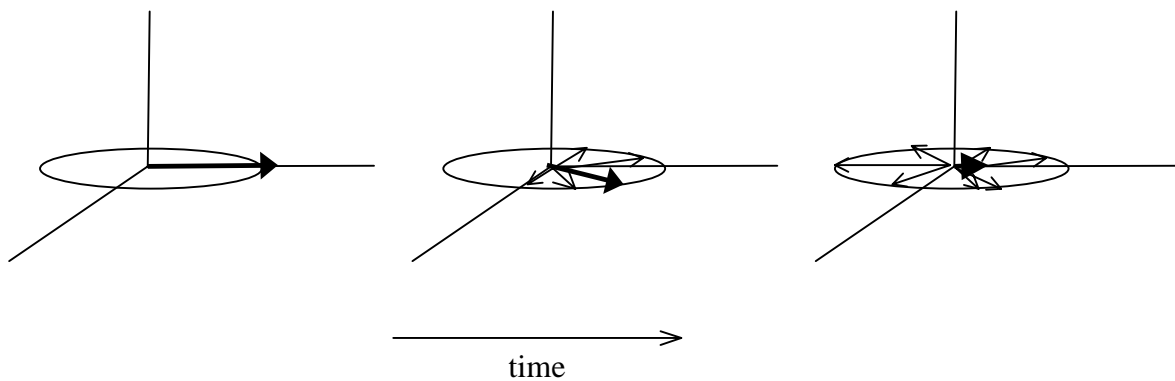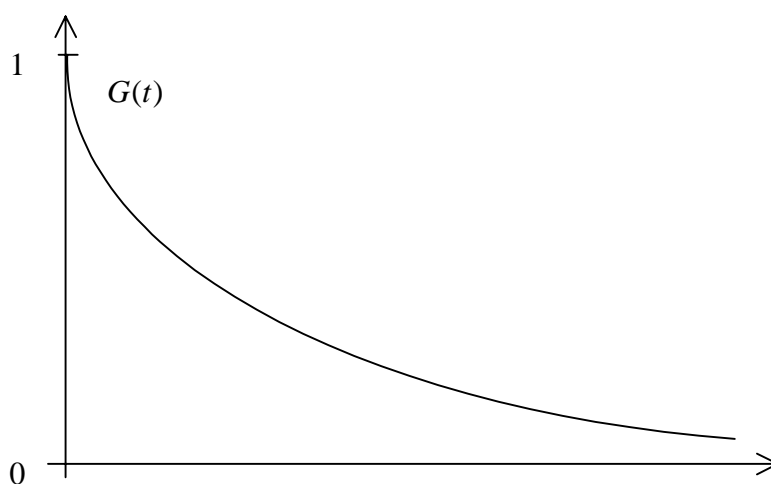
Figure 1.4 a) Decay of the transverse magnetisation **M** as the precessing spins fan out as a result of magnetic field inhomogeneities b) the corresponding decay $G(t)$.

The observable quantity M consists of precessing spins which rotate itself about the magnetic field at the Larmor frequency. If now the induvidual protons experienced slightly different magnetic fields, then the spins comprising M would precess at frequencies perturbed from that of ω_0. Those experiencing a stronger local magnetic field than B_0 will precess faster than the bulk magnetisation, as illustrated in Figure 1.3.

6

It is the quantity **M** as a function of time that is experimentally recorded as the free induction decay (fid) $G(t)$ (see Figure 1.4b), which can be defined as

$$G(t) = M(t)/M(0) \quad .$$ **(1.3)**

1.1.3 The Transverse Relaxation Function

The simplest theoretical model to study the transverse NMR relaxation in polymer molecules consists of two spin ½ nuclei (a proton pair) a vector distance **d** apart, fixed to a single bond in a chain of identical bonds. For a single spin in a magnetic field **B** along z direction, the transverse components (m_x, m_y) of the magnetisation precess about the direction of **B** with the Larmor frequency ω_0. The presence of the other spin contributes a dipolar field at the site of the first spin and leads to an additional interaction energy of

$$\frac{3\gamma^2\hbar}{4d^3}\left[3\cos^2 \upsilon(t) - 1\right] \quad ,$$ **(1.4)**

where $\upsilon(t)$ is the angle that the vector **d** makes with the applied magnetic field and γ is the gyromagnetic ratio. The dipolar interaction causes the dephasing of the transverse components and the subsequent relaxation of the magnetisation is described[2] by

$$G(t) = \left\langle \cos\frac{3\gamma^2\hbar}{4d^3}\int_0^t (3\cos^2 \upsilon(t') - 1)dt' \right\rangle \quad ,$$ **(1.5)**

The averaging in equation (**1.5**) is taken over all the dynamically accessible configurations of the chain available in the time interval 0 to t. It is assumed that the

proton pair is rigidly attached to the main chain so that the dynamical behaviour of the polymer chain is monitored through the integrated time dependence of the angle $\upsilon(t)$.
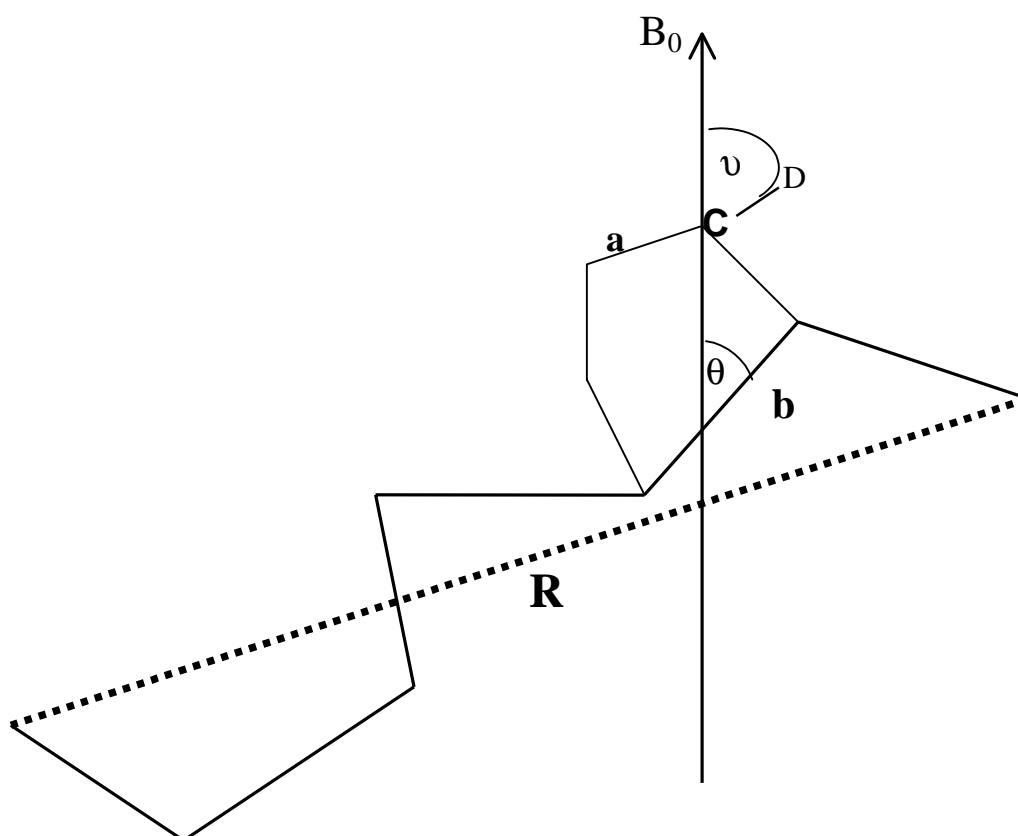
Figure 1.5 A schematic representation of the relation between the atomic bond vectors $\{d_s\}$ and the submolecule bond vector **b**. The atomic bond carrying NMR active spin ½ nuclei and makes an angle $\upsilon(t)$ to the applied magnetic field B. The configurations of the atomic bonds $\mathbf{d}_s$ are averaged out for a given **b** vector. The complete polymer chain is considered as a sequence of {**b**} bond vectors. **a** represents a monomer. In the case of deuterium (spin 1 nuclei) $\upsilon(t)$ is the angle the C–D bond makes with the applied magnetic field B.

Clearly the complexity of the local connectivity of an actual polymer chain in terms of bond angles and steric hindrances makes an analytic calculation of the relaxation function $G(t)$ at this level of molecular details difficult. However, the notion of scale invariance[3] enables to simplify the large scale connectivity of polymer chains. This

makes many of the details at the molecular level irrelevant to the large scale and long time behaviour of the polymer chain. Cohen-Addad successfully pioneered this approach to the NMR properties of polymers[4-8]. A short sequence of s=1,2,..N_a atomic bond vectors $\mathbf{d}_s$ containing the NMR active bond is considered. A semilocal description is provided by the end to end vector $\mathbf{b}$:

$$b = \sum_{s=1}^{N_a} d_s \tag{1.6}$$

and the dipolar interaction energy (**1.4**) is averaged over all configurations of the $\{\mathbf{d}_s\}$ subject to the constraint that the vector $\mathbf{b}$ is held constant. The leading term, δ_b, of the rescaled interaction associated with this semilocal submolecule bond vector $\mathbf{b}$ is found to have essentially the same form as the original dipolar interaction[2,3], i.e.,

$$\delta_b = \delta'\{3\cos^2\theta(t') - 1\} \quad, \tag{1.7}$$

where

$$\delta'(t') = \frac{3b^2(t')}{N_a d^2}\frac{\gamma^2\hbar}{4d^3 N_a} \quad .$$

$\theta(t')$ is now the angle between $b(t')$ and the magnetic field B. The situation is schematically shown in Figure 1.5.

Form (**1.7**) does not bring out the full significance of the rescaling operation. To see this let (x,y,z) be the coordinates of the submolecule vector $\mathbf{b}$, with $b^2 = x^2 + y^2 + z^2$ then equation (**1.7**) can be written as[2]

$$\delta_b = \frac{3\Delta}{2b^2}\{2z^2 - x^2 - y^2\} \quad, \tag{1.8}$$

9

where

$$\Delta = \frac{\gamma^2 \hbar}{2d^3 N_a} \quad \text{and} \quad b^2 = N_a d^2 .$$

Δ^{-1} determines the NMR time scale for the experiment and b^2 is the average length (squared) of the submolecule.

Now whereas the original dynamics of the chain were effective only through the angular variable $\theta(t)$, in the rescaled form they appear in the coordinate variables $x(t), y(t), z(t)$ of the semilocal bond vector $\mathbf{b}(t)$. The essential simplification occurs because the semilocal variables $x(t), y(t), z(t)$ can adequately be described by a Gaussian random type process, whereas those for angular variables $\theta(t)$ involve detailed molecular conformational changes. It is this fact that makes an analytic solution of this problem possible. The transverse relaxation function can be written as

$$G(\Delta, t) = \left\langle \cos\left(\frac{3\Delta}{2b^2}\right) \int_0^t \left\{2z^2(t') - x^2(t') - y^2(t')\right\} dt' \right\rangle , \tag{1.9}$$

where the averaging is taken over all dynamical configurations of the submolecule bond vector $\mathbf{b}(t)$.

The starting point of this work essentially the equation (**1.9**), with all that follows being methods of solving this NMR problem for various systems and environments. The physics of the polymer melt, cross links, entanglements and other chain interactions, is introduced into the transverse decay through the averaging denoted by $\langle ... \rangle$ in (**1.9**). The type of reorientation undergone by the probe molecule is indicative of its environment and can be revealed through the shape of the transverse relaxation curve.

1.1.4 Deuterium NMR

Unlike protons deuterium nuclei are spin 1 particles. It is found that nuclei with spin quantum numbers greater than 1/2 possess an asymmetric nuclear charge distribution, known as a quadrupole moment[9]. In a polymer sample a deuterium nucleus is covalently bonded to a carbon atom. This deuterium nucleus will interact with the electric field gradient (EFG) that is oriented along the C-D bond axis. A quadrupole moment in the presence of a local EFG experiences a torque. As with the dipolar interaction this perturbs the resonant Larmor frequency of the nucleus. The magnitude of this interaction depends on the relative orientation of the C-D bond through[10]

$$\Delta\omega(t) = \frac{3\pi}{4} v_q (3\cos^2 \upsilon(t) - 1) \qquad , \tag{1.10}$$

where v_q denotes the static quadrupolar coupling constant (~200 kHz) and $\upsilon(t)$ is the angle the C-D bond makes with the applied magnetic field at a time t. This is identical in form to (1.4) and so the mathematical approach to deuterium NMR follows that set out by the proton spin pair analysis above.

1.1.5 NMR on Polymers

Through measurements of spin relaxation times, Nuclear Magnetic Resonance (NMR) has been a profoundly useful technique for providing insights into segmental dynamics in dilute polymer solutions. Recent advances in solid state NMR give access to a wide range of dynamical processes in solid polymers. The dipole-dipole interactions between a pair of protons and the quadrupolar interaction along the C-D bond are inherently the most sensitive ways to draw out dynamical information from NMR.

There exists wide range of time scales for dynamical processes in the condensed fluid phases of entangled polymer melts, concentrated solutions and amorphous networks above the glass transition temperature. These include fast, localised processes like intramonomer librations ($\sim 10^{-12}$s time scale) and correlated conformer isomerisations ($\leq 10^{-9}$s), which are comparable to motions in liquids comprised of flexible, low molecular mass molecules. In contrast with such liquids the linking together of monomers imposes constrains on molecular motions that give rise to slow dynamical processes unique to polymer chains. For example, the so-called Rouse modes correspond to subchain reorientations that exhibits dynamics on the microsecond time scale. And cooperative multichain processes that involve whole chain reconfigurational dynamics (e.g. reptative diffusion) can be operative on a tens of seconds time scale for high molar mass polymers. Consequently, the way in which microscopic properties appear to be averaged will depend on the time scale of the experimental window associated with the particular technique employed.

Local order parameter associated with nuclear spin interactions of rank 2 tensorial character is among the many important average molecular properties that can be measured by NMR. Especially these include the proton-proton dipolar interaction of magnitude $\nu_H = (3/2)\gamma^2 \hbar r^{-3}$, associated with a pair of protons affixed at a separation r within a monomer, and the quadrupolar interaction of magnitude $\nu_D = (3/4)e^2 Qq/\hbar$ experienced by deuterons in the presence of a magnetic field gradient q associated with the local molecular orbital. These interactions, which are bilinear in the spin operators, transform under rotation as $P_2(\cos\vartheta) = (1/2)\left[3\cos^2\vartheta(t) - 1\right]$, where $\vartheta(t)$ is the angle the polarising magnetic field makes with the internuclear vector in the case of pair of protons, or the electric field gradient symmetry axis in the case of deuterons. The corresponding local order parameters involve the temporal average over relevant dynamical processes. In the case of isotropic polymer melts or solutions $\overline{P_2(\cos\vartheta)} = 0$ on a sufficient long time scale. However, on the operative NMR time scale, $\left[\nu_{H,D}\right]^{-1} \approx 10^{-6}$ s, the whole chain reconfigurational processes are too slow, and the rank 2 spin interactions are incompletely averaged. J.P. Cohen Addad originally suggested that one might

investigate aspects of the topological restrictions in networks and entangled phases (slow dynamical process) by studying residual nuclear spin interactions - dipolar and quadrupolar interactions that have been pre-averaged over the fast daynamical processes[11,12]. Subsequently it was shown that, in mechanically ordered fluid polymers, deformed networks, and sheared melts $\overline{P_2(\cos\vartheta)} \neq 0$, irrespective of the time scale. In particular, the deuterium NMR spectroscopic signature of mechanically induced anisotropy, the quadrupolar splitting $2\nu_D \overline{P_2(\cos\vartheta)}$, has been extensively used[13-17]. In principal, knowledge about the strength of the dipolar and quadrupolar interactions and the orientation of their relevant principal axes can reveal important information about local order and dynamics. In practice, such knowledge depends on the effectiveness with which the interaction can be distinguished from other terms in the nuclear spin Hamiltonian, especially from those associated with Zeeman-like magnetic interactions. In the case of ^{2}H-NMR, this distinguishability is relatively straightforward and has led to the wide spread use of deuterium labelling experiments.

CHAPTER 2

2.1 Materials and Methods

2.1.1 Materials

Polybutadiene (PB) is used as the testing material throughout this study. Cis and anionic (cis+trans) polymer microstructures were obtained by employing two different polymerisation procedures.

Ziegler-Natta polymerization[18] procedure resulted in cis microstructure. The partially deuterated poly(butadiene) was polymerised on the basis of $(1,1,4,4-D_4)$-butadiene (Promochem 98%, stabilized by Hydrochinon) by a conventional (commercially used) Ziegler-Natta catalyst. The result is a methylene labeled high cis-1,4 Poly(butadiene) (98% cis microstructure). Toluene (Aldrich, 99.8%) was used as solvent. 2,4-Di-tert.-butyl-p-cresol was used for ageing protection. The following is the composition of the catalyst:

$$Ni(OOC - \underset{\underset{C_2H_5}{|}}{CH} - C_4H_9)_2 + 9\ BF_3 {}^*Et_2O + 10\ AlEt_3 + 3\ CH_2 = CH - CH = CH_2$$
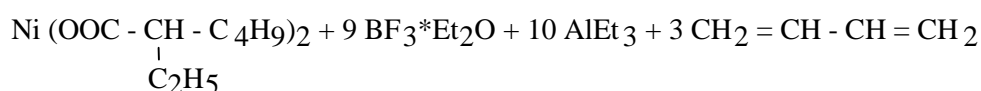
The microstructure was determined by ^{13}C-NMR and showed a 98% cis-microstructure. Molecular weights were performed by gel permeation chromatography (GPC) (see Table 3.1). This polymer was mixed in a ratio 1:9 with the nearly corresponding commercial non-deuterated poly(butadiene) BUNA cis 132 (for the case of cis polymers $M_n(H) = 120000$ g/mol, $M_w(H) = 450000$ g/mol, and for the case of anionic polymers see the Table 3.1). Dicumyl Peroxide (DCP) was used as the crosslinking agent for all networks prepared. The samples were vulcanised in a vulcameter press at 145°C and 100 bar for 1h. Latter vulcanisation conditions were valid for all the samples describe hereafter. The resulting mean molar mass between two crosslinks, Mc, determined from mechanical stress-strain measurements[19], swelling measurements[18] and NMR relaxation[20] for individual samples, and the average values are shown in Table 3.1. BUNA cis 132

$(M_n(H) = 120000$ g/mol, $M_w(H) = 450000$ g/mol, $U = 3.75)$ is used to prepare non deuterated samples.

Sample	Deuterated free chains				Protonated free chains (BUNA cis 132)				Filler N220 (phr)	M_c (g/mol)
	M_n (g/mol)	M_w g/mol	U	%	M_n g/mol	M_w g/mol	U	%		
CD2A	25000	120000	4.80	10	120000	450000	3.75	90	-	8000
CD2B	25000	120000	4.80	10	120000	450000	3.75	90	-	6500
CSM1	-	-	-	-	120000	450000	3.75	100	-	10000
CSM2	-	-	-	-	120000	450000	3.75	100	-	8000
CD1	190000	700000	3.68	10	120000	450000	3.75	90	-	8000
CD2F25	25000	120000	4.80	10	120000	450000	3.75	90	25.0	6500
					(BAYER 150000)					
AD1	152000	162000	1.06	10	125000	129000	1.03	90	-	3300
AD2	135000	140000	1.04	10	125000	129000	1.03	90	-	3600
AD3	70000	72000	1.03	10	61000	64000	1.05	90	-	6800
AD4	50000	52000	1.04	10	61000	64000	1.05	90	-	5400

Table 2.1 Description of all Polybutadiene samples used in the experiments. $U=M_w/M_n$. The used polymer fractions, in order to prepare test samples, are described in the columns titled %. All the samples starting from the label letter **C** correspond to cis-1,4 Poly(butadiene), PB, while that of **A** corresponds to anionic polymer. It is important to note that the four anionic polymer samples have made by using different precursor chain lengths of the deuterated polymer. **F** in the sample labels indicate that the samples were filled with carbon black and **D** in the labels indicate that the samples were made using also the deuterated polymer. M_c value is the average of the values determined from NMR relaxation, swelling and stress- strain measurements.

In order to prepare the filled samples, Carbon black N220 was used as the filler. The desired amounts of carbon black were incorporated by mixing the polymer, crosslinker and filler together in a mixer of rotating frequency of 60 min^{-1} for 10 minutes at a temperature of 50°C, and then the vulcanization procedure was applied.

The series of prepared cis-1,4 Polybutadiene samples can be summarised as follows with the help of Table 2.1:
CD2A and CD2B are unfilled, deuterated samples while CD2F25 is the only deuterated sample also with filler (25 phr). CSM1 and CSM2 are protonated (non deuterated),

unfilled samples. The labels CF0.2 – CF60 are corresponding to the protonated polymer networks with different amount of the filler. For all the anionic, CSM1, CSM2 and CD2B samples the mixing procedure was done in solution state. Toluene was used as the solvent and after mixing the polymer was dried in a vacuum oven. Vulcanisation procedure was applied after removing the solvent.

The anionic polymer samples were prepared by employing the procedure of anionic polymerisation[18]: (1,1,4,4-D$_4$)-butadiene (Promochem 98%, stabilised by Hydrochinon) was used as monomer. The reaction medium was Cyclohexan and as initiator for the polymerisation sec-Butyllithium (Merk, 1,3m in Cyclohexan) was used. To avoid breaking of the reactions, all the chemicals were dried and cleaned as the first step. Cyclohexan was distilled over CaH$_2$, cleaned by using BuLi and evacuated. Monomers were distilled by Mg(Bu)$_2$ (Aldrich, 2m in Heptan) and then stired at room temperature. The monomer was distilled off and condensed on to BuLi, after which is was stirred at – 70 °C during 10 hours. In order to determine activity of the initiator it was titrated with 0.1n Benzoic acid, before each polymerization step. After that necessary amount of Butylithium was calculated in order to get required molecular mass.   In the polymerisation step, the calculated amount of initiator was spurt in a vacuum vessel at first, and then the solvent and at the end the monomer were condensed. Reaction temperature was about 30-40°C. Finally, the resulting amorphous Poly(butadiene) was dried in vacuum. Vulcanisation procedure was the same as described above. The samples labelled as AD1, AD2,AD3 and AD4 were with the anionic microstructure. They were composed of 45% cis, 45% trans and 10% 1,2 vinyl microstructure.

The samples have been prepared by Sabine Hotof, a former member of the research group.

2.1.2   Methods

All NMR experiments were carried out on a Varian Unity 400 (later INOVA) wide-bore spectrometer (400 MHz proton frequency) operating at 61.3 MHz for deuterons. Spectra were obtained using a standard 90 rf pulse of approximate 7 µs.

The deuteron measurements under mechanical deformation were performed by a simple stretching device parallel and perpendicular to the static magnetic field B_0. The aim of the one-dimensional stretching of the samples was to induce an orientation of the network chains. The stretching ratio was determined from the distance between two marks on the sample, before and after stretching. Figure 2.1 shows the NMR probe used to perform the NMR experiments of the polymer samples under deformation perpendicular to the magnetic field. This probe was built with the help of Dr. Manfred Knögen. The important features of this probe for deforming the polymer networks is its simplicity, easy to build and accurate measurements of deformation.

Rubber sample **s** is driven through the radio frequency (**RF)** coil and then turn down to vertical direction from both sides over the freely rotatable rollers **b** and **b´**. Both ends of the sample are clamped tightly by the clamps **c** and **c´**(opposite to the c) respectively. These two clamps are fixed to the plate **e**. A threaded rod **f** goes freely through the plate g and again it goes through the female threads in the plate **e**.

The top end of the rod **f** is free to rotate and the bottom end of it is fixed to a lever **h**. Suppose the distance between two threads of rod **f** is x. When the lever **h** is turned clockwise one round, the plate **e** is moved vertically downward by an amount of x (and vise versa). Since **c** and **c´** are fixed to **e** , the sample **s** is extended from both sides by amounts of x. Therefore, one clockwise turn of the lever **h** corresponds to $2x$ macroscopic deformation of the sample. Since the distance x between two threads can be made in sub-millimeter scales, the above described probe can be used as one of the accurate tools of deforming the rubber samples in NMR experiments.
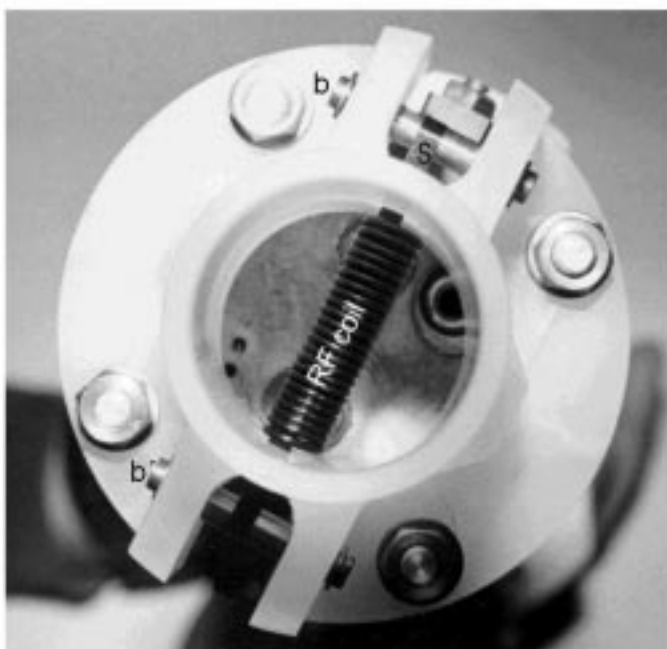
Standard Hahn-Echo pulse sequence was employed in the relaxation experiments. The pulse sequence used to generate the experimental data of Beta function will be described in the Chapter 6.
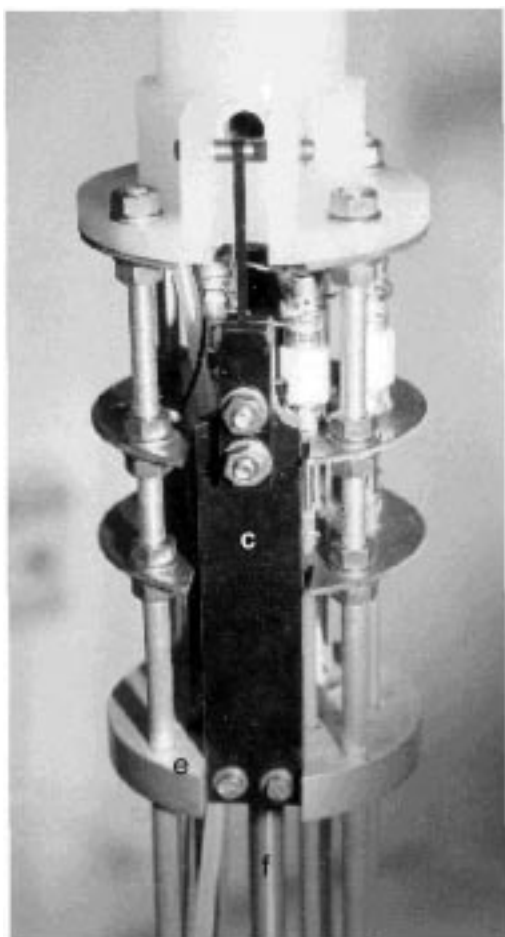
View from side
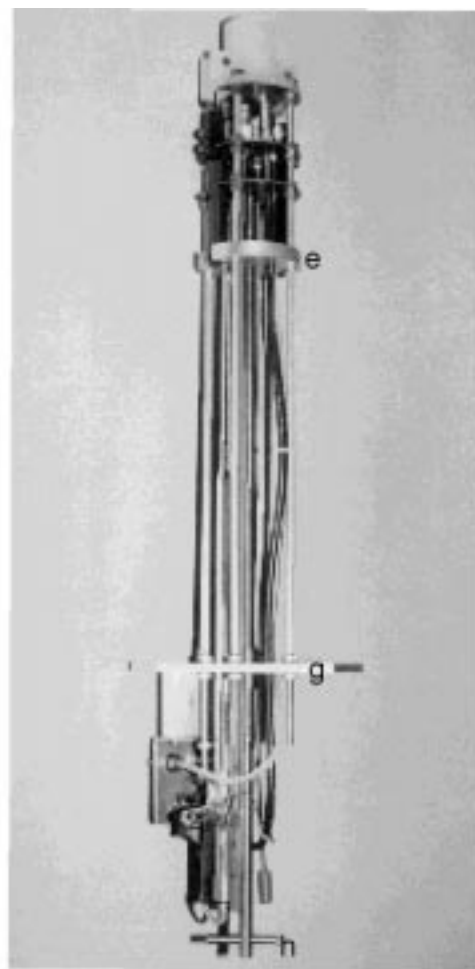
The complete probe

View from top

Figure 2.1 The probe used to perform NMR experiments on deformed (perpendicular to the external magnetic field) polymer networks.

CHAPTER 3

3.1 Contributions to the Total Orientation of Deformed Rubbers Arising from the Network Constraint and Chain Interactions as Measured by NMR

3.1.1 Introduction

Macroscopic strain applied to elastomeric networks induces orientation to the constituent polymer chains. Several experimental techniques, such as rheo-optical and deuterium nuclear magnetic resonance, have been devoted to the study of the anisotropy at a molecular level in strained elastomers[23-25]. The important feature considered in this work is the contribution to the total orientation coming from interchain interactions in the deformed rubber.

For an undeformed rubber a single resonance line in the deuterium NMR spectrum is observed[26]. Under uniaxial deformation the spectrum splits into a well-defined doublet structure corresponding to an oscillation in the free induction decay[27]. A non interacting phantom Gaussian network theoretically shows no splitting under deformation[28]. These results therefore indicate that to model the chain reorientation in a strained elastomer one must introduce segmental interactions[29]. In strained rubbers there is a higher degree of anisotropy than that merely induced by the crosslinks.

Several explanations have been put forward to account for the oscillations seen in the free induction decay from strained deuterated networks, these include: nematic interactions[30], excluded volume interactions[31], and anisotropic junction fluctuations[32]. In this chapter it will be shown, without the need to assume a particular model for the chain interactions, that the oscillations are indicative of an anisotropic mean field due to the many segmental interactions. Furthermore the decay envelope of the oscillations reveals the distribution of network vectors, each formed by connecting

together consecutive crosslinks. A general analytic result that includes the effect of anisotropic mean field and network constraint will then be derived.

It is shown, from analysing a range of deformed network sample signals, that for small deformations, the assumption of initially Gaussian distributed network vectors that then undergo affine deformation adequately describes the NMR response. The NMR interaction term, the static quadrupolar constant, is effectively reduced in magnitude by rapid local level reorientations subject to both the constraint from the monomers being attached between crosslinks and the interactions of the segments with their environment. In a network a polymer segment interacts with many neighbouring ones. These many interactions can be described by an effective mean field[33-34]. NMR is able to monitor the average orientation due to the crosslinks and this mean field separately, allowing the two contributions to the total average orientation $\overline{P_2(\cos\theta)}$ to be evaluated.

A theoretical interpretation by Brereton and Ries[31] attributes the higher degree of anisotropy implied by the splitting to excluded volume interactions within the rubber. Under deformation the distribution of monomeric units generate, through their excluded volume interactions, an anisotropic mean field. All chains within the rubber matrix experience this mean field that causes an induced alignment along the strain direction[35-38]. The resultant splitting due to this interaction is dependent on the size of the excluded volume interaction[31].

This work is based on an earlier NMR study that analysed a range of linear poly(butadiene) melts[39]. In that work the deuterium transverse relaxation was investigated to determine the size of a statistical segment and the magnitude of its corresponding rescaled quadrupolar coupling constant v_o. Rapid internal conformational changes within a single statistical segment reduce the magnitude of the static quadrupolar coupling constant, giving rise to a rescaled value. These two parameters found in the previous study of well-characterised monodisperse linear chains are required in analysing the spectra from strained deuterated networks.

3.1.2 Theory

3.1.2.1 Introduction

A scale invariant model consisting of a series of statistical units $\{\mathbf{b}_j\}$ is taken to represent the network chains. As introduced by Cohen-Addad[4-7,40] and further developed by Brereton[2,41] the quadrupolar interaction is rescaled by rapid local reorientations onto this coarse-grained representative chain.

The effect is to reduce the magnitude of the static quadrupole interaction strength and make the perturbations of the energy levels of the deuterium nuclei dependent on the instantaneous orientations of the statistical units. For a nucleus within a particular statistical segment $\mathbf{b}_j$ this orientation gives rise to a perturbation of the precessional Larmor frequency by $\Delta\omega(\mathbf{b}_j)$, which in reference (31) was written as

$$\Delta\omega(\mathbf{b}_j) = v_o \frac{2b_z^2 - b_y^2 - b_x^2}{b^2} \quad ,$$

where $\{b_x^2, b_y^2, b_z^2,\}$ are the Cartesian coordinates of the labelled NMR statistical segment and v_o is the rescaled interaction constant. In this work, as it is the aim to focus on the average orientation of the chain segments, it is more convenient to write this as

$$\Delta\omega(\mathbf{b}_j) = 2v_o P_2(\cos\theta) \quad ,$$

where θ is the angle the applied magnetic field makes with the statistical bond vector $\mathbf{b}_j$ and $P_2(\cdots)$ is the second order Legendre polynomial.

In the regime where the local level bond dynamics is fast compared to the time scale set by v_o^{-1} the relaxation of the transverse components of the magnetisation can be written as[42]

$$G(t,\lambda) = \exp\left(\frac{-t}{T_2}\right)\overline{\cos\left[2v_o\langle P_2(\cos\theta)\rangle t\right]} \quad . \tag{3.1}$$

The $\langle\cdots\rangle$ is an annealed average over all the available conformations subject to the network constraint imposed by the deformation λ through the crosslinks, whilst the $\overline{(\cdots)}$ indicates a quenched average over all crosslink points. The T_2 term corresponds to the intrinsic line width of the poly(butadiene) sample and is related to the fluctuating part of the NMR Hamiltonian[42]. At temperatures sufficiently above T_g in a network this contribution evolves much slower than the cosine term. In an earlier study on poly(butadiene) it was measured T_2 s from a range of linear uncrosslinked samples giving a measure of the intrinsic line width term[39]. The network samples decay on a time scale that is approximately 20 times shorter than linear chains of a corresponding molecular weight to that of the crosslink density. This reveals that this broadening can be neglected with very little loss in accuracy, i.e. we can write[31]

$$G(t,\lambda) = \overline{\cos\left[2v_o\langle P_2(\cos\theta)\rangle t\right]} \quad . \tag{3.2}$$

3.1.2.2 An Interacting Network

The important point in this work is that there are two principle factors that influence the averaging over all the available conformations of the NMR active bond. Firstly there is the constraint caused by the junction points. The end-to-end vector formed by two consecutive crosslinks determines a static residual average orientation of the labelled bond. Secondly there are the interactions of the chain segments in the rubber with their many neighbours. The average orientation of an NMR active segment can be written as $\langle P_2(\cos\theta)\rangle_{\mathbf{R},V}$, where the subscript $\mathbf{R},V$ indicates that both the constraints of the network vector $\mathbf{R}$ and the interactions V have been included.

The network constraint **R** and the interactions V will contribute to the average orientation of the chains. The orientation due to the network constraint in the absence of interactions is[43] $\sim N^{-1}$, where N is the number of statistical segments between crosslinks. The interchain interactions V collectively form a mean field, which in an undeformed state is isotropic[34] and therefore does not contribute to the orientation. However, in the deformed rubber, the mean field becomes anisotropic and makes a contribution. The effect of the mean field on a single chain is expressed as a deformation dependent screened potential[31] $V^*(\lambda)$. Only the anisotropic part contributes to the orientation and its effect, through the Boltzmann factor, can be treated as a perturbation, i.e.

$$\exp\left[\frac{V^*(\lambda)}{kT}\right] = 1 + \frac{V^*(\lambda)}{kT} + \ldots$$

In an earlier work it was shown that the effect of $V^*(\lambda)$ in the deformed state was also the same as[31] $\sim N^{-1}$, justifying the perturbative approach of present work. Hence to this order it can be written[11-13,44]

$$\langle P_2(\cos\theta)\rangle_{\mathbf{R},V} \approx \langle P_2(\cos\theta)\rangle_{\mathbf{R}} + \langle P_2(\cos\theta)\rangle_V \tag{3.3}$$

where $\langle\cdots\rangle_{\mathbf{R}}$ indicates an averaging over all conformations subject to the limiting imposed by the end to end vector, but without the interactions and $\langle\cdots\rangle_V$ is subject to these interactions, but conversely not to the network vector constraint. In this way the effect of the network constraint and the interchain interactions are additive[31].

Combining this expression (3.3) for the average orientation with the equation for the transverse relaxation signal (3.2) gives

$$G(t,\lambda) = \mathrm{Re}\left\{\overline{\exp\left[2i\nu_o\left(\langle P_2(\cos\theta)\rangle_{\mathbf{R}} + \langle P_2(\cos\theta)\rangle_V\right)\right]t}\right\} \tag{3.4}$$

It is possible to see the effect of including the extra term $\langle P_2(\cos\theta)\rangle_V$ on the transverse relaxation, without as yet going into the details of the mathematics. A segment of a chain in a network is interacting with many neighbouring chains. The total effect is found by summing over the interactions from these many chains, with this then naturally self averaging the interactions. These interactions can therefore be well described by an effective mean field[34]. Furthermore this mean field by its very nature is not unique to any specific network vector, but is common to all segments. The $\overline{(\cdots)}$ indicates an averaging over each network vector, but since $\langle P_2(\cos\theta)\rangle_V$ will be the same for each segment considered, it can come out from under the $\overline{(\cdots)}$. This means that the NMR response can be simplified to

$$G(t,\lambda) = \text{Re}\left\{ \exp\left[2i\nu_o\langle P_2(\cos\theta)\rangle_V\, t\right] \times \overline{\exp\left[2i\nu_o\langle P_2(\cos\theta)\rangle_{\mathbf{R}}\right]t} \right\} \quad . \qquad (3.5)$$

The resultant NMR signal **(3.5)** is seen to consist of a product of two terms. The first term corresponds to an oscillation, or a splitting, whose frequency depends on the mean field contribution to the average orientation. The second term determines the decay envelope, or lineshape, and is fully specified by the network constraint contribution to the average orientation.

3.1.2.3 Fourier Transformed Signal

The ability of NMR to separate the two contributions was first mentioned by Sotta et al[13]. What follows here is a new analytic result for the NMR Fourier transformed spectrum of equation **(3.5)**. This expression will then be compared to a range of experimental data, enabling NMR to be a probe of the mean field and cross-link density. The NMR spectrum in frequency space ν, $G(\nu,\lambda)$, can be derived from

$$G(v,\lambda) = \int e^{2\pi i vt} G(t,\lambda) dt \quad .\tag{3.6}$$

Before this calculation is made, a form is needed for the averaging over all network vectors, $\overline{(\cdots)}$, in (3.5) and a relationship between the network end-to-end vector and the average orientation of a subsequent segment. In this work it will be assumed that the initial Cartesian components of the network end-to-end vectors, $\{X_o, Y_o, Z_o\}$, are Gaussianly distributed and that these then undergo uniaxial affine deformation. This means that the averaging $\overline{(\cdots)}$ denotes an integration over a probability distribution, i.e.

$$\overline{(\cdots)} = \left(\frac{3}{2\pi Nb^2}\right)^{3/2} \int\limits_{-\infty}^{+\infty} \int\limits_{-\infty}^{+\infty} \int\limits_{-\infty}^{+\infty} (\cdots) \exp\left[\frac{-3\left(X_o^2 + Y_o^2 + Z_o^2\right)}{2Nb^2}\right] dX_o Y_o Z_o \quad .\tag{3.7}$$

Under an affine, uniaxial deformation λ it can be shown that the average orientation of a segment attached to an initial network constraint (X_o, Y_o, Z_o) is given by[31]

$$\left\langle P_2(\cos\theta)\right\rangle_{\mathbf{R}} = \frac{1}{2N}\left[\frac{2\lambda^2 Z_o^2 - X_o^2/\lambda - Y_o^2/\lambda}{Nb^2}\right] \quad ,\tag{3.8}$$

where N is the number of Gaussian statistical segments of average size b between the junction points. If this value is averaged over all the network vectors, using the above averaging equation, (3.7), this gives the mean orientation due solely to network constraint, $\overline{P_2(\cos\theta)}_{\mathbf{R}}$, as

$$\overline{P_2(\cos\theta)}_{\mathbf{R}} = \frac{1}{3N}\left(\lambda^2 - \frac{1}{\lambda}\right) \quad .\tag{3.9}$$

The NMR problem posed by equations (3.5) - (3.8) requires an integration over all possible network vectors. Each network vector orientation produces a particular frequency of oscillation in the NMR signal, or in Fourier space two Dirac delta

functions. The magnitude of this frequency depends on the total contribution from the network constraint and the mean field to the average orientation, recall equation **(3.4)**. The summation over all network chains, giving the resultant theoretical spectrum $G(v, \lambda)$ is derived in the Appendix. There it is shown that the NMR spectrum can be determined from

$$G(v, \lambda) = \left(\frac{3N\pi}{2v_o} \right) \left[2\lambda + \frac{1}{\lambda^2} \right]^{-1/2} \left[g_+ \left(|v| + \frac{\Delta v}{2}, \lambda \right) + g_- \left(|v| - \frac{\Delta v}{2}, \lambda \right) \right] , \quad \textbf{(3.10)}$$

where

$$\Delta v = 2 \frac{v_o}{\pi} \left\langle P_2(\cos\theta) \right\rangle_V \quad , \quad \textbf{(3.10a)}$$

with

$$g_+(v, \lambda) = \exp\left[-\frac{3N\pi\lambda}{v_o} v \right] \quad \textbf{(3.10b)}$$

and when $|v| \le \dfrac{\Delta v}{2}$

$$g_-(v, \lambda) = \exp\left[\frac{3N\pi\lambda}{v_o} v \right] \quad \textbf{(3.10c)}$$

or when $|v| > \dfrac{\Delta v}{2}$

$$g_-(v, \lambda) = \exp\left[\frac{3N\pi\lambda}{v_o} v \right] \left\{ 1 - erf\left[z(v) \sqrt{\frac{3}{2}\left(2\lambda + \frac{1}{\lambda^2} \right)} \right] \right\} \quad \textbf{(3.10d)}$$

with

$$z(v) = \sqrt{\frac{N\pi v}{v_o}} \quad . \quad \textbf{(3.10e)}$$

Parts **b** and **d** of equation (**3.10**) correct a minor numerical error in the result of (**3.8**) in reference 28, which has also been noted elsewhere[29]. However, (**3.10**) represents a substantial correction to the result (**5.2**) in reference 28, although both expressions give qualitatively similar results.

In the absence of a mean field contribution to the orientation $\Delta v = 0$ this result **(3.10)** agrees with the theoretical result for a non-interacting network. The calculation of the Fourier transformed phantom network signal can be found in the literature and has been the concern of a recent paper by Warner et al[29]. An important point to note is that the non-interacting network does not generate the oscillation that is seen in experimental data. By contrast the interacting network result above generates a doublet structure, where the splitting, i.e. the distance in frequency space between the peaks, is given by Δv. This means that the NMR free induction decay is a measure of the induced orientation produced by the mean field. It is also important to stress that the splitting consequently does not give the total orientation of the chain segments but merely the contribution from mean field. In this way NMR can decouple the resultant orientation due to the chain interactions from that of the network constraint. This is the main result of this chapter.

3.1.3 Results and Analysis

The NMR spectra for a range of deformations from a poly(butadiene) network have been recorded. The signal intensities have been normalised so as to have unit area under each spectrum, with these displayed in Figure 3.1.

The aim of the subsequent work is to quantify the two contributions to the average orientation of the polymer segments. To achieve this equation **(3.10)** will be employed to interpret the NMR frequency response of the deformed networks. This expression has three independent parameters; the rescaled interaction constant divided by the number of statistical segments between crosslinks v_o/N, the magnitude of splitting in frequency space Δv that depends on the mean field contribution to the anisotropy through **(3.10a)** and the deformation λ. A Mathematica program has been written to fit the theoretical spectrum **(3.10)** to the data, by minimising the root mean square difference between the theoretical lineshapes and the data recorded.
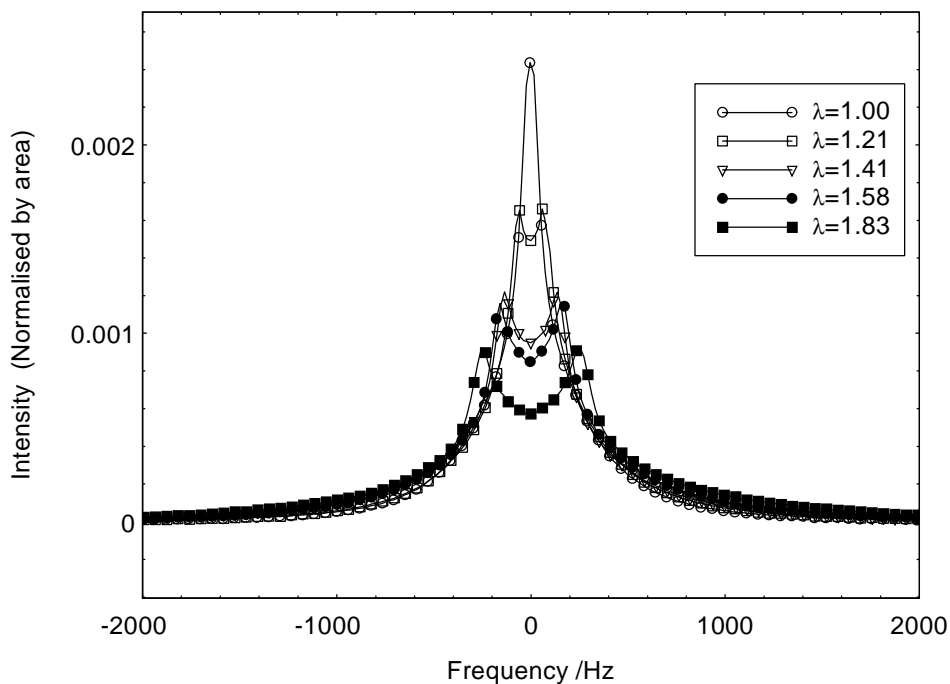
Figure 3.1 A range of NMR spectra from a strained poly(butadiene) network, where λ is the deformation ratio. The solid lines are to guide the eye.

There is a ~5% experimental error in determining λ, so the fitting procedure allows for small changes in the required theoretical deformation ratios. As the same network is examined at each λ, v_o/N must be the same for each theoretical spectrum, therefore this will be treated as a global fitting parameter. Essentially only $\langle P_2(\cos\theta)\rangle_V$ is allowed to vary between data sets.

In an earlier study[39] on poly(butadiene) linear melts it was found the molecular weight of a NMR statistical segment is $(260\pm30)\,\text{g/mol}$ and the corresponding rescaled interaction constant for the methylene deuterium is $v_o = 7730\,\text{Hz}$. From these values and the v_o/N required to fit the data it is simple to determine N, thus the actual molecular weight between crosslinks and the mean orientation $\overline{P_2(\cos\theta)}_\mathbf{R}$ due to the network constraint from equation **(3.9)**. The fitting parameters can be found in Table 3.1 and the corresponding theoretical decays are compared to the data in Figure 3.2.

	Experimental λ	Fitting λ	$\overline{P_2(\cos\theta)}_{\mathbf{R}}$	$\langle P_2(\cos\theta)\rangle_V$	$\left.\langle P_2(\cos\theta)\rangle_V \middle/ \overline{P_2(\cos\theta)}_{\mathbf{R}}\right.$
	1.00	1.00	0	0	
	1.21	1.29	0.086	0.024	0.28
	1.41	1.49	0.15	0.055	0.37
	1.58	1.56	0.17	0.063	0.37
	1.83	1.83	0.27	0.10	0.38
v_o/N (Hz)	2200 +/-200				
M_x (g/mol)	900 +/-200				

Table 3.1 The parameters required in the theoretical NMR signal **(3.10)** to model the data in Figure 2

$\lambda=1.00$

(a)

λ=1.21

(b)

λ=1.41
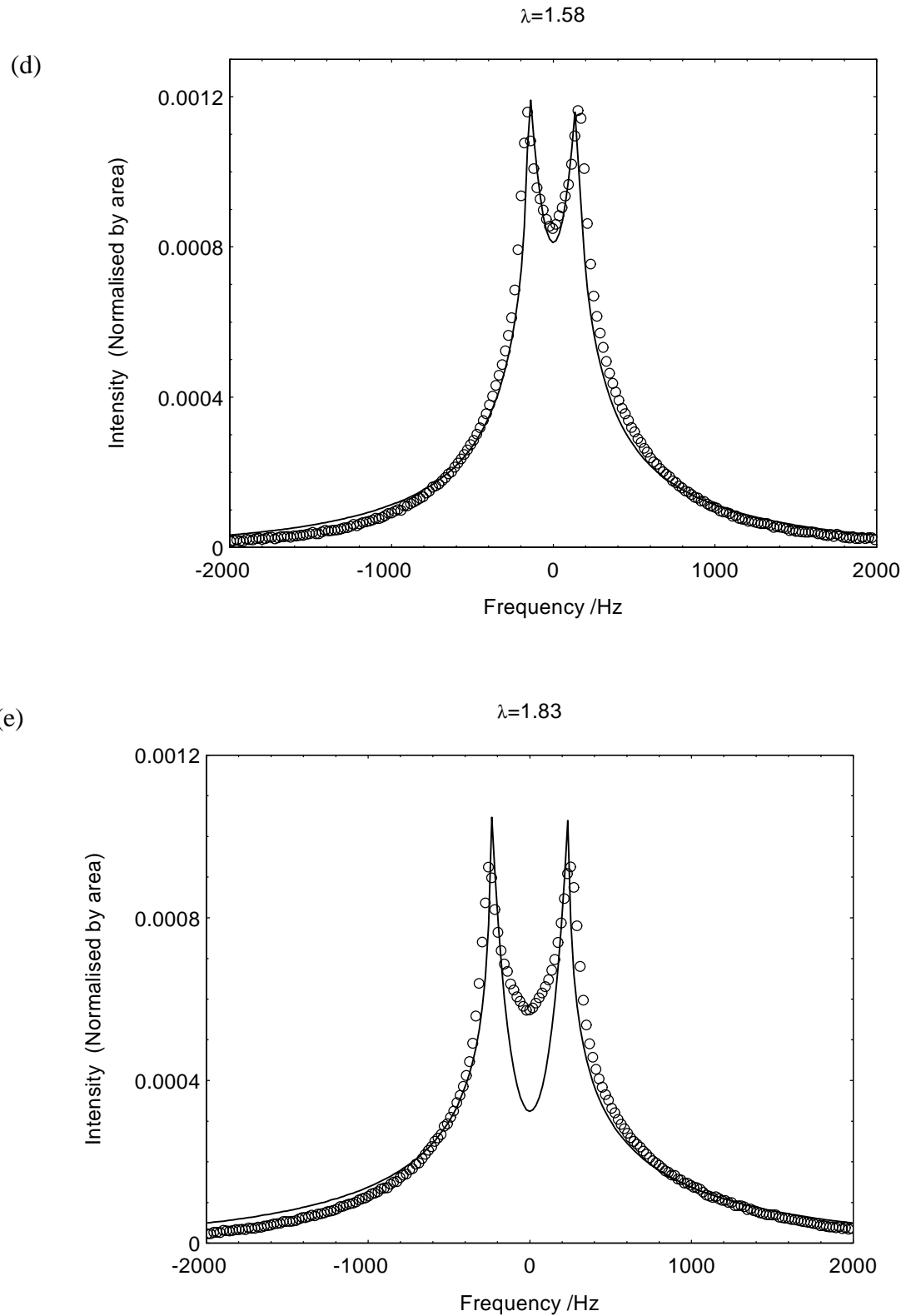
(c)

(d)

λ=1.58

(e)

λ=1.83
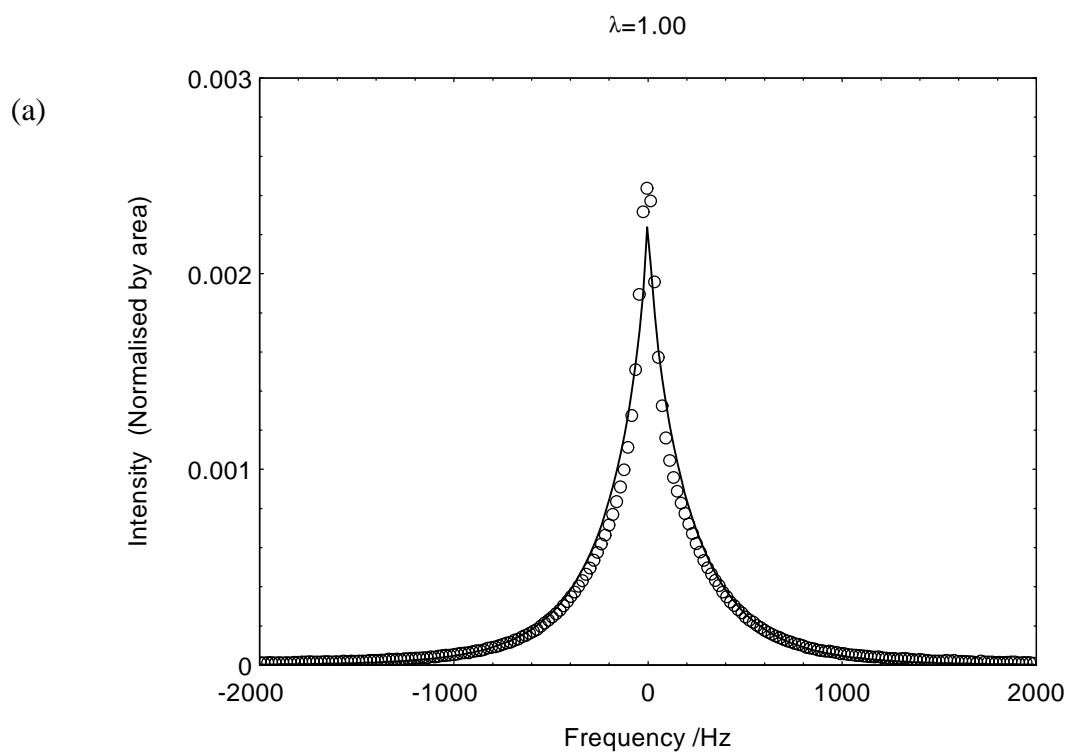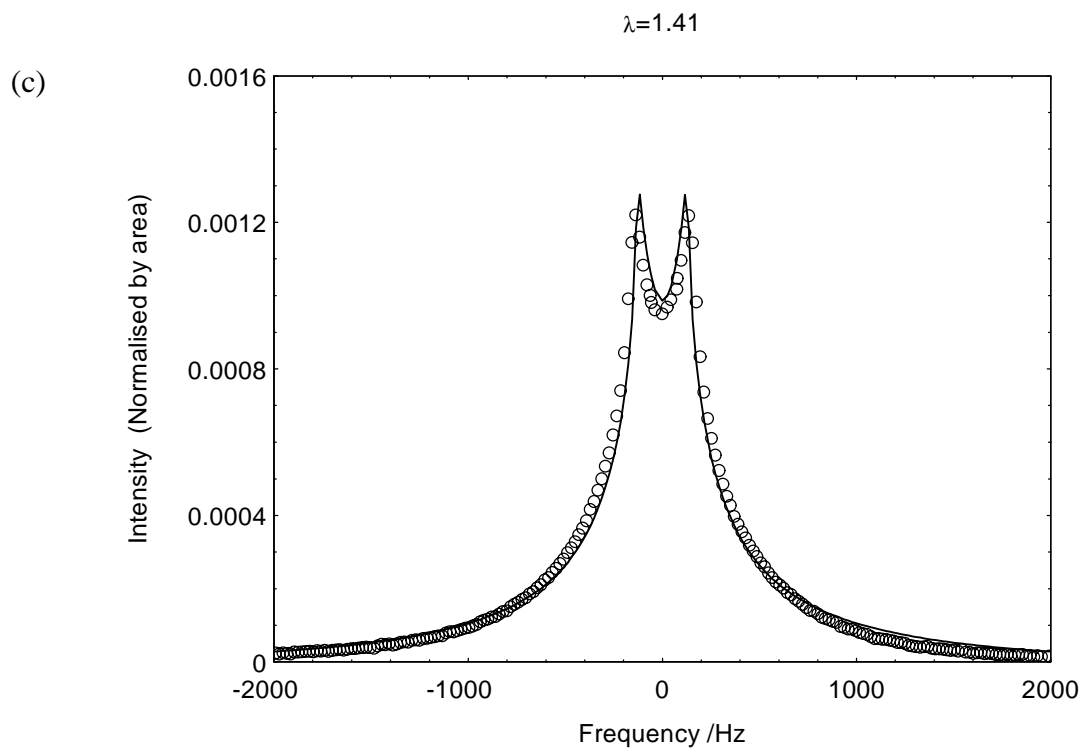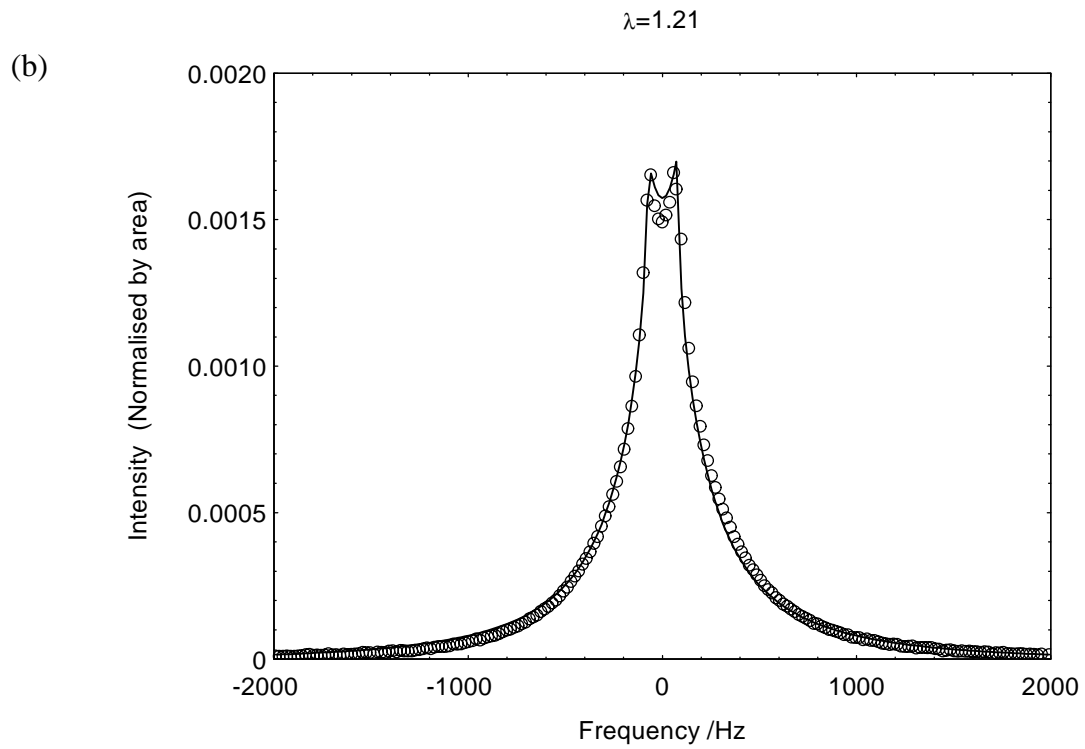
Figure 3.2(a)-(e) The solid lines are the theoretical fits from equation **(10)** to strained poly(butadiene) network using the parameters in Table 1. λ is the deformation ratio. (a) $\lambda = 1.00$ (b) $\lambda = 1.21$ (c) $\lambda = 1.41$ (d) $\lambda = 1.58$ (e) $\lambda = 1.83$.

From Table 3.1 it can be seen that the theoretically required deformation ratios are close to the experimentally determined ones and indeed are within the ~5% estimated error in λ. This means that NMR was able to measure the deformation of the samples from the NMR Fourier transformed signals. It is only at the highest deformation, $\lambda = 1.83$, that the theoretical lineshape deviates from the experimental data. This could be attributed for example to non-affine deformation of the effective crosslink points at high elongations.

Stress strain measurements[19] on this network have determined the molecular weight between chemical crosslinks, M_c, as 6500g/mol and the molecular weight between entanglements, M_e, as 1970g/mol at room temperature. The effective molecular weight between crosslinks, M_x, can be estimated from[42]

$$\frac{1}{M_x} = \frac{1}{M_e} + \frac{1}{M_c} \qquad . \tag{3.11}$$

This gives a value of $M_x = 1500\text{g/mol}$ which is close to the above NMR determined value in Table 1. Through the new analytic result **(3.10)** it is therefore possible to measure the average molecular weight between effective crosslink points.

In Table 3.1 the relative contribution to the orientation of the mean field to the network constraint has been determined. The mean field appears to increase the alignment, in terms of a resultant $\left\langle P_2(\cos\theta) \right\rangle_{\mathbf{R},V}$, by approximately 30%. The remaining part of the analysis section shall consider a proposed model for this anisotropic mean field.

3.1.3.1 Edward's Screening Length

A segment in a polymer melt interacts through excluded volume interactions with its many neighbouring chains. These many interactions of the segment with its environment give rise to an effective interaction potential between any two segments on a particular chain, $V^*(\mathbf{r})$, given by[34]

$$V^*(\mathbf{r}) = V\left[\delta(\mathbf{r}) - \frac{\exp(-r/\xi)}{4\pi r\xi^2}\right] \qquad , \tag{3.12}$$

where V is the bare excluded volume interaction strength, ξ is the Edward's screening length and $\mathbf{r}$ is the vector separating the two segments. This potential consists of a strong repulsive short range component, $\delta(\mathbf{r})$, and a weak attractive part of range ξ. The Edward's screening length can be related to V through[31]

$$\xi = b\sqrt{\frac{kT}{12Vc}} \qquad , \tag{3.13}$$

where c is the number of statistical segments per unit volume and k is the Boltzmann constant.

From equation (**3.12**), the effective interaction potential satisfies[34] $\int V^*(\mathbf{r})d\mathbf{r} = 0$. This effect is known as the screening of the excluded volume interactions. In an undeformed melt it is this screening that gives rise to Gaussian statistics.

The Fourier transform components V_q^* of the screened interaction potential (equation (**3.12**)) can be written in terms of the components of the bare interaction V_q as[34]

$$V_q^* = V_q - \frac{V_q^2 g_q}{1 + V_q g_q} \quad , \tag{3.14}$$

where in the case of a network g_q becomes the sum of the structure factors of the network chains divided by the number of network chains[31,45-47]. These network chain structure factors then depend on the deformation λ. It is through this dependence of the structure factors on elongation that the interaction potential itself becomes anisotropic.

In a paper by Brereton and Ries the average orientation due to this anisotropic screened potential was calculated to be[31]

$$\langle P_2(\cos\theta)\rangle_V = \frac{1}{15N\pi}\frac{b}{\xi}\left(\lambda^2 - \frac{1}{\lambda}\right) \tag{3.15}$$

with this depending on the crosslink density and the ratio of the length scales b/ξ.

In Figure 3.3 the orientation due to the mean field is plotted as a function of $\left(\lambda^2 - \lambda^{-1}\right)$. As the molecular weight between crosslinks, N, is already known a straight line fit to the data in Figure 3.3 specifies the ratio of the screening length to the average statistical segment size. This gives $\xi = b/6.0$, which as expected is close to unity[48].
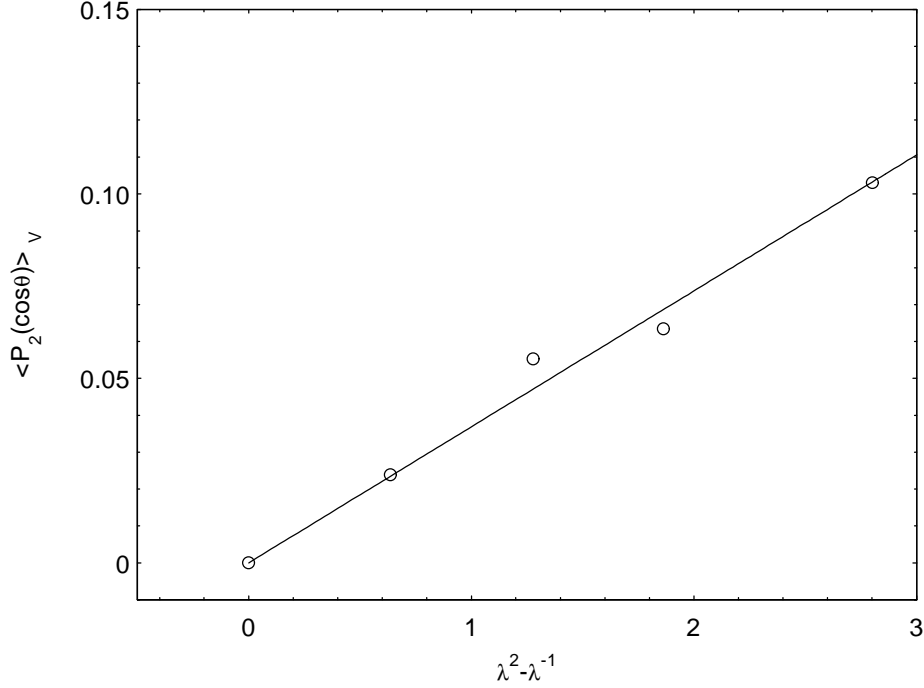
Figure 3.3 The average orientation of the deformed poly(butadiene) network due to the contribution from mean field $\left\langle P_2(\cos\theta)\right\rangle_V$ as a function of $\lambda^2 - \lambda^{-1}$.

If this model of excluded volume interactions for the mean field had been adopted earlier in the analysis, as opposed to having taken the more general approach, it would have been possible to fit all the NMR signals simultaneously using only two parameters; $v_o/N = 2200$ and $\xi = b/6.0$. This is a strong indication of the above theoretical framework to correctly model the NMR response.

From the characteristic ratio C_∞ an absolute value of the screening length can be estimated. This ratio gives the average end to end distance $\left\langle \mathbf{R}^2\right\rangle$ for a chain comprising N' atomic bonds of length l_i through the expression[49]

$$C_\infty = \frac{\left\langle \mathbf{R}^2\right\rangle}{\displaystyle\sum_{i=1}^{N'} l_i^2} \quad . \tag{3.16}$$

For poly(butadiene) both the cis- and trans- forms have a characteristic ratio near to[50] 5. From this the average end-to-end distance of the statistical segment, b, of molecular weight (260 ± 30) g/mol can be calculated as approximately $1.5\,nm$. The ratio $\xi = b/6.0$ gives an Edward's screening length therefore of $0.2\,nm$. At distances greater than that of the order of a bond length the excluded volume interactions are therefore screened. This is a reasonable length scale for screening and supports the notion that excluded volume interactions are sufficient to account for the observed splitting seen in NMR spectra from strained networks.

CHAPTER 4

4.1 Concentration, Molecular Weight and Temperature Dependence of the deformation-Induced Line Splitting

4.1.1 Introduction

When a deuterated network is stretched, an oscillation, corresponding to a splitting in frequency space, is produced in the transverse deuterium NMR decay[16] , see Figure 4.1.

FID   Spectrum

a)

no oscillation   single line

b)

with oscillation   splitting

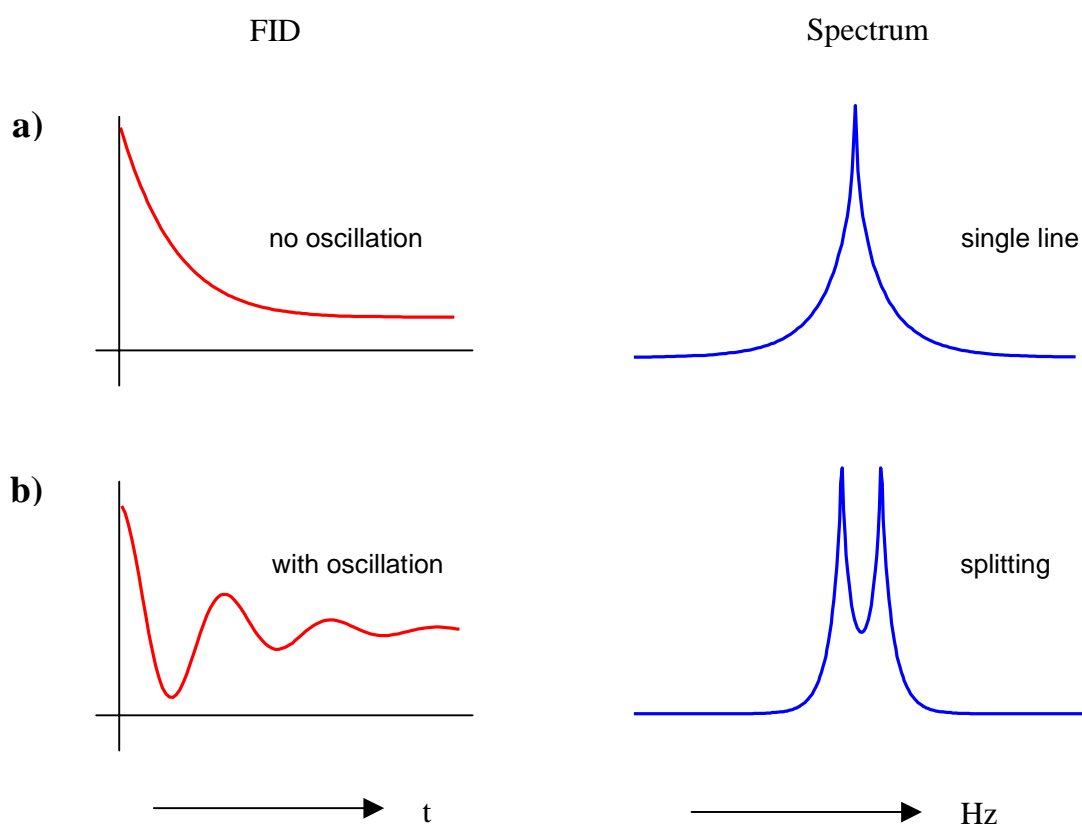t   Hz

Figure 4.1 The NMR response in time domain and after Fourier transformation. a) FID without oscillation corresponds to a single line while b) FID with oscillation corresponds to a splitting.

This indicates an anisotropic tumbling of the chain segments. Indeed this can be understood undoubtedly: if a network is elongated it would induce an anisotropy into the conformations of the network chains translated through the juction points. It was only later realised by Brereton[28], Sotta and Deloche[15] that for a non interacting (phantom) network the oscillation would disappear when averaged over all network chain orientations. This doublet produced in the frequency domain was indicative of a higher degree of anisotropy than that induced merely by the crosslink points.

This section is devoted to strengthen the idea of mean field introduce in Chapter 3, in order to explain the latter mentioned higher degree of anisotropy. To achieve this task it is introduced here the experimental results from deuterated dry networks, protonated networks incorporated with deuterated free chains and deuterated networks incorporated with protonated free chains. It will be shown how the experimental results can be discussed using the theoretical framework constructed on mean field idea. Also it will be discussed here the effect of Flory interaction parameter χ on the observed deuterium NMR line splitting.

4.1.2 Results and Discussion

4.1.2.1 Network Probe and Free chain Probe

The interesting observation is that deuterated free chains within a protonated deformed polymer network exhibit the same line splitting as it does a deuterated deformed network. This result is presented for PB networks in Figure 4.2b while the situation is schematically represented in Figure 4.2a.

It is shown in Figure 4.2b the line splitting of three different networks. Two of them are protonated PB networks (CSM1 and CSM2), (M_C=10 000 g/mol and 8000 g/mol respectively), which were incorporated with deuterated free PB chains of M_n=25000 g/mol. The free chain incorporation procedure was a simple one: free chains were laid

firmly on the network and allowed enough time (few weeks) to be well incorporated to the network. Finally, the remaining free chains on the surface were well wiped out.
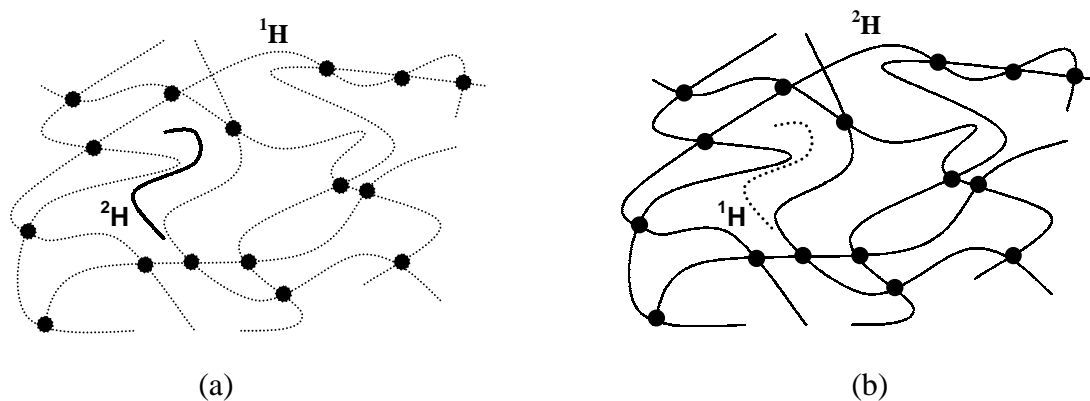

(a)   (b)

Figure 4.2a A schematic representation of the (a) deuterated free chains in a protonated polymer network and (b) protonated free chains in a deuterated polymer network

For comparison, the line splitting of a deuterated dry network (M_C= 6500 g/mol) is also shown in Figure 4.2b. The magnitude of the splitting for all components, the signal from the free chain or network, are comparable and have the same dependence on extention ratio ($\lambda^2 - 1/\lambda$).
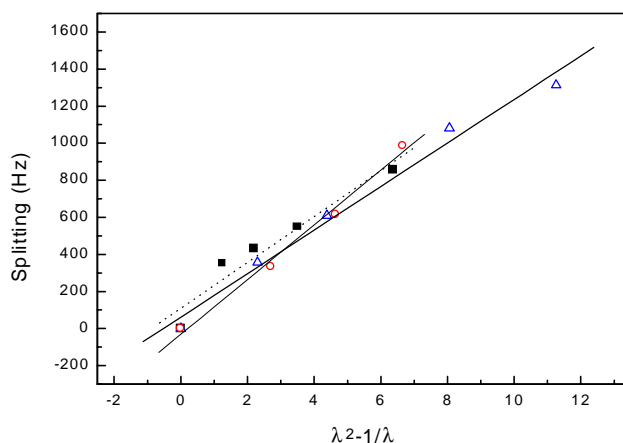

Figure 4.2b A comparison of the line splitting from a deuterated dry network and from deuterated free chains (Mn=25000 g/mol) within protonated networks. ■ - deuterated dry network (Mc=6500 g/mol), △ - deuterated free chains dissolved in protonated network (Mc=8000 g/mol), ○ - deuterated free chains dissolved in protonated network (Mc=10000 g/mol).

An oscillation in the free chain signal reveals that the splitting does not depend explicitly on the presence of crosslinks, i.e. only the constraint arising from the network due to crosslinks is not responsible for the line splitting. In the literature, it was reported similar observations from deuterated solvent molecules within a protonated deformed Polydimethylsiloxane (PDMS) network[10,35,51]. Sotta et al. demonstrated that when oligomers of deuterated PDMS were dissolved into a uniaxially deformed PDMS network they also showed the characteristic doublet[52]. Further these oligomers displayed the usual orientational dependence, ($3\cos^2\theta - 1$), of their splitting on the angle θ between the applied strain and the magnetic field. This clearly revealed that all the chains in the sample, both network and free chains, were aligned along the strain direction.

Previously, Sotta and Deloche[52] introduced nematic interactions occuring between neighbouring segments to explain this phenomenon. These nematic interactions would both enhance the anistropy of the network segments and generate it in any dissolved free chains. In a later work Brereton[28] showed that it was sufficient to include only excluded volume interactions in order to account for the observed line splitting. For the network these were treated as the mean field level and it was shown that an anisotropic mean field arises when the network is deformed. Subsequently numerical simulations[53,54] on deformed one component systems have demonstrated the ability of excluded volume interactions to produce the experimentally observed splitting. Brereton and Ries[31], recently, dealt directly with network vectors, which were treated as quenched variables, to show explicitly how they collectively determine the anisotropy in the mean field.

The latter approach is shortly discussed here and then it will be shown how the experimental observations can be discussed on the light of it. It will also be shown that the splitting on either kind of chain (network or free) for a uniaxial extension λ to vary linearly with ($\lambda^2 - 1/\lambda$), and the magnitude is to be determined by the mean field. This can be experimentally controlled by blending the network with free chains. For the chains, identical to the network chains, the principle effect is simply to dilute the contribution to the mean field from the network chains, with the chain length playing a

minor role. Also, it is derived the contribution to the mean field arises by choosing free chains of a different chemical nature and compared with the experimental results.

The splitting is linearly dependent on the network fraction and determined by the excluded volume interaction as expressed by the ratio of the Edward's screening ξ to the chain segment length b. Taking into account all the above facts Brereton and Ries[31] [RS1] have shown that the deuterium NMR line splitting $\Delta v_{A/B}$ from either the network (A) or free chains (B) can be written as

$$2\pi\Delta v_{A/B} = 2(\lambda^2 - \lambda^{-1})\Delta_{A/B} \quad . \tag{4.0}$$

The deformation dependence is entirely contained in the pre-factor, whereas the molecular weight, concentration and temperature dependence are contained in the term $\Delta_{A/B}$, given by

$$\Delta_{A/B} = \frac{2}{15\pi}\frac{1}{cb^3}\frac{\upsilon_o}{N_A}\frac{c_A}{c}\left[\frac{b}{\xi}+\frac{c_B}{c}F_{A/B}\right] \quad , \tag{4.1}$$

where

$$F_A = \frac{\sqrt{12}\left(\frac{1}{N_B}-\frac{1}{N_A}-2c_B\chi\right)\left(\frac{1}{N_B}+6\left(\frac{c_Ac_B}{c}(\chi_o-\chi)-2c_B\chi\right)\right)}{\left[\frac{2c_Ac_B}{c}(\chi_o-\chi)\right]^{3/2}} \quad , \tag{4.2}$$

$$F_B = \frac{\sqrt{12}\left(\frac{1}{N_B}-\frac{1}{N_A}+2c_A\chi\right)\left(\frac{1}{N_B}+6\left(\frac{c_Ac_B}{c}(\chi_o-\chi)\right)\right)}{\left[\frac{2c_Ac_B}{c}(\chi_o-\chi)\right]^{3/2}} \quad . \tag{4.3}$$

Here N_A, N_B - number of statistical segments per chain (network and free, respectively),

c_A, c_B, c - concentrations of network chain, free chain and total, respectively

$$2\chi_0 = \frac{1}{c_A N_A} + \frac{1}{c_B N_B} \quad .$$

There are two contributions to the splitting given by equation (**4.1**). Contribution of the first term, i.e. b/ξ, is of the order of 1 and the contribution of the second term, i.e. $F_{A/B}$, is of the order of $1/N_A$. If the network chains and free chains are chemically identical but of different molecular weights (i.e. $N_A \neq N_B, \chi = 0$), the second term becomes (from equation (**4.2**) and (**4.3**))

$$F_{A/B} = \frac{\sqrt{12}\left(\frac{1}{N_B} - \frac{1}{N_A}\right)\left(\frac{1}{N_B} + 6\left(\frac{c_A c_B}{c}(\chi_o)\right)\right)}{\left[\frac{2c_A c_B}{c}(\chi_o)\right]^{3/2}} \tag{4.4}$$

and is the same for both kind of chains. That means the line splitting is the same from network and free chains.

It would be interesting to investigate experimentally the above theoretical predictions, especially how the line splitting is affected by network concentration c_A. For this purpose one of the previously described PB dry networks (deuterated, M_C=6500 g/mol) was used. The network volume fraction was gradually reduced by inserting protonated free chains of M_n=1800 g/mol to the network. Deuterium NMR line splitting was measured at different network concentrations. The effective mass between two crosslinks of the same network is 1500 g/mol (see Chapter 3). Since the mass of a statistical segment of methylene deuterated PB is 260 g/mol[39], it is calculated the N_A as 5.7. Number of statistical segments of the protonated free chains N_B is calculated as 6.9. In Chapter 3 it was shown that length of a statistical segment divided by Edward's screening length, b/ξ, is 6.0 and v_0 =7730 Hz. Using these values and equation (**4.0**), (**4.1**) and (**4.2**), the experimental data of the network concentration dependence of line splitting were fitted to

the theoretical function (**4.0**), for $\lambda = 1.8$ and is shown in Figure 4.3. It was noticed that there was a slight departure from the usual linear dependence of the splitting on network concentration. Indeed it is difficult to decide whether these data points corresponds to a linear dependence or a non-linear dependence, since lack of data points. The difficulty of obtaining more experimental data points lies in the long time it takes to dissolve a polymer chain of sufficient length to be considered as a statistical chain into a network. In the case of $\chi = 0$ (i.e. there is no role of Flory interaction parameter although the chains are slightly chemically different), the theoretical curve shows the linear dependence. In a similar work Ries[55] introduced a value of 0.05 for the χ into a system of protonated and deuterated PDMS polymer chains in order to model the experimental data. Hence we can discuss our results on the point of view of non-linear behaviour. Here the second term in equation (**4.1**) is beginning to compete with the Edward's screening length. This is because a small Flory interaction parameter has been introduced due to the slight dissimilarity between the deuterated chemically cross linked chains and the protonated chains. Data can be modeled by constant $\chi = 0.1$ and where the splitting from the network has been normalized to a dry network result. Error of the data is about 5%.

The dependence of the splitting with $\lambda^2 - 1/\lambda$ for a series of deformations is shown in Figure 4.4. In the case of the probe on network chain, deuterated network, the contribution from F_A is predominantly negative, as can be seen in equation (**4.1**). However, the sign can be changed especially when $N_B > N_A$.

To model the results from PB network it has to be used a value of $\chi = 0.1$ which is slightly higher value than that used by Ries[55] to model the data from PDMS network.
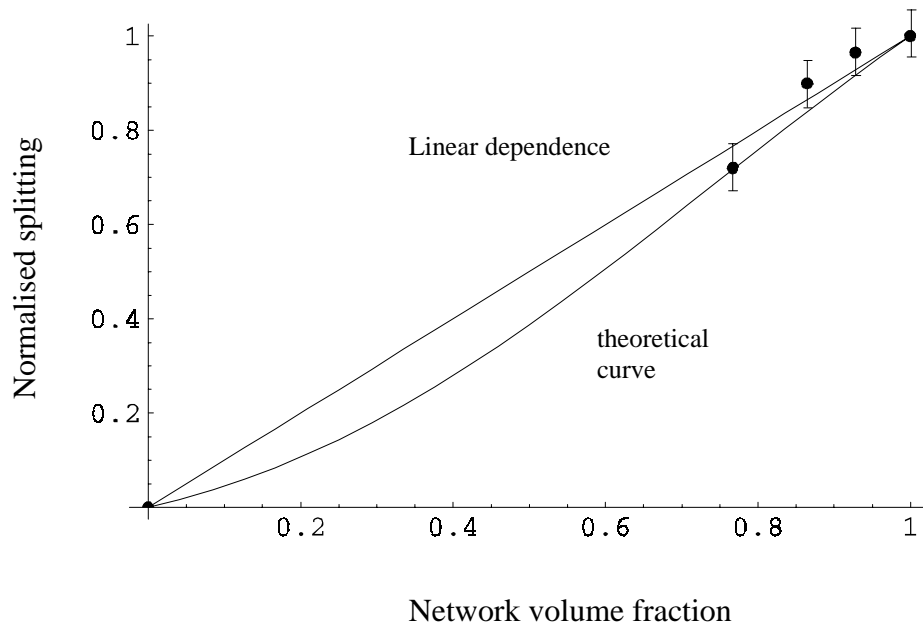
Figure 4.3 The magnitude of the splitting, normalised to the dry network, for deuterated strained (λ =1.8) network which is incorporated with protonated free chains as a function of network volume fraction. The straight line is the linear dependence of line splitting without including the χ dependent part.
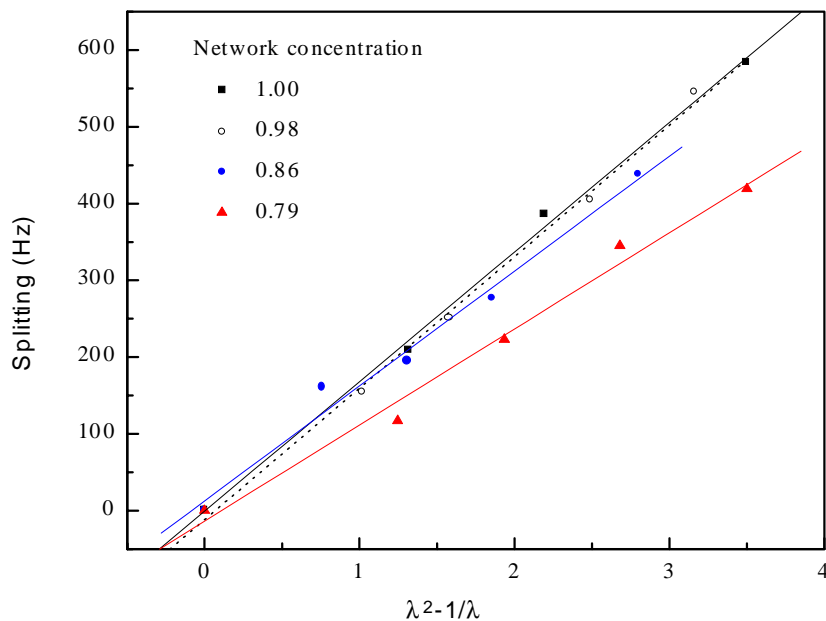

Figure 4.4 The magnitude of the splitting at a series of deformation ratios, for deuterated network which is incorporated with protonated free chains as a function of network volume fraction.

Although the chemical structural difference (protonated and deuterated) in the cases of PDMS and PB are almost the same there exists a large difference of the effective molecular weights between cross links M_x. It was 6500 g/mol for the PDMS[10] and 900 g/mol for the PB. So that the difference of M_x is about seven times. The difference of the crosslink densities of PDMS and PB may cause to differ the values of χ parameter.

The values of χ for some polymers which are in different solvents are shown in Table 6.1 and hence one can get a general idea about the range of the parameter.

Polymer	Solvent	Temperature Range (°C)	χ
PDMS	Benzene	25 – 70	0.81 – 0.75
	n-Hexane	20	0.5
Poly(isoprene)	Benzene	25 – 55	0.46 – 0.43
	n-Hexane	25 - 55	0.54 – 0.50

Table 6.1 χ parameter obtained for different polymers in different solvents [Polymer Hand Book]

During a study on swelling in crosslinked natural rubber, McKenna et al.[56] have shown that χ depends on crossslink density and furthermore, the value of χ in the crosslinked polymer was a linear function of the crosslink density (see Figure 4.5). In the same study it was shown the variation of χ with volume fraction of rubber. Therefore, it is argued here that the apparent increase of χ in PB is due to its higher crosslink density than that of PDMS. Additionally this opens a new way to investigate χ using deuterium NMR spectroscopy.
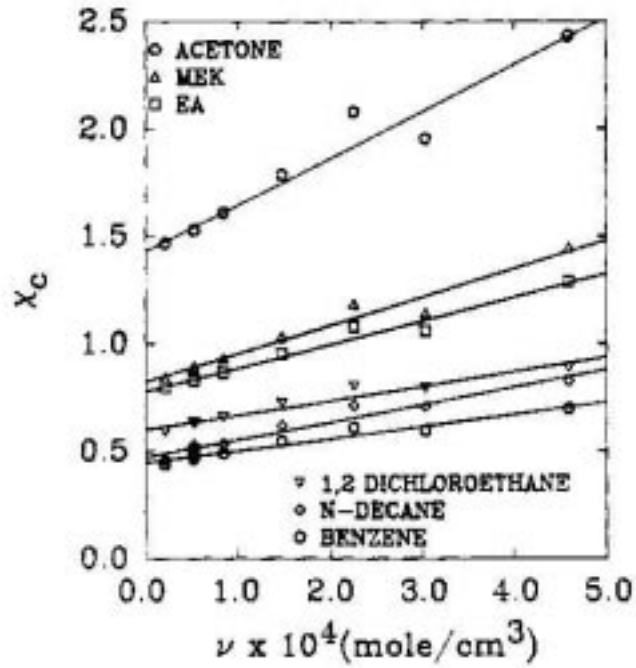
Figure 4.5 Dependence of χ on crosslink density ν for dicumyl-peroxide-crosslinked natural rubber swollen in different solvents, as indicated[56].

4.1.2.2 Temperature Dependence

The term b/ξ in equation (**3.15**) and (**4.1**) is the temperature dependent part of the deuterium NMR line splitting. To show the relation between b/ξ and T recall equation (**3.13**) $\xi = b\sqrt{\dfrac{kT}{12Vc}}$. According to this relation the line splitting depends on temperature as $1/\sqrt{T}$.

In an earlier work by Deloche and Samulski[13] considering nematic-like interactions between chain segments, it was reported that segmental order parameter S has the dependence on temperature according to

$$S = S_{seg}^* (1 + \frac{\phi E}{\alpha(T - T^*)}) \qquad\qquad (4.5)$$

where S_{seg}^* is the ideal segment order parameter deduced from kinetic theories of rubber elasticity[57], ϕ is the rubber volume fraction, E is a constant related to elastic module, and α is a constant related to an interaction constant between segments.

T^* in equation (4.5) corresponds to a critical temperature of the polymer sample. In the present study T^* can be considered as the glass transition temperature. Since the experiments are conducted at a temperature (-20 °C – +60 °C) well above the glass transition temperature (~ -105 °C), the effect of T^* can be neglected and hence the segmental order parameter has the temperature dependence as $1/T$. NMR line splitting Δv is related to S according to the relation[10]

$$S = K \Delta v / v_q \quad, \qquad\qquad (4.6)$$

where v_q is the static quadrupolar interaction constant and K is a numerical constant which depends on the chemical structure of the polymer. From the above formulations by Deloche and Samulski it can be revealed that Δv has the temperature dependence as $1/T$. However, it is hard to find in literature an experimental work which has been done in order to accomplish this temperature dependence.

Experiments were conducted on deuterated PB networks in order to investigate the temperature dependence of the NMR line splitting. At each temperature it was allowed 30 minutes time to stabilise the temperature over the network while the temperature increase was 1 degree per 3 minutes. The deformation ratio was kept at 1.60, 1.85 and 2.20.
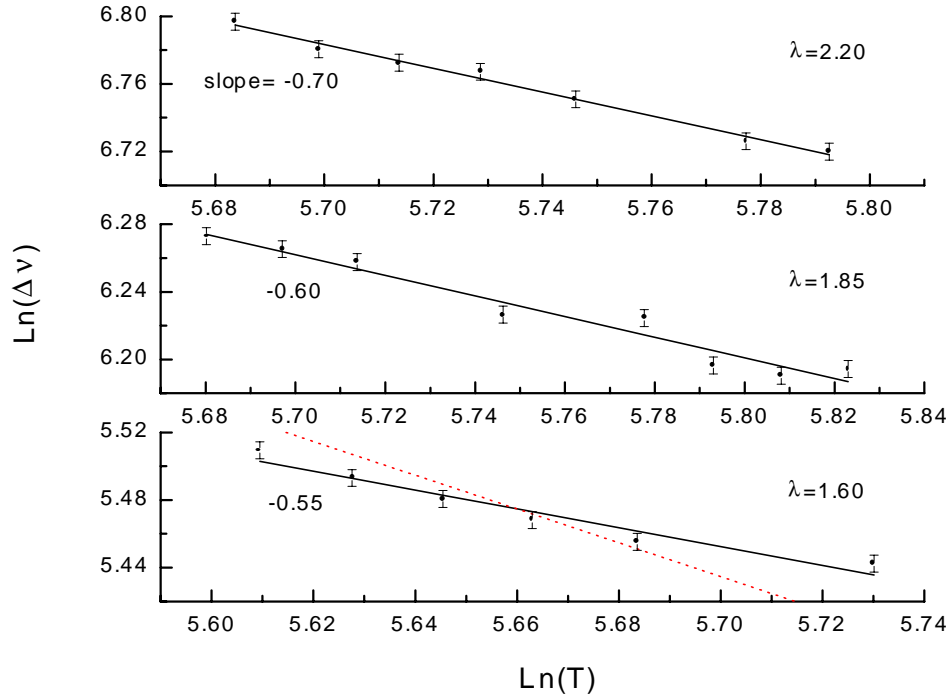
Figure 4.6 Temperature dependence of the NMR line splitting at different deformation ratios (λ=1.60, 1.85 and 2.20). The dotted line corresponds to the slope of –1.0.

The results are depicted as a logarithmic plot in Figure 4.6. The slopes of the plots, which are –0.55, –0.60 and –0.70 in this case, indicates the temperature dependence of the line splitting, i.e. the NMR line splitting depend on the temperature according to $1/\sqrt{T}$ (see equations (**3.13**), (**4.0**) and (**4.1**)). The dotted lines represent the lines with slope –1.0. The interesting feature is the behaviour of the temperature dependence of the NMR line splitting not depend on the applied deformation ratio (see Figure 4.6), giving a strong evidence for the correctness of the nature of temperature dependence of the theoretical frame work which was constructed in Chapter 3.

4.2 Effect of Cross Link Density on the Screening Length and Rescaled Quadrupolar Interaction

4.2.1 Introduction

This section is devoted to study deuterium NMR line shape of PB networks with different cross link densities. It will be addressed, with the help of experimental results fitted to the equation (**3.10**), the behaviour of screening length on the changing cross link densities of the network. In Chapter 3 it is shown that the screening length is a unique quantitiy for a polymer and it is independent of cross link density. Rescaled quadrupolar interaction constant, which depends on the number of statistical segments between two cross links, extracted from the above fitting results used to estimate the cross link densities of the network samples and compared with the results from stress-strain measurements.

4.2.2 Results and discussion

Deuterium NMR has been employed to determine the average orientation of chain segments in the poly(butadiene) networks AD1, AD2, AD3 and AD4 (M_c=3300, 3600, 6800 and 5400 g/mol respectively). The NMR spectrum lineshape reveals the orientational distribution of the network vectors due to the crosslinks, whereas the observed splitting gives information about the orientation due to segmental interactions. Both the lineshape and the splitting has been fitted to the equation (**3.10**) simultaneously for a range of deformed poly(butadiene) networks. The ^{2}H NMR spectra of the networks under study were analysed in dependence on the deformation ratio λ. A qualitative representation of the fitting of experimental data to the equation (**3.10**) is shown in Figure 4.7. The spectra are well represented by fitting of the latter mentioned fitting equation for all the samples.
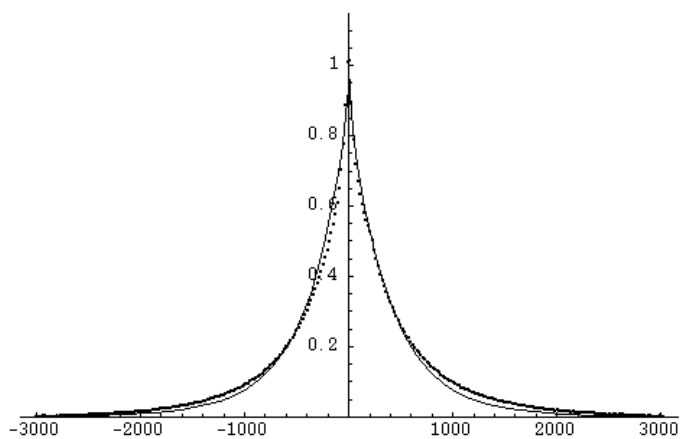
(a)
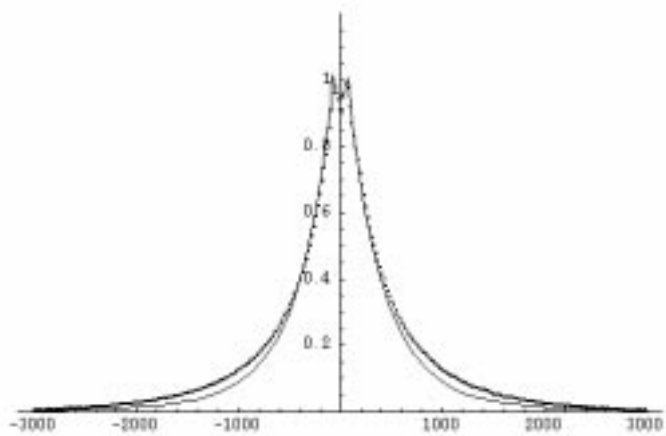
(b)
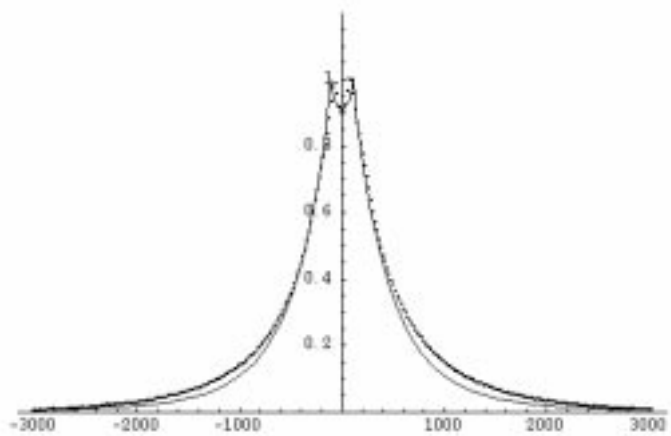
(c)

Figure 4.7 Experimental ^{2}H NMR spectra and the fit by equation (**3.10**) for sample D4 with 0.5 phr DCP at (a) λ=1.0 (b) λ = 1.1 and (c) λ=1.2.

All the ^{2}H NMR spectra could be described with only three independent parameters: the rescaled quadrupolar interaction divided by the number of statistical segments ν_0/N, the magnitude of splitting in the frequency space $\Delta\nu$ that depends on the mean field contribution to the anisotropy through equation (**3.10a**) and the deformation ratio λ. From the fitting parameters the separate contributions to the average orientation of the chain segments arising from the network constraint and from the interactions are calculated. The quantity b/ξ is found to be unique for all networks under study. It was determined to a value of 3.4 which is as expected in the order of unity and independent on the length of the precursor chains and even on the crosslink density. In Chapter 3 it is shown that this ratio b/ξ should remain constant for a series with different crosslink densities which was ascertained here. This is a strong indication of the above mentioned theoretical framework.

In the case of peroxide vulcanisation the radicals are created where the peroxide molecules are happen to be located. This implies that there is a risk of local concentrations of radicals, as the peroxide molecules tend to agglomerate rather than dissolve in the polymer matrix. The rate of termination is dependent on the collision frequency which in turn is strongly dependent on the mobility of the system. If the molecular mobility decreases, the polymer chains in which the radicals are located will be less able to move freely to collide with other radicals. Before the radical terminates, it will have time to perform more reactions than a less hindered radical. A lower mobility will, thus, lead to a larger number of crosslinks per initiated radical. However, it is not only the decrease in segmental mobility that is responsible for the increase of crosslink density, even thought it is probably the main reason. When the mobility decreases for long-chain segments, the mobility of smaller parts of the chain, e.g. methyl groups in natural rubber or vinyl groups in poly(butadiene), are not affected that much. The vinyl groups therefore are favoured over main chain unsaturations for reactive species, even more pronounced at higher pressures[58]. The fact that vinyl unsaturations are prefered in crosslinking was shown already by Lavebrett et al.[59] who investigated butadiene rubber (BR) with different microstructure.

The mean M_c-values between two chemical crosslinks of the networks were estimated from ^1H and ^2H-NMR relaxation, stress-strain and swelling measurements[60] to be 7500 (3300 from swelling only), 3600, 6800 and 5400 g/mol for the networks AD1, AD2, AD3 and AD4. The much larger precursor chain length (see Table 2.1) for D1 and D2 (it is about 2 times larger compared to D3 and D4) yields to a more restricted mobility of the polymer chains. Therefore, the resulting crosslink density is increased (reduced M_c-value) for this networks despite of the fact that the inserted amount of crosslinker was the same (about 0.5 phr DCP for all networks under study here). The large discrepancy in the M_c-values calculated from the different methods for the network D1 is probably caused by irregularities in the spatial distribution of the radicals which may give rise to variations in the homogeneity of the resulting network.

The ratio ν_0/N was estimated to be 5200, 5100, 3800 and 3700 Hz for the networks AD1, AD2, AD3 and AD4, respectively, by fitting the spectra using equation (**3.10**). This trend is in good agreement with the G'-modulus measurements which give plateau values for G' of 1,37 MPa, 1,46 MPa, 1,13 MPa and 1,09 MPa for the same networks. Due to these results it is believed that the M_c-value for the AD1-network of about 3300 g/mol is the more correct one. The networks prepared from larger precursor chains yield the larger ratio ν_0/N than those built from shorter chains, however, they differ by a factor of two in the crosslink density. But if the protonated precursor chain length is the same and the deuterated chain length is larger, one could observe only a small increase in this ratio. This ratio ν_0/N in turn is used to determine an effective molecular mass M_x ($1/M_x = 1/M_c + 1/M_e$) which contains the topological hindrances due to crosslinks and entanglements. The value of the corresponding rescaled interaction constant ν_0 for methylene deuterium was taken from an earlier published paper on poly(butadiene) melts[39] where it was estimated to be 7730 Hz. In the same study[19] it was found the molecular weight of a NMR statistical segment is $(260 \pm 30 / 294*)$ g/mol. Using this values, the effective molecular masses M_x of these networks were determined to 390/590*, 400/604*, 530/920* and 540/960* g/mol, resp. (* is upper limit). The entanglement contribution M_e was found to be about 1700 g/mol for the given microstructure[61]. Based on this value for M_e and the above summarised mean molar masses between crosslinks M_c estimated from

other independent experiments, the expected effective molar masses M_x can be calculated as 1120, 1160, 1360 and 1290 g/mol for the AD1, AD2, AD3 and AD4 networks, respectively, which is close to the above NMR determined value for the effective molecular weight.

The ability of the theoretical result (**3.10)** to measure a crosslink density that compares well with mechanical tests and a screening length of a resonable size of about 0.2 nm which is found to be independent on the precursor chain length and crosslink density, strongly supports the use of this framework to interpret the NMR response from strained elastomers.

CHAPTER 5

5.1   The Susceptibility Effect of Carbon Black Filler on the Deuterium NMR Line Shape from Poly(butadiene) Networks

5.1.1 Introduction

The aim of this chapter is to explain the asymmetric NMR spectra observed from deformed carbon black filled poly(butadiene) networks[62]. To illustrate this asymmetry it is shown in Figure 5.1 a comparison between a NMR spectrum from a filled and unfilled strained network. In this study the effect of the susceptibility of the carbon black filler on the local field of polymer chains that are in the vicinity of these particles is considered. It is proposed that the magnetic field near carbon black particles is different to the rest of the sample. Therefore, the polymer chains near to the filler particles experience a different resonance frequency. This change in frequency causes a shift of their NMR spectrum in the Fourier transformed signal relative to the unbound segments. In order to quantify this shift, the theoretical expression **(3.10)** to model the NMR lineshape and splitting[63] is employed. Then the expected shift in frequency is calculated by using susceptibility data[64] of carbon black, and it is shown that this compares favorably with the results obtained from our fitting procedure.

As well as the susceptibility of the carbon black filler it is also considered that the applied macroscopic deformation does not affect the chains closely attached to filler particles to the same degree as it do the remaining chains. Figure 5.2 shows schematically the various possibilities of polymer chain attachments to the filler particles[65]. Chain segments E, F and D are not affected directly by the macroscopic deformation.

In this work the approach is to consider the asymmetric spectrum as consisting of two main components. The first corresponds to the NMR signal of polymer that are far away from the filler particles. These chains have a spectrum that is essentially

identical to that of an unfilled network. The second is the spectrum from the polymer chains that are very close to the filler particles such as segments E in Figure 5.2. The carbon black causes a shift in the resonance frequency and a different bulk strain orientation dependence of these chains attached to the filler particles. The two components of the resultant NMR lineshape are schematically shown in Figure 5.3a and 5.3b. What experimentally observed from the filled polymer network is the collective effect of the spectra 5.3a and 5.3b. The signal consists of
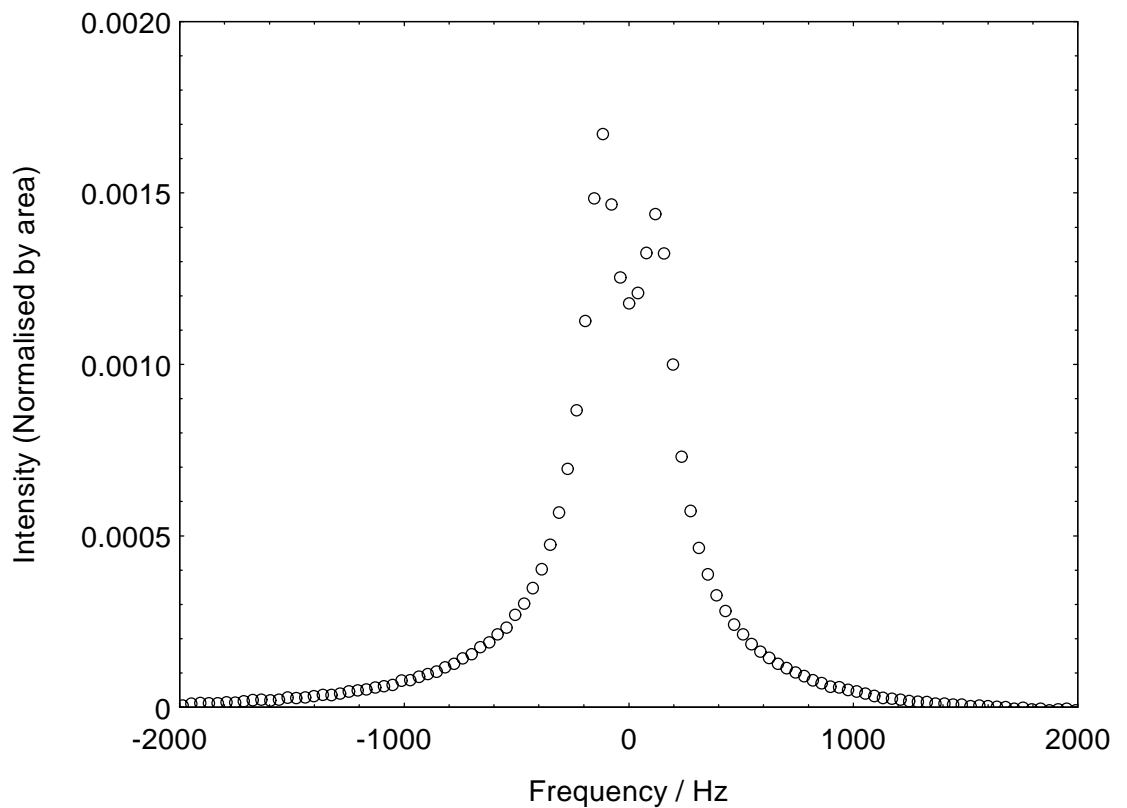

Figure 5.1(a) The NMR spectrum from a carbon black filled deformed poly(butadiene) network $(\lambda = 1.80)$ showing the asymmetry in the peak heights.
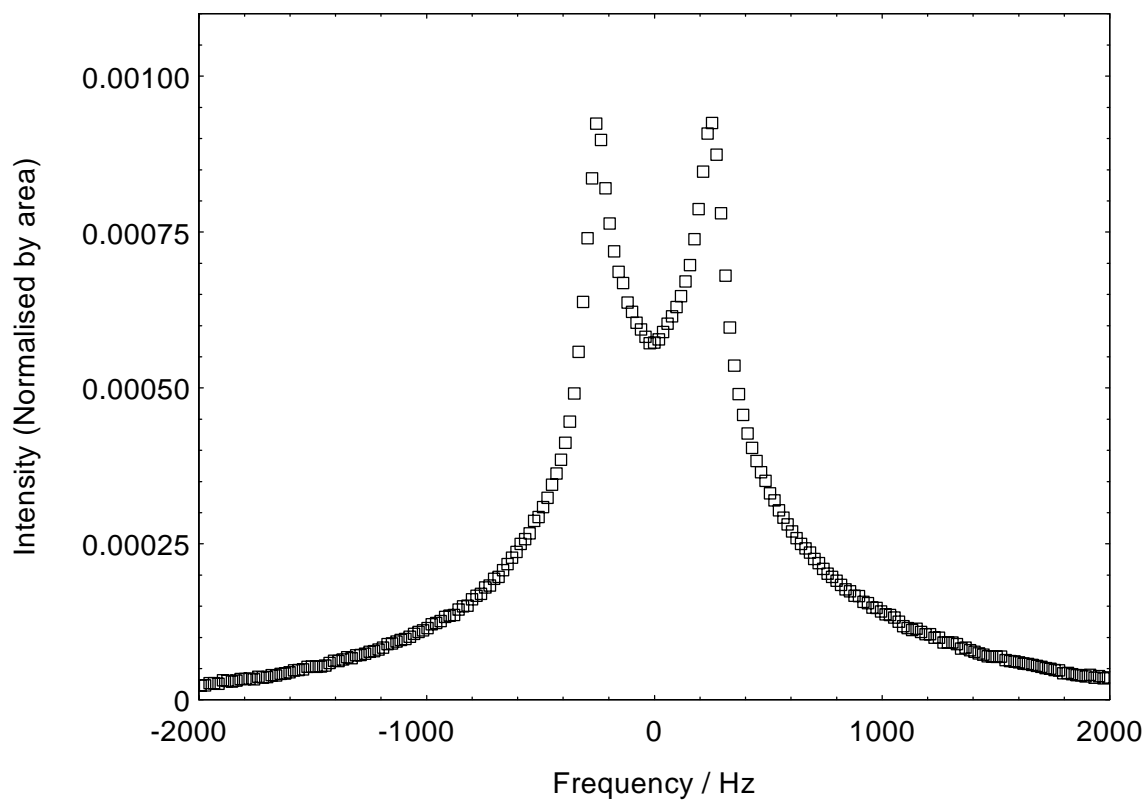
Figure 5.1(b) NMR spectrum from an unfilled deformed network $(\lambda = 1.83)$ showing the symmetry in the peak heights.
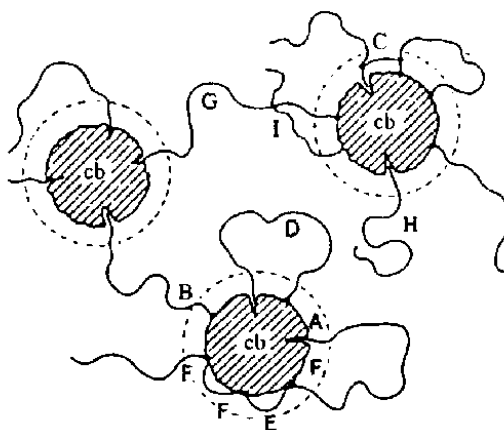

Figure 5.2 Model of the filler-elastomer interactions, cb: carbon black. A: physical attachment. B: chemical attachments. C: cross-linked rubber chain. D: loose fold. E: tight fold. F: multiple adsorptive attachments. G: inter-particle tie chain. H: cilium. I: entanglements (from reference 4).
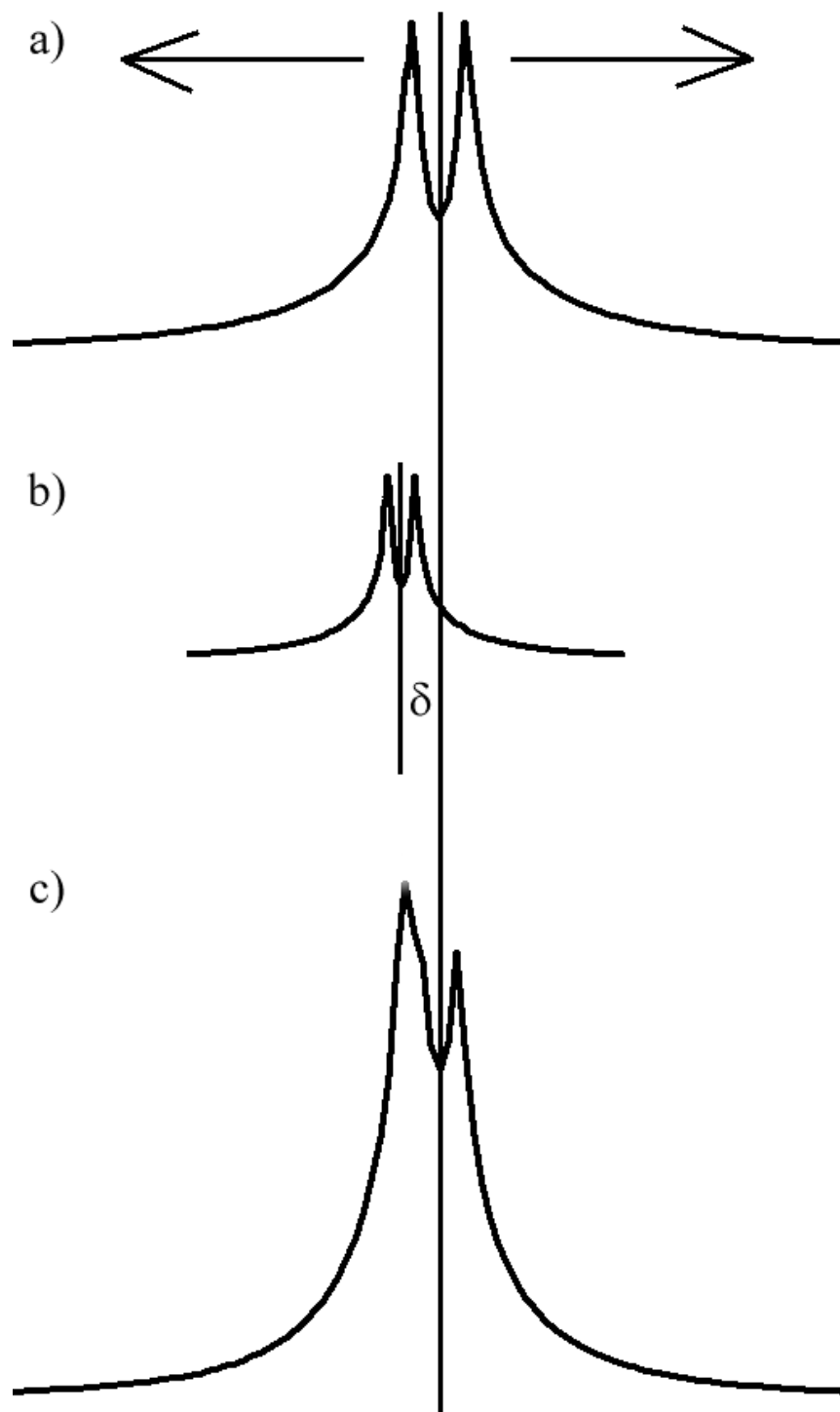
Figure 5.3 Schematic diagram showing how the resultant asymmetric NMR spectrum is formed from two symmetric signals. a) Represents the NMR spectrum from segments not in the vicinity of the carbon black particles. b) The signal from polymer chains that are close to carbon black filler particles and are therefore shifted by $-\delta$ Hz. c) The collective effect gives rise to the resultant asymmetric NMR spectrum.

two doublets with one centered on zero frequency and the other being allowed to have some offset δ. The two doublets in Figure 5.3a and 5.3b have different splittings (distance between peaks in a doublet) indicating that the attached and unattached segments are subject to different deformations. Therefore, the resulting NMR spectrum is asymmetric as shown in Figure 5.3c.

The next step is to find out experimental evidence for the existence of the shifted spectrum of the carbon black closely associated segments as shown in Figure 5.3b. With increasing deformation of the polymer network the line splitting of spectrum of Figure 5.3a and 5.3b will increase as indicated by the arrows. It is anticipated that the chains between the carbon black particles will experience a larger deformation, and so their splitting will increase more rapidly, revealing the off resonance component. In principle at a sufficiently large macroscopic deformation λ, a third or possibly fourth peak should become visible in the resultant spectrum Figure 5.3c.

5.1.2 Background

Deuterium nuclear magnetic resonance (^{2}H NMR) has been used extensively to study the orientational order induced in rubber networks under uniaxial stress[10,15,23,66-68]. The spectrum of network chains exhibits a characteristic doublet structure. It is known that classical theories fail in giving a description for the existence of such a doublet structure[28,29]. This doublet structure has been attributed to orientational interactions between segments[68].

However, the ^{2}H NMR line shape observed from carbon black filled elastomers is somewhat different from that of unfilled elastomers[62]. In the case of carbon black filled cis-1,4 poly(butadiene) networks it has been observed that the peaks of the spectrum of the Fourier transformed NMR signal are not equal in height, recall Figure 5.1a. No model in the literature for the NMR lineshape from strained networks predicts this asymmetry. A similar situation was already stated by Gronski et al[62]. They observed that increasing the filler content of cis-1,4-poly(butadiene) network at constant deformation results in an overall broadening of the doublet line shape at

nearly constant splitting and an increase in the asymmetry of the outer signal wings. In order to explain the above observations they considered the filled network as consisting of two parts. One is formed by the pure rubber phase, whereas the second contains the filler and a fraction of rubber coupled in series. However, the proposed model, based on the free induction decay of the strained sample, which was approximated by superposition of two exponentials modulated by the frequencies of the quadrupolar splitting of the two rubber phases, was unable to explain the observed asymmetry.

In carbon black filled elastomers there exist three different spin-spin relaxation times (T_2), which have been associated with three microregions[69,70]:

1. a tightly adsorbed layer, where the motion of the chains is severely restricted surrounding the filler particles,
2. a more loosely bound domain,
3. a third domain where the motion of the chains is similar to that of unfilled polymer.

A recent investigation on the surface morphology of carbon black particles with an atomic force microscope suggests that rubber-filler interaction is likely to reflect strong topological constraints exerted by the black complex surface on elastomer chains[71].

5.1.3 Analysis

The two main ideas motivating this work are: (a) that the chains in the vicinity of the filler particles have a different resonance frequency due to the susceptibility of the carbon black; (b) these chains experience a different deformation from that of the bulk sample due to their close attachment.

The analytic result, equation **(3.10),** for the lineshape $G(v; \lambda, M_x)$ of a uniaxially deformed network will be used.

Recall equation (**3.10**):

$$G\left(\nu;\lambda,N,\nu_o,\frac{b}{\xi}\right)=\left(\frac{3N\pi}{2\nu_o}\right)\left[2\lambda+\frac{1}{\lambda^2}\right]^{-1/2}\left[g_+\left(|\nu|+\frac{\Delta\nu}{2},\lambda\right)+g_-\left(|\nu|-\frac{\Delta\nu}{2},\lambda\right)\right] \quad \textbf{(5.1)}$$

In this result ν is the NMR frequency in Hz, λ is the deformation and M_x (which is related to N) is the molecular weight between effective crosslinks. This expression has been successfully employed in the analysis of unfilled poly(butadiene) networks[63] (see chapter 3).

In present model the spectra are viewed as comprising two components, a signal from segments closely associated with the carbon black and those that are not. It will assume that the chains not in the local vicinity of the carbon black experience to a first approximation the macroscopic applied deformation λ. This means that the signal from these segments is fully specified by their effective crosslink density M_x and so simplifies the analysis by keeping the number of parameters to a minimum. Next a fraction f of signal that is from the segments closely associated to the carbon black (cb) is introduced. As these chains are bound to the carbon black we allow them to have a different effective crosslink density $M_{x,cb}$ and to experience a different local deformation λ_{cb}. The resultant signal $S\left(\nu,\lambda;f,\lambda_{cb},M_{x,cb},M_x,\delta\right)$ can be written as a linear combination of the two components

$$S\left(\nu,\lambda;f,\lambda_{cb},M_{x,cb},M_x,\delta\right)=\left(1-f\right)\times G(\nu;\lambda,M_x)+f\times G\left(\nu-\delta;\lambda_{cb},M_{x,cb}\right) \quad , \quad \textbf{(5.2)}$$

where δ is the shift in the NMR frequency spectrum from the chains attached to the carbon black due to the local field strength difference (recall Figure 5.3b).

It is only under deformation that the NMR spectra become significantly asymmetric. The signals then clearly reveal that they have this off-resonance component. For successful analysis it is important to examine data that displays enough features such that the parameters in the model can be reliably determined. If

the deformation becomes too great $(\lambda > 2)$ though the theoretical result $G(\nu; \lambda, M_x)$, which is based on Gaussian statistics, is no longer valid[63]. For these reasons the analysis is begun with the $\lambda = 1.8$ data.

In Figure 5.4 the resultant fit to the NMR spectrum from the network under deformation $\lambda = 1.8$ is compared. The required fitting parameters are: $M_x = 1600 \text{ g / mol}$, $M_{x,cb} = 1100 \text{ g/mol}$, $\delta = -49.8 \text{ Hz}$, $f = 0.28$ and $\lambda_{cb} = 1.1$.
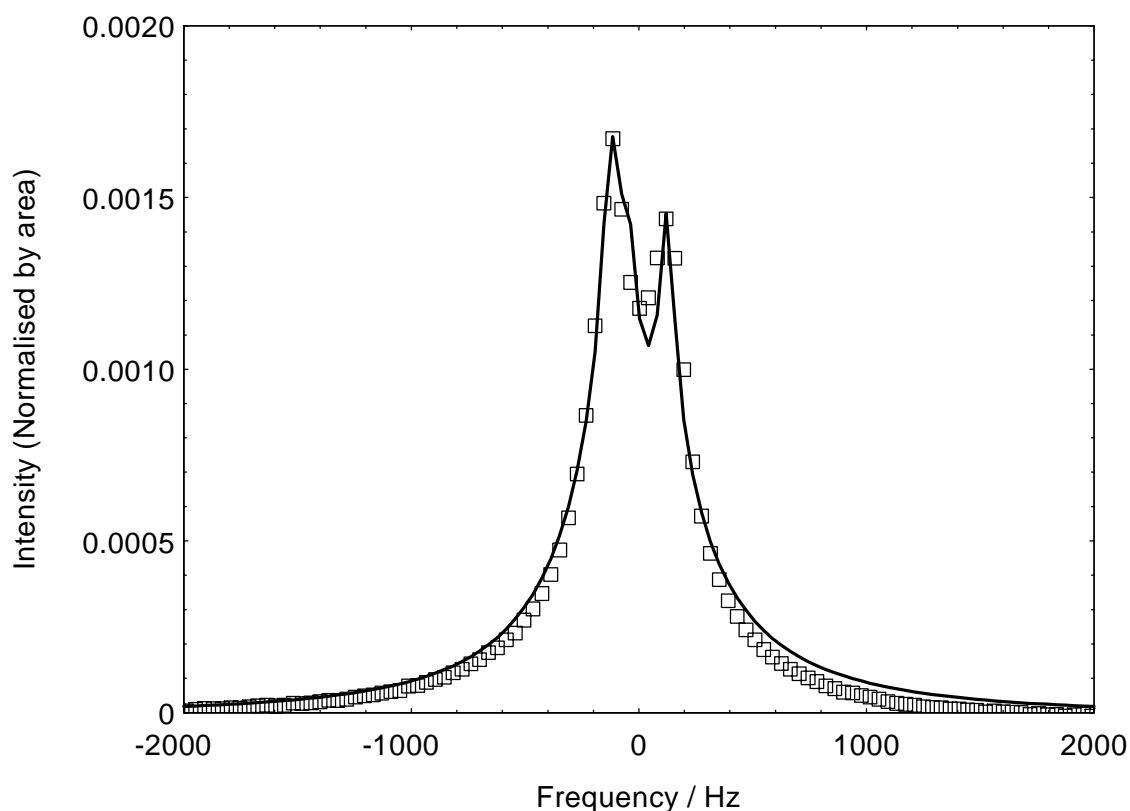

Figure 5.4 Solid line shows the theoretical fit of equation **(5.2)** to NMR spectrum from the strained poly(butadiene) $(\lambda = 1.80)$ carbon black filled network. The required fitting parameters are; $M_x = 1600 \text{ g / mol}$, $M_{x,cb} = 1100 \text{ g/mol}$, $\delta = -49.8 \text{ Hz}$, $f = 0.28$ and $\lambda_{cb} = 1.1$.

This simple model is able to generate a reasonable fit to the experimental data (Figure 5.4). Better fits could have been obtained by adding more components corresponding to chains in a different environments, recall Figure 5.2.

The effective crosslink density of the chains not in the vicinity of the carbon black particles was found to be 1600 g/mol. This can be compared with the stress-strain measurements[19]. In this work it was found that the molecular weight between chemical crosslinks M_c was 6500 g/mol and entanglements M_e was 1970 g/mol. The molecular weight between effective crosslinks M_x can be estimated from the relationship[42]

$$\frac{1}{M_x} = \frac{1}{M_e} + \frac{1}{M_c} \tag{5.3}$$

From this a value for M_x of 1500g/mol is determined. This is very close to the above found fitting parameter and indicates that the theoretical function $G(v; \lambda, M_x)$ is correctly describing the NMR response. The crosslink density of the chains closely attached to the carbon black particles was found to be 1100g/mol. This again is in good agreement with the estimated value for the crosslink density found from equation (5.3). This slightly higher density of crosslinks is consistent with the chains being attached to the filler particles and these contacts acting as extra crosslink points. It is also interesting to note that the effective deformation for these chains was $\lambda_{cb} = 1.1$. This reveals that these chains remain almost isotropic and do not directly take part in the bulk deformation, due to their close attachments to the filler particles.

In addition the fit based on equation (5.2) gives direct access, through the parameter $f = 28\%$, to the amount of polymer chains in the vicinity of the filler particles. This value compares favorably with work by Gronski et al.[70] on carbon black filled networks. They fitted the proton NMR relaxation after a solid echo using three Gaussian components. They attributed these components to segment in different regions within the sample (Figure 5.2), giving a measure of the fraction of chain closely associated with the carbon black particles. Kraus and Collins measured the magnetic susceptibilities and spin concentrations for a range of different carbon blacks[64]. Their data are shown in Table 5.1. They also broke down the mass susceptibility values into their respective diamagnetic and paramagnetic components this being derived from the spin concentration and susceptibility of free electrons. In

present study the net magnetic susceptibility is used to calculate[1] a value for the frequency shift produced by carbon black N220 of 46.6 Hz. This value of is in remarkable agreement with the frequency shift $\delta = -49.8\text{Hz}$ determined by fitting of the equation (**5.2**) to the experimental data.

Carbon black	Mol% Carbon	Spin conc.$\times 10^6$ spins/g	Mass susceptibility$\times 10^6$		
			Net	Paramagnetic	Diamagnetic
N550	95.77	10.0	-0.82	0.21	-1.03
N330	95.75	8.0	-0.79	0.17	-0.96
N220	-	9.2	-0.76	0.19	-0.95
N110	94.78	8.1	-0.73	0.17	-0.90

Table 5.1 Carbon Black Electron Spin Concentrations and Mass Susceptibilities

Now that the microscopic parameters $\left(M_x, M_{x,cb}, f, \lambda_{cb}\right)$ have been determined from the analysis of an NMR spectrum from the deformed network $\left(\lambda = 1.8\right)$ they can now be used to generate the theoretical signal from the undeformed sample. Figure 5.5 compares the data from the unstrained network $\lambda = 1.00$ and the theoretical signal using the above found parameters.
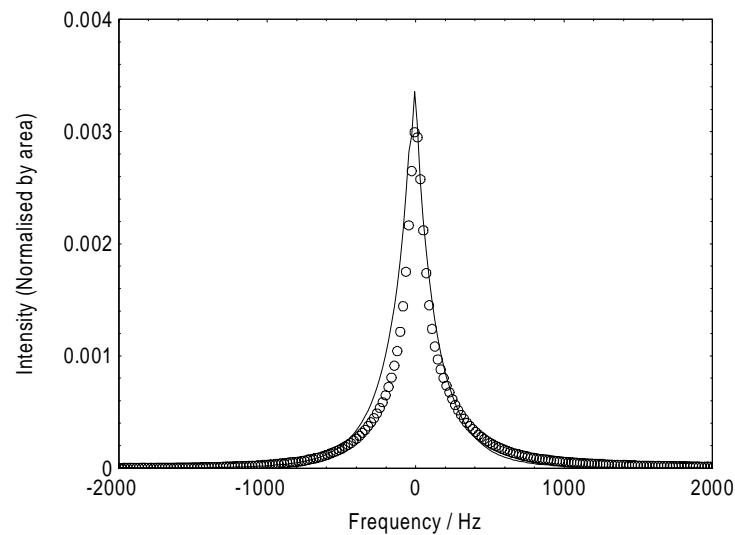

Figure 5.5 Solid line shows a no free parameter fit of Eqn. 5.2 to the NMR spectrum from the undeformed poly(butadiene) carbon black filled network.

For

a no parameter fit the theory compares favorably to the data. It would have been possible to achieve better fits by simultaneously fitting the NMR data from $\lambda = 1.00$ and the $\lambda = 1.80$ deformed networks, but current approach is a stronger test of this off-resonant component model.
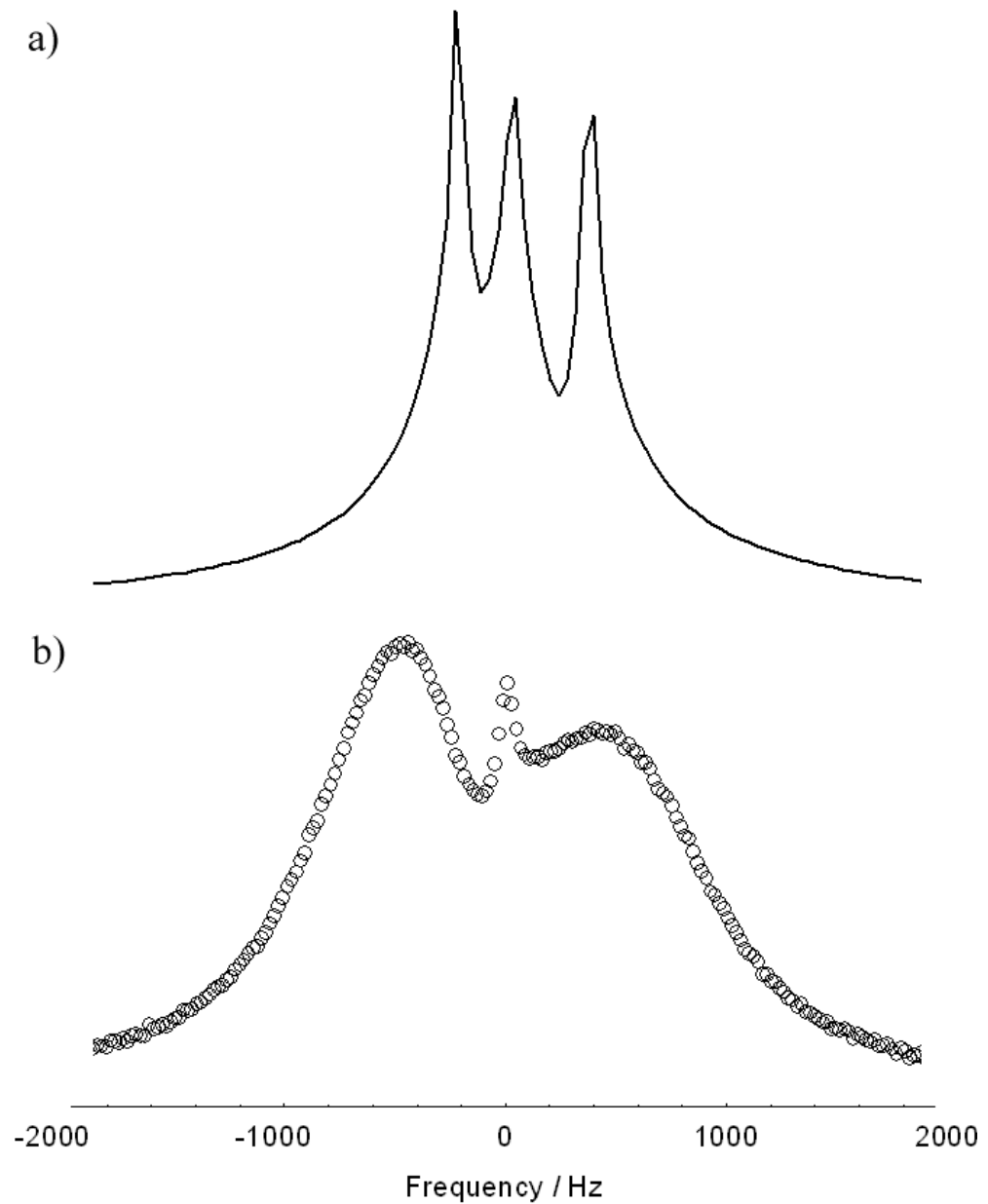

Figure 6 a) The theoretical spectrum from equation (**5.2**), with the parameters found from fitting the $\lambda = 1.80$ network data, predicts the emergence of a third peak to be found at high deformation $(\lambda = 2.5)$. b) This third peak is found experimentally at deformations of $\lambda = 3.00$ in the NMR spectra of the carbon black filled poly(butadiene) network.

It is possible to make a prediction using the current model and the microscopic parameters found from the analysis of the $\lambda = 1.80$ data. At sufficiently high enough deformations the splitting from the chains that are not closely attached to the carbon black particles should become large enough so as to reveal unambiguously the off resonance component. In Figure 5.6a the theoretical spectrum from a sample at deformation $\lambda = 2.5$, using the parameters found from the above analysis, is shown. Here a third peak can be seen in the theoretical response corresponding to the nearly isotropic off-resonance component. In Figure 5.6b the NMR spectrum measured from a network at a high deformation $\lambda = 3.00$ is shown. Here it can be seen that the experimental data does reveal this off resonance component, which qualitatively theoretical function **(5.2)** does. In this study it is not attempted to quantitatively analyse this data as the theoretical function used is only strictly correct for deformations $\lambda < 2$, which is within the validity of the Gaussian chain approximation.

CHAPTER 6

6.1 Molecular Dynamics and Orientation Measured by Sine Correlation Function (β - Function)

6.1.1 Introduction

A new NMR technique, which is a further development of the work done by Collignon et al.[72], was demonstrated by Callaghan et al.[73] that is suitable for the measurement of weak proton dipolar interactions in fluid polymers where rapid segmental dynamics pre-average the rigid lattice dipolar coupling. This method is especially applicable to polymer melts and networks, where such residual interactions can provide valuable information regarding molecular order and reorientational dynamics. The pulse sequence which is employed in this study directly generates a function β, which is zero in the absence of the dipolar interactions, which is completely independent of all Zeeman dephasing associated with chemical shifts or magnetic inhomogeneity, and whose time dependence can yield both the magnitude and the fluctuation rate of the residual dipolar interaction.

In this study, the above mentioned method was employed to deuterium nuclei in order to study the magnitude and the fluctuation rate of the residual quadrupolar interaction. The aim of this work is to investigate the latter properties using this method and compare the results with the same properties obtained by other methods (by deuterium NMR line splitting and by usual NMR relaxation). Also, it will be shown that this method is sensitive enough to detect different classes of interactions present in the polymer.

The β function experiment is composed of a single $90°_x$ pulse; solid echo sequences, $90°_x$ -τ- $90°_y$, $90°_x$ -τ- $90°_x$; and a Hahn echo, $90°_x$ -τ- $180°_y$, where, in the echo examples, τ is the time separating the rf pulses. In each case, it is allowed the density matrix that describe the nuclear spin ensemble will evolve under the influence of the two

offset terms in the Hamiltonian. The details of these evolutions are well known[74]. The superposition of above echoes and the single pulse, in order to create the β function, is as follows.

$$\beta(t,\tau) = [S_1(t,\tau) - S_2(t,\tau) - S_3(t,\tau)]/2S_3(0,0) \qquad \textbf{(6.1)}$$

Where

$$S_1(t,\tau) = 90^0_x - \tau - 90^0_y, \; S_2(t,\tau) = 90^0_x - \tau - 90^0_x, \; S_3(t,\tau) = 90^0_x - \tau - 180^0_y \; and \; S_3(0,0) = 90^0_x.$$

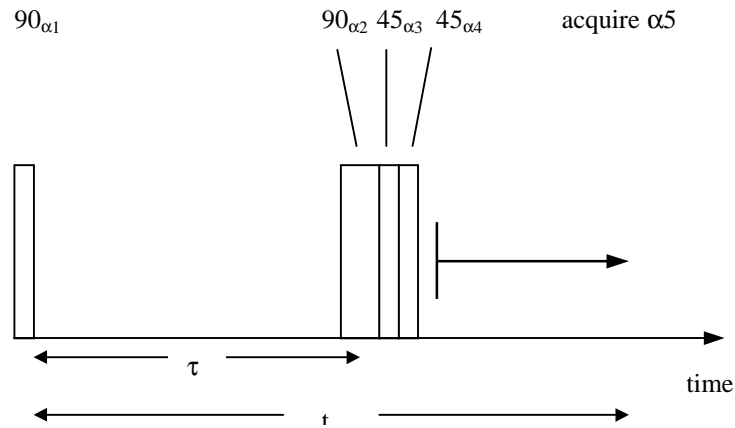This superposition signal is obtained using a single pulse sequence under appropriate phase cycling conditions.

Figure 6.1 The RF pulse sequence used to acquire the β(t,τ) fuction directly. The associated phase cycles are given in reference [cg1].

As the time t=2τ corresponds to the instant that the magnetic precessions are refocused in the spin echo, at this particular moment the effect of Zeeman precession (magnetic field inhomogeneities, chemical shift) vanishes. Therefore, the function β(2τ,τ) is well suited to investigate the weak dipolar interactions, quadrupolar interactions and their fluctuations without perturbations due to Zeeman effects. The exact expression for β(2τ,τ) is derived as[75]

$$\beta(2\tau,\tau) = \exp\left\{-2\overline{Q}_2\,\tau_s^2\left[\exp(-\tau/\tau_s)-1+\tau/\tau_s\right]\right\} \times \sinh\left\{\overline{Q}_2\,\tau_s^2\left[1-2\exp(-\tau/\tau_s)+\exp(-2\tau/\tau_s)\right]\right\},$$

<div align="right">(6.2)</div>

where $\overline{Q}_2$ is residual quadrupolar second moment and τ_s is slow correlation time of the isotropic slow segmental motion.

In many papers[20,73,76,80] a more simple expression, $\sim \tau^2 \exp(\tau/\tau_s)$, is used for the relaxation with the assumption of $\tau \leq (\overline{Q}_2)^{1/2}$.

6.1.2 Experimental and Fitting Procedure

The radio frequency pulse sequence shown in Figure 6.1 was employed to obtain experimental data for the β-function. Indeed, the first combination of the pulse sequence (i.e. S_1-S_2-S_3) was applied first and the pulse $S_3(0,0)$ was applied as the second. The final result (i.e. $\beta(2\tau,\tau)$) was obtained by dividing the maximum point of the result of the first pulse combination by maximum point of the result of the pulse $S_3(0,0)$. 90° radio frequency pulse was approximately 5μs. τ was arrayed between the values 2×10^{-5}s and 0.1s.

An Origin program was written to generate the function (**6.2**). Experimental data were fitted using the latter program by keeping the parameters $A = \overline{Q}_2\,\tau_s^2$, $B = 1/\tau_s$ and C as the weighting factor. The correlation time is determined from B and then from A the residual second moment is calculated. Since the aim here is to calculate the residual quadrupolar interaction v_0, it is necessary to estimate the fraction q of the residual second moment to static second moment $\overline{Q}_{2S}$, which is certainly also the fraction of v_0/v_q, where v_q is the static quadrupolar coupling constant. q is given by[76]

$$q^2 = \frac{\overline{Q}_2}{\overline{Q}_{2S}} \quad .$$ (6.3)

It can be shown that $\overline{Q}_{2S} = (1/5)(\Delta v_S)^2$, where Δv_S is the distance between the two maxima of the NMR powder spectrum which can be measured below glass transition temperature T_g. For methylene deuterated PB it was found[20] that $\Delta v_S = 123$ kHz. The relation between v_q and Δv_s is[39]

$v_q = \frac{4}{3}\Delta v_s$, which give the value for v_q as 165 kHz.

Fitting of the experimental data to equation (**6.2**) lead to estimate $\overline{Q}_2$ and hence q was determined using equation (**6.3**). For the consistency of further discussions it is defined an order parameter S which has value of q.

6.1.3 Results and Discussion

It is discussed here qualitatively the experimental results of the $\beta(2\tau,\tau)$ measurements and their fittings to the theoretical expression (**6.2**). The major aim of this section is to extract information about residual quadrupolar interaction v_0 and its fluctuation, using $\beta(2\tau,\tau)$, and to compare the results with the same properties investigated by using deuterium NMR line splitting and transverse relaxation methods.

Since $\beta(2\tau,\tau)$ starts from near to zero, reach to a maximum value and then decay to zero with time, it is more appropriate for a fitting procedure. Because of the fact that this function exhibits a high degree of sensitivity to the precise nature of dynamics (expressed via correlation function), it is argued that this sensitivity is significantly greater than that found in the measured quantities for other NMR methods which provide information about the strength and fluctuation of dipolar/quadrupolar interactions[77].

Sample	τ_s (ms)	$\overline{Q}_2 .10^{-6}$ (s^{-2})	$S .10^3$	ν_0 (Hz)
CD2A_L0 λ=1.0	62	4.1	5.4	912
CD2A_L1 λ=1.6	100	4.3	5.6	937
CD2A_L2 λ=2.2	20	6.0	7.2	1207
CD2B(first part)	23	1300	103	17000
CD2B(second part)	9	1.3	3.3	559
CD2Freechains M_n=25000 g/mol	100	5.3	5.4	910
AD1 network	58	6.5	7.4	1225
AD2 "	15	6.6	7.3	1210
AD3 "	18	7.5	7.8	1299
AD4 "	10	7.5	7.8	1301
CD2network+free ^{1}H chains (first part)	8	2438	141	23396
CD2network+free ^{1}H chains (second part)	40	2.5	5.8	965

Table 6.1 Results from the fitting of experimental data to the equation.(**6.2**).

The experimental and fitting results of $\beta(2\tau,\tau)$ are discussed in a way that to clarify the latter mentioned ability of $\beta(2\tau,\tau)$ in recognising discrete dynamics, in the PB networks and melts. To illustrate this point, firstly, the results obtained from CD2A network were presented (see Figure 6.2). $\beta(2\tau,\tau)$ was investigated at different deformation ratios of the network, as shown in Figure 6.2 (a), (b) and (c). It is worth to state here that the maximum amplitude of $\beta(2\tau,\tau)$ is a property which is independent on the interaction strength and which depend only on the functional form of time dependence[75,77]. Hence the observed maximum amplitude of the experimental $\beta(2\tau,\tau)$ data will give an idea about the nature of the dominant dynamics in the network. It is also important to note that this height will be sensitive to all dynamical regimes, not just that prevailing at the observational time scale τ.

As one can clearly note in Figure 6.2, there exist an additional broadened maximum at higher τ values (see Figure 6.2(a)) in addition to the major maximum. This broadened second maximum get slightly narrow and move to the left on τ axis with increasing deformation ratio, as show in Figure 6.2 (a), (b) and (c). We argue that if the polymer network contains regions with different chain dynamics, $\beta(2\tau,\tau)$ can detect them and reflect as additional maxima to the major one. This additional maxima can be either side of the major maximum, depending on their dynamics.
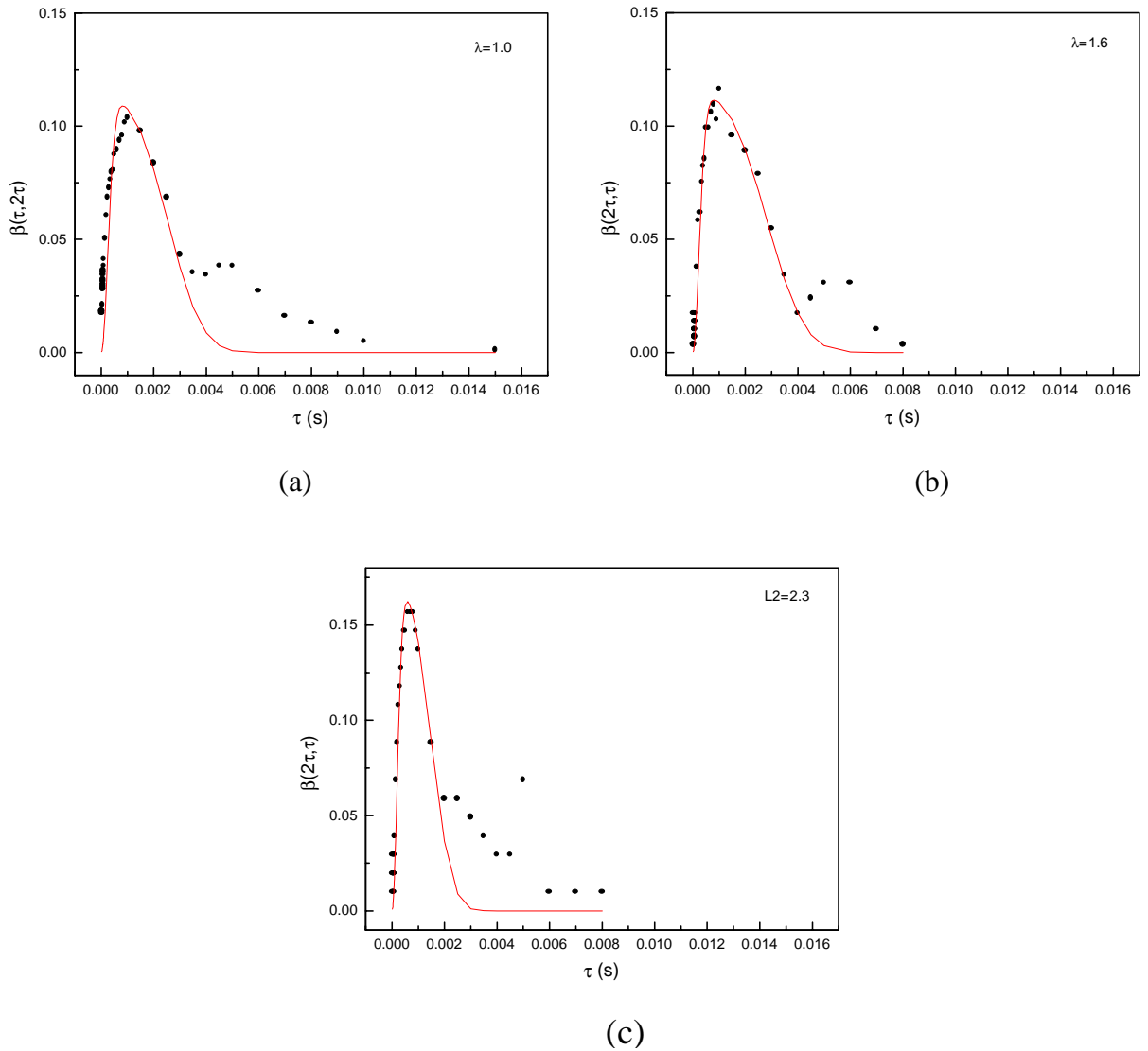

(a)

(b)

(c)

Figure 6.2 Fits of the Beta function (equation **6.2**) to the experimental data obtained from cis PB network (CD2A) under different deformation ratios.

Also it is important to note that in order to derive the expression (**6.2**) it was used the exponential correlation function $C(t) = \overline{Q_2}\exp(-t/\tau_s)$ and this is related to the isotropic slow chain motion, or in other words, to the long-range center-of-mass motion. However, the hierarchy of motions and their correlation functions are well described by Callaghan et al.[77].

From the other NMR methods which were used in this study (deuterium NMR and usual transverse relaxation), one could probably get the information about the dominant dynamics in the network. Therefore, for the comparison, the major maximum of the $\beta(2\tau,\tau)$ experiments were considered for the discussion.

However, before starting of the discussion of the latter subject the attention was paid to Figures 6.3 and 6.4 in order to strengthen the idea about the possible sub-dynamics which can be detected by $\beta(2\tau,\tau)$ experiments. Figure 6.3 shows the experimental and fitted results of $\beta(2\tau,\tau)$ for the network CD2B (refer to Table 2.1 to learn the details of the network samples).
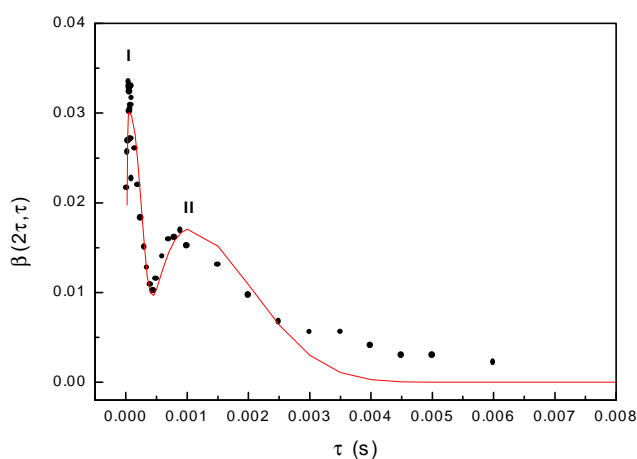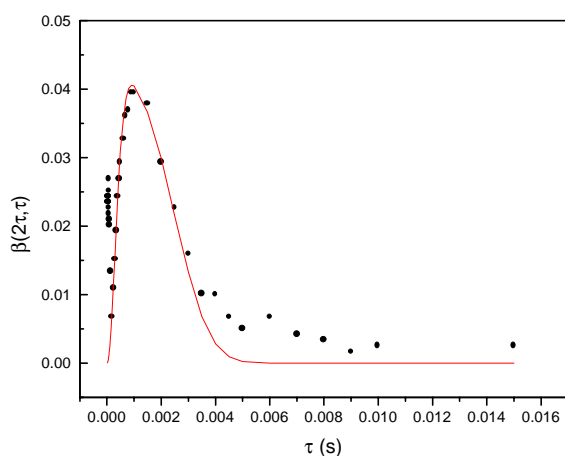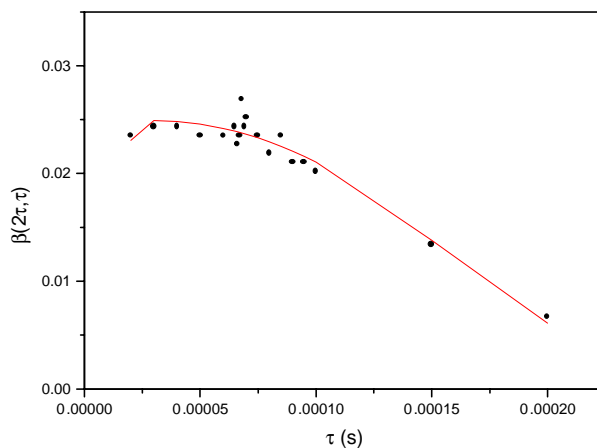

Figure 6.3 Fits of the Beta function (equation **6.2**) to the experimental data obtained from cis PB network (CD2B). The two peaks (I and II) reveal two distinguishable dynamics in the polymer network.

Obviously, there are two maxima named as I and II. Experimental data were fitted by using an addition of two $\beta(2\tau,\tau)$, each contained different $\overline{Q_2}$ and τ_s parameters. According to the fitting results, peak I corresponds to a region of polymer which is much more solid like (obtained $\nu_0 \sim 17$ kHz).

(a)

(b)

Figure 6.4 (a) Fit of the Beta function (equation **6.3**) to the experimental data obtained from CD2 network which is incorporated with high amount of free protonated PB chains (b) The fit for the peak at very small time scale shown in (a).

In Figure 6.4(a), one can see the results of $\beta(2\tau,\tau)$ obtained from a polymer network which was swollen to a higher degree by incorporating protonated free chains(M_n=1800 g/mol) (refer to Table 6.1 and to the section Chapter 4). Much narrow maximum was observed in the short time scales (short τ values). This region was expanded and fitted to the $\beta(2\tau,\tau)$ as shown in Figure 6.4(b). As expected the fitting resulted in a high value of residual quadrupolar interaction ($\nu_0 \sim$23 kHz) indicating a highly solid like behaviour. Indeed, the polymer sample was more solid like by the appearance one could break it simply by bending. The discussion on the sub-dynamics which can be detected by $\beta(2\tau,\tau)$ will be stopped here.

Hereafter, the discussion is mainly on the major maxima which were observed in $\beta(2\tau,\tau)$ experiments. Once again the attention would be paid to the Figure 6.2 which represents the results obtained at different deformation ratios. The macroscopic deformation applied to the network increases the degree of orientation of the polymer chains resulting more solid like behaviour. The $\beta(2\tau,\tau)$ maximum moves slightly to the left, that is to the region of low τ values, when the deformation was increased. This confirms the major idea which was discussed in last two paragraphs, and similar results from deformed polymer networks were reported by Callaghan et al[73].

Fittings of $\beta(2\tau,\tau)$ to the experimental data in Figure 6.2(a), (b) and (c) resulted in giving an increasing value of ν_0 when the deformation was increased, as was expected (see Table 6.1). In other words, this analysis shows a monotonous increase in the value of $\overline{Q}_2$ and hence in the values of ν_0 with the increasing deformation. The reliability of τ_s values derived from fittings appears to be robust. For example, the τ_s values were independent on the magnitude of $\overline{Q}_2$. However, it is not obvious what kinds of deformation dependent dynamical processes are responsible for the behaviour of the correlation[73]. The 2nd maximum of Figure 6.3 and Figure 6.4(a) gave the values of the ν_0 which are comparable with the similar property investigated from CD2A network,

indicating that it was the responsible maximum which gives the dynamics and orientation that are comparable with other networks.
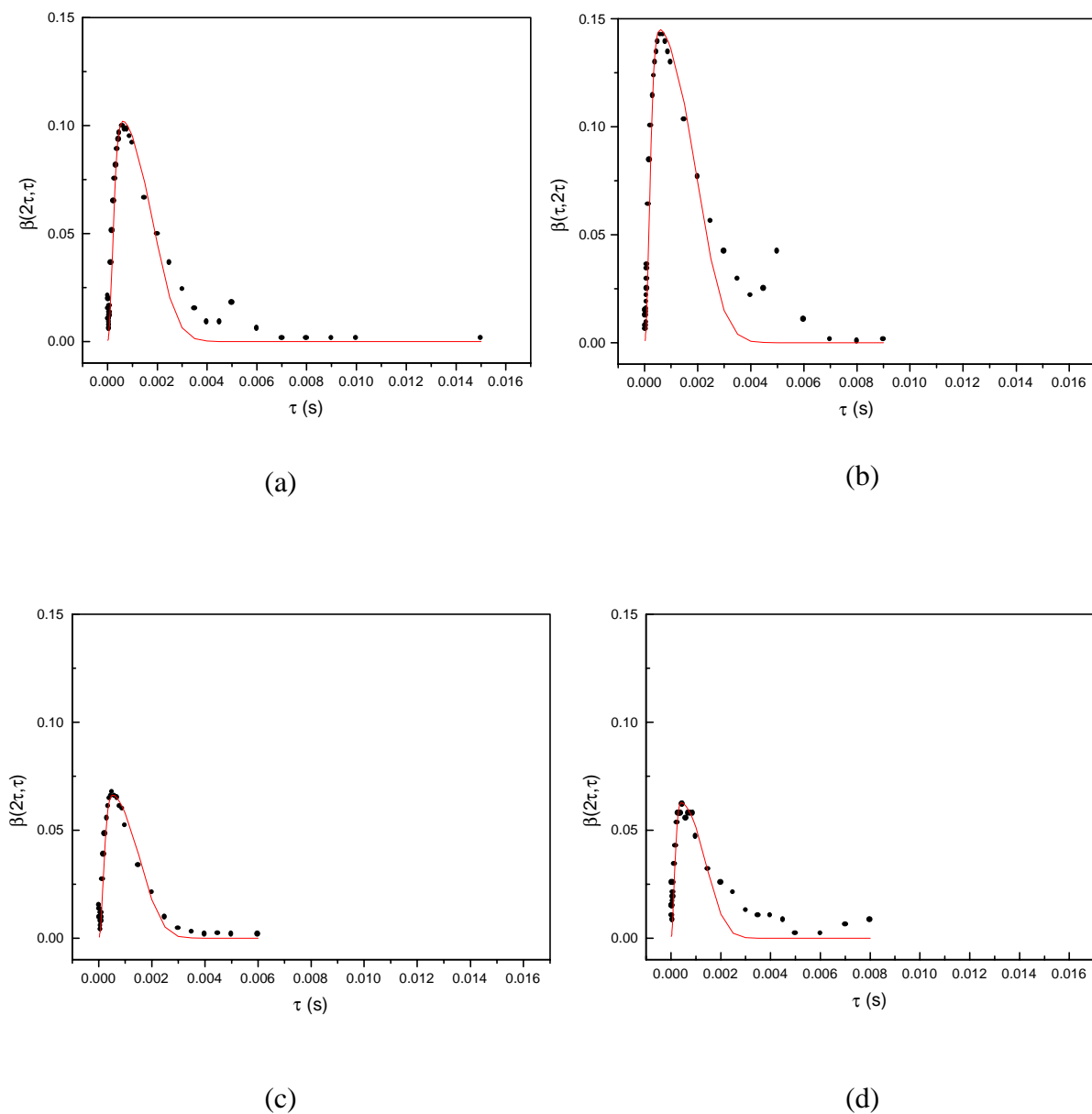

(a)

(b)

(c)

(d)

Figure 6.5 Fits of the Beta function (equation **6.3**) to the experimental data obtained from anionic PB networks. (a): AD1 (b): AD2 (c): AD3 (d): AD4.

A series of anionic PB networks were subjected to investigate $\beta(2\tau,\tau)$ and are shown in Figure 6.5. The length of the precursor chain was varied in this prepared anionic PB networks as AD1 has the longest and AD4 has the shortest deuterated precursor chains (see Table 2.1). Mean molecular mass between two crosslinks M_c is above the entanglement length (~1900 g/mol) for all the four networks as shown in Table 6.1, and hence the effect of M_c must be less dominant. Accordingly, the observed ν_0 values were ranging from 5200 Hz to 7900 Hz. ν_0 was decreasing slightly with increasing precursor chain length. This changes would be due to the different M_c values. However, the ν_0 values obtained from relaxation were by a factor of 2 to 4 less than that observed from $\beta(2\tau,\tau)$. In the relaxation experiment the most important information is concentrated at the beginning of the relaxation curve. Therefore, in case, if one or few first data points were missed (due to the receiver dead time), most of the information would be probably lost (especially the information about highly oriented or solid like features) and hence gives rise to a low ν_0 values.

Also this networks were used to observe deuterium line splitting and then to determine the ν_0 (see Chapter 4). The results obtained from the latter method were in good agreement with the results obtained from $\beta(2\tau,\tau)$ and hence give strong evidence for the correctness of the theoretical framework presented in Chapter 3 to explain the deuterium NMR line splitting.

CHAPTER 7

7.1 Orientation and Dynamics of Polymers Measured by Employing Relaxation from Hahn-Echo

7.1.1 Introduction

In this chapter it will be discussed an another method presented by Simon et al.[20] for investigating the local order and dynamics of polymers well above glass transition temperature. Also the results from this method will be compared with results discussed in Chapter 3 and Chapter 6.

Firstly, it will be recapitulate the basic ideas for the interpretation of the relaxation of the transversal proton magnetisation in polymer networks well above T_g in terms of a modified single-chain approximation[78]. The second step will be a comparison with the deuteron relaxation.

7.1.2 The Transverse NMR Relaxation Function

Since transversal ^{1}H-NMR relaxation is determined by the dipolar magnetic interaction of protons, a motional averaging of this interaction and, consequently, the nuclear motions itself are detectable in this way. Therefore, at $T>T_g$ a contrast in such a relaxation picture of a polymer network can be formed by different mobile molecular parts which produce separate relaxation signals of different form and/or length. In Figure 7.1 a rough sketch illustrates the principal different mobile parts.

Most of the chains are inter cross-linked chains. As a first step they could be thought of as fixed at both ends. In this case the motional statistics provides a mean, small anisotropy of the fast local motion[78] (correlation time $\tau_f \approx 10^{-8}$s) of the chain segments.
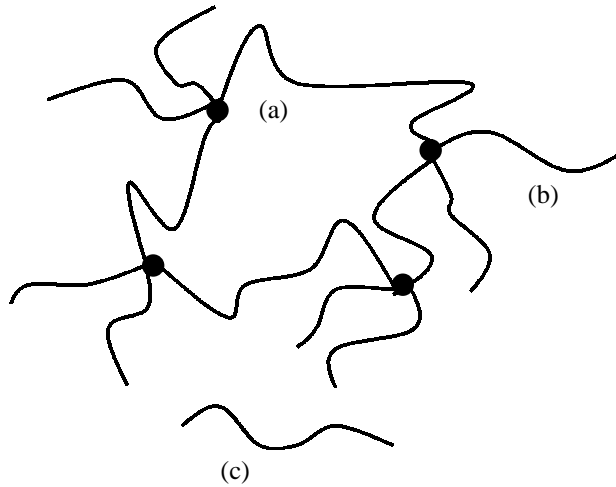
Figure 7.1 A schematic representation of the different mobile molecular parts in a polymer network (a) inter-crosslink chains (b) dangling chain ends (c) sol molecules.

Consequently, a small, mean residual part q' ($q' \approx 10^{-4}$) of the second moment M_2 of the dipolar interaction in the rigid lattice[1] (T<T_2) remains. The residue can only be destroyed by an overall isotropic motion of the whole inter cross link chain. This motion is much slower ($\tau_s \approx 10^{-3}$s) as a result of the larger size of the moving object.

For dangling chain ends a reason for an anisotropy of the local motion (also τ_f) does not exist (q'=0), and so τ_s cannot be detected. Connecting this dynamical model with the NMR theory of the transversal magnetic relaxation, a sum of two relaxation components follows according to the two dynamical types of chains of a network.

7.1.2.1 Dangling Chain Ends

Since $x^2 = (2\pi f_0 \tau_f)^2 \leq 1$ (liquid like, f_0 - resonance frequency) and q=0 is valid for chain ends, this component of the decay can be described by BPP (Bloembergan,

Purcell, and Pound)[79,80] theory. Consequently, this component is purely exponential function of the type $\exp(-t/T_2)$ with the transversal relaxation rate $1/T_2$ (BPP) formula:

$$1/T_2 = M_2\tau_f \left[1 + (5/3)/(1+x^2) + (2/3)/(1+4x^2)\right] \quad . \tag{7.1}$$

It must be emphasised that this formula was established by assuming an intramolecular interaction of single spin pairs and an isotropic rotary motion of these pairs. The real case of more than two interacting nuclei is taken into consideration by assuming that spins are fixed at the Kuhn statistical segments[78]. Under these circumstances the resulting decay should remain exponentially[79].

Therefore, the τ_f values, which are derived according to equation (**7.1**), are effective values and represent an average over several closely attached interacting spin pairs mainly along the monomeric unit.

7.1.2.2 Inter-Crosslink Chains

The inter-crosslink component is influenced by the fast anisotropic motion as well as by the slow isotropic motion. Since $x^2 = (2\pi f_0\tau_f)^2 \leq 1$ (liquid like) and $x^2 = (2\pi f_0\tau_f)^2 \gg 1$ (solid like) is valid, the relaxation function has to be described by a combination of the BPP theory[1,79] and the Anderson-Weiss formula[1]. The latter takes into consideration the residual solid like behaviour ($q' \neq 0$) and leads to a shortening of the decay and to an observable deviation from a simple exponential decay form (Gaussian-like). According to Anderson-Weiss the magnetisation decay is given by

$$M(t) \sim \exp(-\int_0^\infty G(\tau)(\tau-t)d\tau) \quad . \tag{7.2}$$

The correlation function $G(\tau)$ should reflect the fact that the fast local motion is anisotropic and cannot eliminate the dipolar interaction (M_2) totally:

$$G(\tau) = M_2 \left[(1-q')\exp(-\tau/\tau_f) + q'\right]\exp(-\tau/\tau_s)$$

$$\approx M_2 \exp(-\tau/\tau_f) + q'M_2 \exp(\tau/\tau_s) \quad . \qquad (7.3)$$

The latter expression is valid since $\tau_f \ll \tau_s$ and $q' \ll 1$.

7.1.2.3 Total Relaxation Function

Including equation (**7.2**) and (**7.3**) and all the above dynamical and structural assumptions, it follows for the total transversal magnetisation decay that

$$M(t) = A\exp\left[-t/T_2 - q'M_2\tau_s^{\,2}(\exp(-t/\tau_s) + t/\tau_s - 1)_s\right] + B\exp\left[-t/T_2\right] \qquad (7.4)$$

with $1/T_2 = M_2\tau_f$. The latter expression is identical with the more general formula of equation (**7.1**) if $(2\pi f_0 \tau_f)^2 \gg 1$ (slow motion). That is the point of the formal combination of BPP and Anderson-Weiss: $1/T_2$ will always be identified with equation (**7.1**). A and B are the portions of proton magnetisation (equivalent to mass portions) of the inter cross link chains and dangling chain ends, respectively.

For the transversal ^{2}H-NMR quadrupolar relaxation the principal formalism[1] is the same. However, from the theoretical point of view the advantage of this relaxation is the fact that most of the formulas, equations (**7.1-4**) (with changes indicated below) are valid more strictly since the quadrupolar interaction is restricted to the C-^{2}H bond and corresponds to a "single proton pair" interaction. The second moment of dipolar interaction M_2 must be replaced by the second moment of the quadrupolar interaction $\overline{Q_{2s}}$. The resonance frequency f_0 is 61.3 MHz for deuterons.

An order parameter S can be defined as $\qquad S = \left(\dfrac{q'\overline{Q_{2s}}}{\overline{Q_{2s}}} \right)^{1/2}$.

The transversal magnetisation decay of deuteron was measured by the common Hahn spin-echo technique which eliminates inhomogeneities of the magnetic field and of the chemical shift.
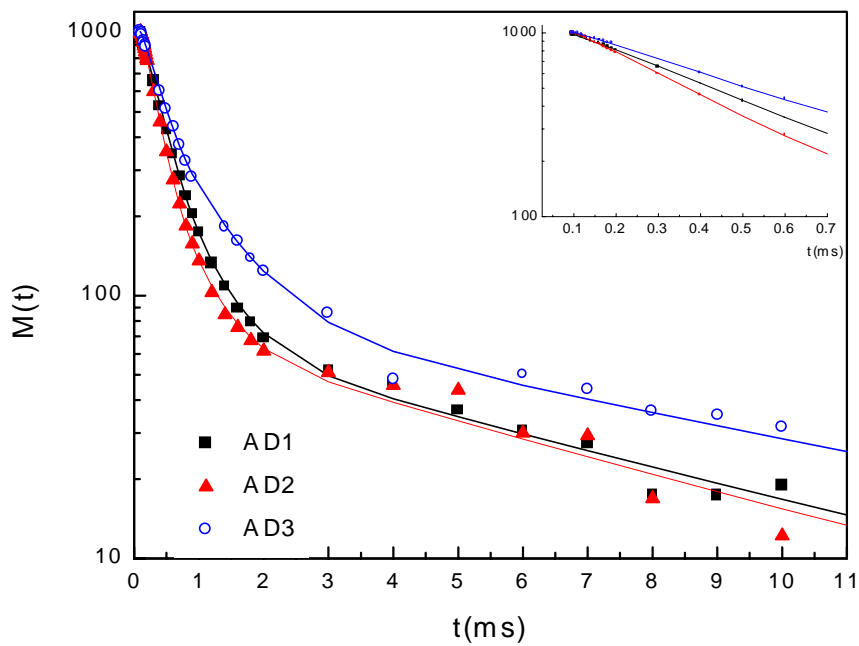
7.1.3 Results and Discussion

Figure 7.2 Fits of the equation (**7.4**) to the experimental data. Top right of the figure shows the fitting curves in short time region. ■ - AD1, ▲ - AD2, ○- AD3

Figure 7.2 shows relaxation data after Hahn echo experiment and the fits to the equation (**7.4**). At the top right of the latter figure it is shown fit curves in the short time region. If one looks at the table 2.1 it can be found that AD2 has the highest M_c value among these three samples while AD1 has the intermediate and AD3 has the lowest M_c

Sample	Relaxation (Hahn-Echo)			
	τ_s (ms)	$q´Q_2 \cdot 10^{-6}(s^{-2})$	$S \cdot 10^3$	ν_0 (Hz)
CD2B	100	4.1	6.0	970
AD1	100	26	15.0	2438
AD2	100	31	16.0	2663
AD3	100	19	13.1	2085
AD4	100	18	12.1	2029

Table 7.1 The parameters obtained by fitting equation (**7.4**) to the data obtained from relaxation.

values. Accordingly, in Figure 7.2, it can be noticed that the magnetisation from AD2 relaxes faster than that of the others. Due to the high crosslink density of AD2, polymer chains experience more constraints and therefore shows the solid like behaviour. On the other hand the polymer sample AD3 relax slowly showing experiencing less constraints. Results from the fitting are shown in Table 7.1. The behaviour of the fast decay at the very short time scales (Figure 7.2) influence strongly to the parameters determined by fitting the relaxation function (**7.4**) to the data.

7.2 A Brief Comparison of Results

7.2.1 Introduction

In this chapter the results obtained from the three different methods, which were already explained in Chapter 3, 6 and 7, are discussed. The main focus is to the residual quadrupolar interaction v_0 observed from these methods. Approaches of the different methods is briefly analysed in order to understand the final results.

7.2.2 Background of the Methods, and Comparison of the Results

In Chapter 3, an analytic result (**3.10**) was derived that takes into account two contributions to the total orientation of the constituent polymer chains. It was found that the free induction decay readily separates the effect of chain interactions with their environment from that of the network constraint, i.e. the presence of crosslinks within the rubber matrix, on the polymer segmental anisotropy. The residual quadrupolar interaction v_0 is extracted from the fitting of the analytical expression to experimental data as a ratio of v_0 / N. Here N is the number of statistical segments between two effective crosslinks. Hence, the result is giving the residual quadrupolar interaction which is rescaled to the N. In this chapter, v_0 itself is an averaged quadrupolar interaction which is rescaled to number of monomers per statistical segment N_a. This primary averaging has done in an earlier study[39] by employing computer simulations. In that study v_0 is expressed as

$$v_0 = \frac{3}{2}\frac{\kappa}{4}\frac{v_q}{N_a} \quad ,$$
(8.1)

κ is the constant to be found by employing the simulations using the expression:

$$\left\langle P_2(\cos v)\right\rangle = \frac{\kappa}{N_a}P_2(\cos\theta) \quad ,$$
(8.2)

where υ and θ are the angles that C-D bond and a segment make with the applied magnetic field (Figure 1.5). In fact (**8.2**) compares averaging of two fast dynamics of the C-D bond and the statistical segment.

For methylene deuterated poly(butadiene), it was found[39] the value of κ as 0.55 and N_a as 4.4 and hence giving the value of 7730 Hz to ν_0.

However, in the derivation of the beta function[73,75,77] (Chapter 6) there exist no such primary rescaling. It takes into account the slow re-orientation of a chain in which the both ends are crosslinks. This chain is divided into small sub-units in order to rescale the residual interaction of a bond. Latter sub-units seem to be approximately the number of monomers between two crosslinks. In this manner the residual interaction of the bond is directly rescaled to a chain which consists of a certain number of sub-units. It is the similar scaling procedure used in the model explained in Chapter 7, which is based on relaxation[20]. Therefore, it is difficult to compare straightforward the results from above three models. However, one can discuss qualitatively the trend of the results.

	Line Splitting	β - Function		Relaxation	
	ν_0 / N (Hz)	ν_0 (Hz)	τ_s (ms)	ν_0 (Hz)	τ_s (ms)
AD1	5200	1225	58	2438	100
AD2	5100	1210	15	2663	100
AD3	3800	1299	18	2085	100
AD4	3700	1301	10	2029	100

Table 8.1 The residual quadrupolar interaction determined by employing three different methods for anionic polymer samples. All the residual interactions stated here are rescaled values although only in the first case (line splitting) it is indicated up to which stage it is rescaled.

Table 8.1 compares some of the results from the three models. Residual quadrupolar interaction determined by usual relaxation and β function seem agree qualitatively each

other. These values remain more or less constant although the network structure of the anionic poly(butadiene) samples slightly differs.

In contrast, the result obtained from NMR line splitting seems sensitive to this difference of the network structure. Polymer sample AD1 is prepared with the longest precursor chains, the length of it is reduced consecutively for AD2, AD3 and AD4. Therefore, one can expect a heavier entangled situation for AD1 and reducing the effect for others. Effect of the different entangled situation is to give different values for the N through the effective molecular mass M_x, the lowest value for AD1 while the highest value for AD4. This difference of the values of N gives feasibility to understand the reducing values of v_0 / N from AD1 to AD4. In any case the residual interaction observed from this method is almost two times higher than the results from the other methods.

τ_s represents an apparent correlation time of slow motion of the entire chain. Both β function and relaxation models constructed without taking into account a correlation time distribution. However, in networks there exists a distribution of chain lengths between crosslinks. The results observed for τ_s do not show any systematic trend.

CONCLUSIONS

NMR has been used to measure the orientation of chain segments within deformed poly(butadiene) networks. An analytic result was derived that takes into account two contributions to the total orientation of the constituent polymer chains. It was found that the free induction decay readily separates the effect of chain interactions with their environment from that of the network constraint, i.e. the presence of crosslinks within the rubber matrix, on the polymer segmental anisotropy. This makes NMR a useful complementary tool to techniques such a birefringence that measure the total average orientation.

The theoretical NMR relaxation function from a strained network was found to consist of an oscillation within a decay envelope. The oscillation is related to the anisotropy stemming from the interactions of the chains with their environment. This interaction of a monomer with its many surrounding segments can be described by an effective mean field[34]. Under deformation this mean field becomes anisotropic in nature[31]. The frequency of the oscillations in the signal is directly related to the magnitude of the induced orientation from this mean field through equation (**3.10a**). Therefore the splitting in frequency space is indicative of chain interactions. In contrast the decay envelope is specified by the distribution of network vectors in the rubber.

The analytic result for the NMR response of a strained network was compared to experimental data from a range of deformed poly(butadiene) rubbers. It was found that the theoretical decay modelled the data well, until the deformation became too large $\lambda \sim 2$. Here assumptions such as the affine deformation of effective crosslink points are expected to break down[63].

The theoretical decay envelope is fully specified by the crosslink density through (**3.10**). A value of ~1000g/mol was required to fit the experimental signals, with this comparing well with the mechanical tests on the same sample[19]. This analytic result therefore allows NMR to monitor crosslink density.

It was found that the contribution to the orientation from the mean field corresponded to a ~30% perturbation from the non-interacting case. Brereton and Ries[31] have attributed this anisotropic mean field to the excluded volume interactions between chain segments. The contribution from this mean field was expressed in terms of an Edwards' screening length via equation (**3.15**). By comparing the λ dependence of this contribution with their theoretical predictions, Figure 3.3, it was possible to determine an Edward's screening length of $2.5\overset{o}{A}$. This indicates that at distances greater than that of one or two bond lengths the excluded volume interactions are screened.

The ability of the theoretical NMR result to measure a crosslink density that compares well with mechanical tests and a screening length of a reasonable size, strongly supports the use of this framework to interpret the NMR response from strained elastomers.

The NMR line splitting is found to be depend on the network concentration and also on the Flory interaction parameter χ. It is shown that one should take into account not only the χ parameter arising from different chemical structures but also that arising from the crosslinks of the network, in order to explain the experimental NMR line splitting. The latter is found to be proportional to $1/\sqrt{T}$. The Edward's screening length is found to be independent of precursor chain length and crosslink density.

It is shown that the asymmetric NMR spectra observed from strained filled networks could be explained by considering the susceptibility of the carbon black particles. Polymer segments closely associated with the filler particles experience a different local field and contribute an off-resonance term to the free induction decay. In the NMR spectrum this appears as a frequency shifted component relative to the non closely attached chain signal. The resultant spectrum is then asymmetric.

We applied the theoretical work (equation **3.10)** to model the NMR lineshapes quantitatively. A very simple approach was adopted in that the signal was considered to comprise of only two components; polymer segments closely attached to the carbon black particles and those that are not. It was found that the signal from the attached chains needed to be off resonance by -50Hz, with this comparing extremely well with susceptibility measurements on carbon black[64]. The crosslink density determined from this analysis was in close agreement with the stress-strain measurements on this sample[19]. The fraction of signal attached to the carbon black was found to be 28% with this being in reasonable agreement with other NMR work on similar filled networks[70]. An interesting point is that the chains attached to the carbon black experience a different local deformation to that from the bulk sample, with these segments remaining isotropic.

As a test of this two component model we used the parameters determined from the analysis of the $\lambda = 1.8$ data to predict the undeformed network result. It was found that for a no free parameter fit that the theory and data were in good agreement. It is interesting to note that the undeformed sample shows little asymmetry and that this off-resonance component also theoretically remains somewhat hidden at low deformations.

From our model a prediction was made that at high deformations the isotropic off-resonance component will become visible as a third peak in the NMR spectrum. This was illustrated qualitatively by the theoretical function (eq 5.2) in Figure 5.6a. In Figure 5.6b data from a highly deformed filled network $\left(\lambda = 3.0\right)$ is shown for comparison, where this predicted third peak can clearly be seen.

The sine correlation function (introduced by Callaghan et al.)[73,75,77] and the NMR relaxation function (introduced by Simon et al.)[20] were also employed to study the NMR response of the poly(butadiene) networks and linear chains. The residual quadrupolar interaction determined by all the above mentioned procedures was compared. It is shown that the results from sine correlation function and conventional NMR relaxation show the same tendency though they differ in the numbers.

REFERENCES

1. Abragam, A. *Principles of Nuclear Magnetism* 1961, Clarendon Press, Oxford.

2. Brereton, M. G. *J. Chem. Phys.* 1991, **94**, 213.

3. De Gennes, P. G. *Scaling Concepts in Polymer Physics* 1979, Cornell University, Ithaca.

4. Cohen-Addad J. P.; Dupeyre, R. **Polymer** 1983, **24**, 400.

5. Cohen-Addad J. P. *ibid.* 1983, **24**, 1128.

6. Cohen-Addad J. P.; Guillermo, J. *J. Polym. Sci.* 1994, **22**, 931.

7. Cohen-Addad J. P.; Feio, G. *ibid.* 1984, **22**, 957.

8. Cohen-Addad J. P.; Domard, M.; Herz, J. *J. Chem. Phys.* 1982, **76**, 2744.

9. Harris, R. K. *Nuclear Magnetic Resonance Spectroscopy* 1983, Pitman Books Limited, London.

10. Sotta, P.; Deloche, B.; Herz, J. *Polymer* 1988, **29**, 1171.

11. Cohen-Addad J. P. *J. Chem. Phys.* 1974, **60**, 2440.

12. Cohen-Addad J. P. *Prog. NMR Spectrosc.* 1993, **25**, 1 and references therein.

13. Deloche, B.; Samulski, E. T. *Macromolecules* 1981, **14**, 575.

14. Deloche, B.; Beltzung, M.; Herz, J. *J. Phys. Lett.*1982, **43**, 1763.

15. Sotta, P.; Deloche, B. *Macromolecules* **1990**, **23**, 1999.

16. Samulski, E. T. *Polymer* 1985, **26**, 177.

17. Nakatani, A. L.; Poliks, M. D.; Samulski, E. T. *Macromolecules* 1990, **23**, 2686.

18. Lechner, M. D.; Gehrke, K.; Nordmeier, E. H. *Makromolekulare Chemie* 1993, Birkhäuser Verlag, Basel.

19. Matzen, D.; Straube, E. *Colloid & Polym. Sci.* 1992, **270**, 1.

20. Simon, G.; Baumann, K.; Gronski, W. *Macromolecules* 1992, **25**, 3624.

21. Gronski, W.; Stöppelmann, G. *Teubner-Texte Phys.* 1986, **9**, 148.

22. Deloche, B.; Dubault, A.; Durand, D. *J. Polym. Sci. Part B: Polym. Phys.* 1992, **30**, 1419.

23. Litvinov, V.; Spiess, H. W. *Makromol. Chem.* 1992, **193**, 1181.

24. Sotta, P.; Deloche, B. *J. Chem. Phys.* 1994, **100**, 4591.

25. Klinkenberg, M.; Blümler, P.; Blümich, B. *Macromolecules* 1997, **30**, 1038.

26. Sotta, P. *Macromolecules* 1998, **31**, 3872.

27. McLoughlin, K.; Waldbieser, J. K.; Cohen, C.; Duncan, T. M. *Macromolecules* 1997, **30**, 1044.

28. Brereton, M. G. *Macromolecules* 1993, **26**, 1152.

29. Warner, M.; Callaghan, P. T.; Samulski, E. T. *Macromolecules* 1997, **30**, 4733.

30. Sotta, P.; Deloche, B.; Herz, J.; Lapp, A.; Durand, D.; Rabadeux, J. C. *Macromolecules* 1987, **20**, 2769.

31. Brereton, M. G.; Ries, M. E. *Macromolecules* 1996, **29**, 2644.

32. Brereton, M. G. *Macromolecules* 1991, **24**, 6160.

33. Edwards, S. F. *J. Phys. A: Math. Gen.* 1975, **8**, 1670.

34. Doi, M.; Edwards, S. F. *The Theory of Polymer Dynamics*; Clarendon Press: Oxford, 1986.

35. Gottlieb, H. E.; Luz, Z. *Macromolecules* 1984, **17**, 1959.

36. Deloche, B.; Dubault, A.; Herz, J.; Lapp, A. *Europhys. Lett.* 1986, **1**, 629.

37. Sotta, P.; Deloche, B.; Herz, J. *Polymer* 1988, **29**, 1171.

38. Jacobi, M. M.; Abetz, V.; Stadler, R.; Gronski, W. *Polymer* 1996, **37**, 1669.

39. Klein, P. G.; Adams, C. H.; Brereton, M. G.; Ries, M. E.; Nicholson, T. M.; Hutchings, L. R.; Richards, R. W. *Macromolecules* 1998, **31**, 8871.

40. Cohen-Addad, J. P. *J. Phys. 1 Fr.* 1982, **43**, 1509.

41. Brereton, M. G. *Macromolecules* 1990, **23**, 1119.

42. Sotta, P.; Fülber, C.; Demco, D. E.; Blümich, B.; Spiess, H. W. *Macromolecules* 1996, **29**, 6222.

43. Kuhn, W.; Grün, F. *Kolloid-Z.* 1942, **101**, 248.

44. Gronski, W.; Emeis, D.; Brüderlin, A.; Jacobi, M. M.; Stadler, R.; Eisenbach, C. D. *British Polymer Journal* 1985, **17**, 103.

45. Brereton, M. G.; Vilgis, T. A. *J. Phys. France*, 1989, **50**, 245.

46. Brereton, M. G.; Vilgis, T. A. *J. Phys. France*, 1992, **2**, 581.

47. Brereton, M. G.; Vilgis, T. A. *J. Phys. France*, 1992, **2**, 2281.

48. Wittmer, J.; Paul, W.; Binder, K. *Macromolecules* 1992, **25**, 7211.

49. Billmeyer, Jr. F. W. *Textbook of Polymer Science 1984*, John Wiley & Sons, Singapore.

50. Flory, P. J. *Statistical Mechanics of Chain Molecules 1989*, Hanser Publishers, New York.

51. Edwards, S. F.; McLeish, T. C. B. *J. Chem. Phys.* 1990, **92**, 6855.

52. Sotta, P.; Deloche, B.; Herz, J.; Lapp, A.; Durand, D.; Rabadeux, J. C. *Macromolecules* **1987**, **20**, 2769.

53. Depner, M; Sotta, P.; Deloche, B. *Macromolecules* 1994, **27**, 5192.

54. Baljon, A. R. C.; Grest, G.; Witten, T. A. *Macromolecules* 1995, **26**, 1835.

55. Ries, M. E. *Ph.D thesis* 1996, University of Leeds, UK.

56. McKenna, G. B.; Flynn, K. M.; Chen, Y. *Polymer* 1990, **31**, 1937.

57. Roe, R. J.; Krigbaum, W. R. *J. Appl. Phys*. 1964, **35**, 2215.

58. Bellander, M.; Stenberg, B.; Persson, S. *Kautschuk Gummi Kunststoffe* 1999, **52**, 265

59. Lavebratt, H.; Persson, S.; Östman, E.; Stenberg, B. *Kautschuk Gummi Kunststoffe* 1990, **43**, 677.

60. Menge, H.; Hotopf, S.; Heuert, U.; Schneider, H. Polymer **1999**, 40, 5303.

61. Roland, C. M. *J. Appl. Polym. Sci.: Appl. Polym. Symp.* 1994, **53**, 29.

62. Baumann, K.; Gronski, W. *Progr. Colloid. Polym. Sci*. 1992, **90**, 97.

63. Ries, M. E.; Brereton, M. G.; Klein, P. G.; Ward, I. M.; Ekanayake, P.; Menge, H.; Schneider, H. *Macromolecules* 1999, **32**, 4961.

64. Kraus, G.; Collins, R. L. *Rubber World* 1958, **139**, 219.

65. Legrand, A.P. *Macromol. Symp*. 1996, **108**, 81.

66. Gronski, W.; Stadler, R.; Jacobi, M. M. *Macromolecules* 1984, **17**, 741.

67. Jacobi, M.; Stadler, R; Gronski, W. *Macromolecules* 1986, **19**, 2887.

68. Sotta, P.; Deloche, B. *Macromolecules* 1990, **23**, 1999.

69. O'Brien, J.; Cashel, E.; Wardell, G. E.; Mc Briertry, V. J. *Macromolecules* 1976, **9**, 653.

70. Lüchow, H.; Breier, E.; Gronski, W. *Rubber Chemistry and Technology* 1998, **70**, 747.

71. Leblanc, J. L. *J. App. Pol. Sci.* 1997, **66**, 2257.

72. Collignon, J.; Sillescu, H.; Spiess, H. W. *Colloid and Polym. Sci.* 1981, **259**, 220.

73. Callaghan, P. T.; Samulski, E. T. *Macromolecules* 1997, **30**, 113.

74. Ernst, R. R.; Bodenhausen, G.; Wokaun, A. *Principles of Nuclear Magnetic Resonance in One and Two Dimensions* 1987, Oxford University Press, UK.

75. Ball, R. C.; Callaghan, P. T.; Samulski, E. T. *J. Chem. Phys.* 1997, **106**, 7352.

76. Simon, G.; Schneider, H.; Haesler, K. G. Progr. *Colloid Polym. Sci.* 1988, **78**, 30.

77. Callaghan, P. T.; Samulski, E. T. *Macromolecules* 1998, **31**, 3693.

78. Gotlib, Yu. Ya.; Lifshitz, M. I.; Shevelef, V. A.; Lishanskij, L. S.; Balanina, I. V. *Vysokomol. Soedin. A* 1976, **10**, 2299. The English version of this journal is entitled Polym. Sci. USSR.

79. Roth, H. K.; Keller, F.; Schneider, H. *Hochfrequenzspektroskopie in der Polymerforschung* 1984, Akademie-Verlag, Berlin and references therein.

80. Fedotov, V. D.; Schneider, H. *Structure and Dynamics of Bulk Polymers by NMR-Methods* 1989, Springer-Verlag, Berlin and references therein.

Appendix: Spectrum from a Strained Network with an added Orientation due to a Mean Field

The aim of this section is to calculate the NMR spectrum, $G(v,\lambda)$, from a strained polymer network. From equations **(3.4)** and **(3.6)** we have

$$G(v,\lambda) = \frac{1}{2}(G_+ + G_-) \tag{A.1}$$

with

$$G_\pm = \int P(\mathbf{R}) \left\{ \delta\left[v \pm \frac{v_o}{\pi} \left(\langle P_2(\cos\theta) \rangle_\mathbf{R} + \langle P_2(\cos\theta) \rangle_V \right) \right] \right\} d\mathbf{R} \tag{A.2}$$

and

$$\int P(\mathbf{R}) d\mathbf{R} = \left(\frac{3}{2\pi Nb^2} \right)^{3/2} \int_{-\infty}^{+\infty}\int_{-\infty}^{+\infty}\int_{-\infty}^{+\infty} \exp\left[\frac{-3\left(X_o^2 + Y_o^2 + Z_o^2 \right)}{2Nb^2} \right] dX_o Y_o Z_o \tag{A.3}$$

where $\{X_o, Y_o, Z_o\}$ are the undeformed Cartesian coordinates of an end-to-end network vector.

The average orientation due only to the network constraint on a statistical segment in a chain comprising N units is given by

$$\langle P_2(\cos\theta) \rangle_\mathbf{R} = \frac{1}{2N}\left[\frac{2\lambda^2 Z_o^2 - X_o^2/\lambda - Y_o^2/\lambda}{Nb^2} \right] \quad . \tag{A.4}$$

For compactness we define a term Δv such that

$$\Delta v = 2\frac{v_o}{\pi}\langle P_2(\cos\theta) \rangle_V \quad . \tag{A.5}$$

The NMR spectrum **(A.1)** combined with **(A.2)** - **(A.5)** can be expressed in terms of scaled cylindrical co-ordinates

$$r^2 = \frac{X_o^2 + Y_o^2}{\lambda Nb^2} , \; z^2 = \frac{\lambda^2 Z_o^2}{Nb^2}$$

(A.6)

as

$$G(v,\lambda) = \frac{1}{2}\left[I_+(v,\lambda) + I_-(v,\lambda)\right] ,$$

(A.7)

where

$$I_\pm(v,\lambda) = \left(\frac{3}{2}\right)^{3/2} \frac{1}{\sqrt{\pi}} \int\limits_{-\infty}^{+\infty} dz \int\limits_0^\infty dr^2 \exp\left[-\frac{3}{2}\left(\lambda r^2 + \frac{z^2}{\lambda^2}\right)\right] \delta\left\{v \pm \left[\frac{v_o}{\pi}\frac{1}{2N}\left(2z^2 - r^2\right) + \frac{\Delta v}{2}\right]\right\}.$$

(A.8)

The two integrals $I_+(v,\lambda)$ and $I_-(v,\lambda)$ must be evaluated separately. The following analysis will only consider $v/v_o \geq 0$, as the signal must be symmetric. It will also be assumed that $\Delta v \geq 0$, which implies that the induced orientation due to the mean field is in the same direction as the strain.

For $I_+(v,\lambda)$ the integrand is zero unless $r^2 = 2\left[\frac{N\pi}{v_o}\left(v + \frac{\Delta v}{2}\right) + z^2\right]$. Since r^2 will remain positive for all z, $v/v_o \geq 0$ and $\Delta v \geq 0$, the remaining integral over z is unrestricted. From the property of a δ function we have

$$I_+(v,\lambda) = \left(\frac{2N\pi}{v_o}\right)\left(\frac{3}{2}\right)^{3/2} \frac{1}{\sqrt{\pi}} \exp\left[-\frac{3\pi N\lambda}{v_o}\left(v + \frac{\Delta v}{2}\right)\right] \int\limits_{-\infty}^{+\infty} dz \exp\left[-\frac{3}{2}\left(2\lambda + \frac{1}{\lambda^2}\right)z^2\right].$$ (A.9)

This is now in the form of a standard Gaussian integral, so

$$I_+(v,\lambda) = \left(\frac{3N\pi}{v_o}\right)\left[2\lambda + \frac{1}{\lambda^2}\right]^{-1/2} \exp\left[-\frac{3N\pi\lambda}{v_o}\left(v + \frac{\Delta v}{2}\right)\right] \quad . \qquad \textbf{(A.10)}$$

For the $I_-(v,\lambda)$ the integrand is zero unless $r^2 = 2\left[-\frac{N\pi}{v_o}\left(v - \frac{\Delta v}{2}\right) + z^2\right]$. The

integration over the variable z must be constrained so as to keep $r^2 \geq 0$. This then

defines two intervals over which $I_-(v,\lambda)$ should be considered.

In the range $v \leq \frac{\Delta v}{2}$ the variable z is unrestricted as $r^2 \geq 0$. In this region we have

$$I_-(v,\lambda) = \left(\frac{2\pi N}{v_o}\right)\left(\frac{3}{2}\right)^{3/2}\frac{1}{\sqrt{\pi}}\exp\left[\frac{3N\pi\lambda}{v_o}\left(v - \frac{\Delta v}{2}\right)\right]\int\limits_{-\infty}^{+\infty} dz \exp\left[-\frac{3}{2}\left(2\lambda + \frac{1}{\lambda^2}\right)z^2\right]. \quad \textbf{(A.11)}$$

The integral is again in a standard Gaussian form, giving

$$I_-(v,\lambda) = \left(\frac{3N\pi}{v_o}\right)\left[\left(2\lambda + \frac{1}{\lambda^2}\right)\right]^{-1/2}\exp\left[\frac{3N\pi\lambda}{v_o}\left(v - \frac{\Delta v}{2}\right)\right] \quad . \qquad \textbf{(A.12)}$$

In the second region $v > \frac{\Delta v}{2}$ the variable z must be constrained so as to keep $r^2 \geq 0$.

Thus for a non zero integrand $|z| > z\left(v - \frac{\Delta v}{2}\right) = \sqrt{\frac{N\pi(v - \Delta v/2)}{v_o}}$, giving

$$I_-(v,\lambda) = \left(\frac{2N\pi}{v_o}\right)\left(\frac{3}{2}\right)^{3/2}\frac{1}{\sqrt{\pi}}\exp\left[\frac{3N\pi\lambda}{v_o}\left(v - \frac{\Delta v}{2}\right)\right]2\int\limits_{z(v-\Delta v/2)}^{+\infty} dz \exp\left[-\frac{3}{2}\left(2\lambda + \frac{1}{\lambda^2}\right)z^2\right].$$

$$\textbf{(A.13)}$$

The integral can then be written in terms of the error function $erf\left(\cdots\right)$ as

$$I_-(v,\lambda) = \left(\frac{3N\pi}{v_o}\right)\left(2\lambda + \frac{1}{\lambda^2}\right)^{-1/2}\exp\left[\frac{3N\pi\lambda}{v_o}\left(v - \frac{\Delta v}{2}\right)\right]\left\{1 - erf\left[z\left(v - \frac{\Delta v}{2}\right)\sqrt{\frac{3}{2}\left(2\lambda + \frac{1}{\lambda^2}\right)}\right]\right\} \quad . \qquad \textbf{(A.14)}$$

The resultant spectrum must be symmetric about $v = 0$, so it can be written from the above analysis as

$$G(v,\lambda) = \left(\frac{3N\pi}{2v_o}\right)\left[2\lambda + \frac{1}{\lambda^2}\right]^{-1/2}\left[g_+\left(|v| + \frac{\Delta v}{2},\lambda\right) + g_-\left(|v| - \frac{\Delta v}{2},\lambda\right)\right] \quad , \qquad \textbf{(A.15)}$$

where

$$\Delta v = 2\frac{v_o}{\pi}\left\langle P_2\left(\cos\theta\right)\right\rangle_V \qquad \textbf{(A.16)}$$

with

$$g_+(v,\lambda) = \exp\left[-\frac{3N\pi\lambda}{v_o}v\right] \qquad \textbf{(A.17)}$$

and when $|v| \le \dfrac{\Delta v}{2}$

$$g_-(v,\lambda) = \exp\left[\frac{3N\pi\lambda}{v_o}v\right] \qquad \textbf{(A.18)}$$

or when $|v| > \dfrac{\Delta v}{2}$

$$g_-(v,\lambda) = \exp\left[\frac{3N\pi\lambda}{v_o}v\right]\left\{1 - erf\left[z(v)\sqrt{\frac{3}{2}\left(2\lambda + \frac{1}{\lambda^2}\right)}\right]\right\} \qquad \textbf{(A.19)}$$

with

$$z(v) = \sqrt{\frac{N\pi v}{v_o}} \quad . \qquad \textbf{(A.20)}$$

Acknowledgements

CURRICULUM-VITAE

Name   : Piyasiri **Ekanayake**
Date of Birth   : 14 September, 1965
Sex   : Male
Nationality   : Sri Lankan
Civil Status   : Married

Academic Qualifications:

Secondary Education

(a) High School

    School   : Central College Kekirawa
    Examination   : **University Entrance Examination**
    Year of Examination : 1984
    Subjects   : Physics, Chemistry, Pure Mathematics,
                           Applied Maths

Higher Education

(a) First Degree

    University   : University of Peradeniya, Sri Lanka
    Degree   : **B.Sc. (Honours in Physics)**
    Year of Graduation   : 1992
    Major Subject   : Physics
    Subsidiary Subject   : Pure Mathematics

(b) Postgraduate degree

    University   : University of Peradeniya, Sri Lanka
    Degree   **Master of Science (in Physics)**
    Year of Graduation   : 1996

Area of Specialization for the Masters degree: *Creep Behaviour of Ceramic Coposite Materials*

Employment:

Feb. 1997 - to date
Scientific Collaborator/ Ph. D Student
Department of Physics
University of Halle-Wittenberg
Friedemann-Bach-Platz 6
D - 06108 Halle/Saale
Germany

July 1994 - Dec. 1996
Guest Student
Swiss Federal Institute of Technology(ETH)
Institute of Non Metallic Materials
NO H 11, Sonneggstrasse 5, 8092 Zurich
Switzerland

November 1992 - June 1994
Research Assistant
Department of Physics
University of Peradeniya
Peradeniya, Sri Lanka

March 1992 - October 1992
Temporary Demonstrator
Department of Physics
University of Peradeniya
Peradeniya, Sri Lanka

Fellowships

1). Gate Mudliyar A.G. Tilakeratne Research Fellowship (1993),
    University of Peradeniya, Sri Lanka
2). Swiss Federal Government Scholarship (ESKAS) (July 1994-Dec.1996)

Erklärung

Ich erkläre hiermit, dass die Dissertation selbständig verfasst wurde und nur die angegebenen Hilfsmittel benutzt wurden. Die Dissertation wurde noch an keiner anderen Universität oder Hochschule eingereicht.

Halle, den 07. 02. 2000

(Piyasiri Ekanayake)